SYNTHESIS AND STUDY OF INTERACTIONS OF NOVEL ACRIDINIUM DERIVATIVES WITH SINGLE STRAND AND DOUBLE STRAND DNA

THESIS SUBMITTED TO
THE UNIVERSITY OF KERALA
FOR THE DEGREE OF
DOCTOR OF PHILOSOPHY
IN CHEMISTRY
UNDER THE FACULTY OF SCIENCE

By

ELIZABETH KURUVILLA

PHOTOSCIENCES AND PHOTONICS
CHEMICAL SCIENCES AND TECHNOLOGY DIVISION
REGIONAL RESEARCH LABORATORY (CSIR)
TRIVANDRUM 695 019, KERALA, INDIA

APRIL 2007

SYNTHESIS AND STUDY OF INTERACTIONS OF NOVEL ACRIDINIUM DERIVATIVES WITH SINGLE STRAND AND DOUBLE STRAND DNA

THESIS SUBMITTED TO
THE UNIVERSITY OF KERALA
FOR THE DEGREE OF
DOCTOR OF PHILOSOPHY
IN CHEMISTRY
UNDER THE FACULTY OF SCIENCE

By

ELIZABETH KURUVILLA

PHOTOSCIENCES AND PHOTONICS
CHEMICAL SCIENCES AND TECHNOLOGY DIVISION
REGIONAL RESEARCH LABORATORY (CSIR)
TRIVANDRUM 695 019, KERALA, INDIA

APRIL 2007

STATEMENT

I hereby declare that the matter embodied in the thesis entitled: **"Synthesis and Study of Interactions of Novel Acridinium Derivatives with Single Strand and Double Strand DNA"** is the result of investigations carried out by me at the Photosciences and Photonics, Chemical Sciences and Technology Division of the Regional Research Laboratory (CSIR), Trivandrum, under the supervision of Dr. D. Ramaiah and the same has not been submitted elsewhere for a degree.

In keeping with the general practice of reporting scientific observations, due acknowledgement has been made wherever the work described is based on the findings of other investigators.

Elizabeth

Elizabeth Kuruvilla

PHOTOSCIENCES AND PHOTONICS
CHEMICAL SCIENCES AND TECHNOLOGY DIVISION
REGIONAL RESEARCH LABORATORY (CSIR)
TRIVANDRUM 695 019, INDIA

Dr. D. Ramaiah
Scientist

Telephone: (91)-471-2515362; Fax: (91)-471-2490186 or 2491712
E. Mail: d_ramaiah@rediffmail.com or rama@csrrltrd.ren.nic.in

April 18, 2007

CERTIFICATE

This is to certify that the work embodied in the thesis entitled: **"Synthesis and Study of Interactions of Novel Acridinium Derivatives with Single Strand and Double Strand DNA"** has been carried out by Ms. Elizabeth Kuruvilla under my supervision and the same has not been submitted elsewhere for a degree.

D. Ramaiah
Thesis Supervisor

ACKNOWLEDGEMENTS

I have great pleasure in placing on record my deep sense of gratitude to Dr. D. Ramaiah, my thesis supervisor, for suggesting the research problem and for his guidance, support and encouragement, leading to the successful completion of this work.

I would like to express my sincere thanks to Professor M. V. George for being an inspiration.

I wish to thank Professor. T. K. Chandrashekhar, Director and Dr. G. Vijay Nair, Dr. B. C. Pai and Professor Javed Iqbal, former Directors of the Regional Research Laboratory, Trivandrum for providing necessary facilities for carrying out the work.

I sincerely thank Dr. Suresh Das, Dr. A. Ajayaghosh, Dr. K. R. Gopidas and Dr. K. George Thomas, Scientists of the Photosciences and Photonics, Chemical Sciences and Technology Division, for all the help and support extended to me.

I thank all the members of the Photosciences and Photonics and in particular, Dr. Joshy Joseph, Dr. K. T. Arun, Dr. Mahesh Hariharan, Mr. Jyothish Kuthanapillil, Mr. P. N. Prakash, Ms. Jisha. V. S., Ms. Rekha Rachel Avirah and Ms. Priya A. Nair, Mr. Robert Philip and Mrs. Sarada Nair for their help and cooperation. I thank Ms. S. Viji and Ms. Soumini Shoji for NMR and elemental analyses. I also thank my friends in other Divisions of the Regional Research Laboratory, Trivandrum for their cooperation.

I am deeply indebted to my parents and my sister for their invaluable support and constant encouragement.

Financial assistance from the Council of Scientific and Industrial Research (CSIR) and the Department of Science and Technology (DST) is gratefully acknowledged.

Elizabeth Kuruvilla

CONTENTS

Study of interactions of small molecules with nucleic acids has gained widespread interest because such studies are not only useful in understanding the molecular basis of carcinogenesis and DNA-protein interactions but also lead to the design of novel drugs targeted to DNA and sensitive probes for nucleic acids. Of the sensitive probes reported for nucleic acids, the small molecule based sensors have attracted much attention in recent years and have found wide range of applications, including in detection and quantification of DNA, DNA damage, real-time monitoring of polymerase chain reaction, DNA hybridization and in DNA microarrays. The thesis entitled: "Synthesis and Study of Interactions of Novel Acridinium Derivatives with Single Strand and Double Strand DNA" reports our efforts towards the design and study of photophysical and DNA binding aspects of a series of novel acridinium derivatives, with a view to developing new molecular probes for selective recognition of various DNA structures.

The first Chapter of the thesis presents a short description of the single strand and double strand DNA structures and provides a brief overview of various interactions of small molecules with DNA, with a particular emphasis to the ligand-DNA non-covalent interactions. Further, a few examples of currently used nucleic acid probes along with their mode of interaction with DNA and the objectives of the present thesis are also briefly described in this Chapter.

Synthesis and results of photophysical and DNA binding studies of a series of aryl acridinium derivatives, wherein steric factors have been varied systematically through substitution at the 9th-position of the acridinium ring are reported in the second Chapter of the thesis. These compounds were synthesized by the reaction of the corresponding acridine derivatives with iodomethane. These derivatives showed high solubility in the aqueous medium and exhibited quantitative fluorescence quantum yields depending on the nature of the substituent present at the 9th-position of the acridinium ring. In presence of the double stranded DNA (dsDNA), the derivatives **1-5** showed a red shift of 2-3 nm in the absorption spectra and efficient quenching in the fluorescence emission, which was attributed to the energetically feasible electron transfer process from the DNA bases to the singlet excited state of the acridinium chromophore. The DNA association constants were found to be in the range of 6.9 - 10 $\times 10^4$ M^{-1}. The *ortho*-substituted derivatives, **6-8**, on the other hand exhibited negligible interactions with dsDNA due to the steric crowding around the acridinium ring. However, in presence of the single stranded DNA (ssDNA), where the nucleobases are more exposed, the *ortho*-substituted derivatives **6-8** showed significant changes in the absorption and fluorescence properties with moderate association constants in the range of 6.3 - 7 $\times 10^4$ M^{-1}. Apart from the spectroscopic studies, the mode of association of these derivatives with ssDNA and dsDNA were characterized using chiroptical and AFM techniques. The results presented in this chapter demonstrate that the subtle variation in the substitution pattern has profound influence on the photophysical and DNA binding properties of these novel acridinium derivatives.

The third Chapter of the thesis deals with the synthesis, photophysical and DNA binding properties of a few bisacridinium derivatives **1** and **2** and the model compounds **3** and **4**. The synthesis of the bisacridinium derivatives **1** and **2** was achieved by the quarternization of the corresponding bisacridine derivatives using methyl trifluoromethane sulphonate, while the starting bisacridines were synthesized by the condensation of diphenylamine with the corresponding dicarboxylic acid. All the derivatives were characterized on the basis of analytical results and spectral data. The bisacridinium derivatives exhibit high extinction coefficient value of 3.3×10^4 M^{-1} cm^{-1} and quantitative fluorescence quantum yields of 0.91-0.98. DNA binding studies through photophysical and biophysical techniques indicate that these systems interact with DNA preferentially through intercalation of the acridinium chromophore with significant DNA association constants of the order 10^5 - 10^7 M^{-1}. These derivatives, depending on the spacer length showed interestingly both mono- and or bis-intercalative interactions at low ionic strengths (2 mM). However, upon increasing the ionic strength (100 mM) of the buffer, all these derivatives exhibited exclusively the mono-intercalative interactions. The observation of efficient quenching in the fluorescence emission of these derivatives in the presence of DNA could be attributed to the theoretically feasible electron transfer from the DNA bases to the excited state of the acridinium chromophore. Further confirmation was obtained from the observation of the photoproducts using laser flash photolysis studies. Laser flash photolysis studies of these systems in buffer gave transients with absorption maxima in the range 480-500 nm and lifetimes 0.6-3 μs, which can be attributed to their triplet exited states based on

the quenching studies with molecular oxygen. The laser excitation of these systems in the presence of DNA and guanosine-5'-monophosphate (GMP) led to the formation of oxidized species like radical cations of DNA and GMP. The efficiency of oxidation of GMP and DNA by these derivatives was further increased in the presence of an efficient electron acceptor such as methylviologen. These results indicate that ionic strength has a profound influence on the DNA mono- and bis-intercalating properties of the novel bisacridinum derivatives and further demonstrate that depending on the spacer and substituents present, these molecules can act as efficient DNA photooxidizing agents.

The development of a fluorimetric method for the quantification of single strand DNA (ssDNA) and for the determination of ratio of ssDNA to double strand DNA (dsDNA) based on the acridinium derivatives forms the subject matter of the fourth Chapter. The *ortho*-substituted acridinium derivatives **1** and **2** were found to exhibit significant changes in their spectroscopic, biophysical and microscopic properties in the presence of ssDNA, when compared to other nucleic acids such as dsDNA and RNA. The selective binding of the acridinium derivatives with ssDNA could be visually observed by the quenching of the acridinium fluorescence in the presence of ssDNA.The study of interactions of these derivatives with single strand oligomers of 19 bases indicated that these derivatives show highest affinity for $(dG)_{19}$ sequences, whereas least affinity (ca. 3-fold) was observed for the cytosine rich sequences $(dC)_{19}$. These observations led to the development of a fluorescence based method for the quantification of ssDNA and for the determination of ratio of ssDNA to dsDNA. This

fluorimetric assay displayed linearity over a wide range of ssDNA concentrations (0 – 1 mM). The linearity was checked in the presence of commonly found impurities in nucleic acid assays such as proteins, micelles like sodium dodecyl sulfate (SDS), Triton X-100, RNA and NaCl. Interestingly, these additives were found to have negligible effects on the assay. Results presented in this Chapter indicate that this assay could be used to quantify the ssDNA in the presence of dsDNA and also in the blood serum, indicating the versatility of the assay based on the acridinium derivatives for various biological applications.

Note: *The numbers of the various compounds given here correspond to those given under the respective Chapters.*

Chapter 1

A BRIEF OVERVIEW OF NUCLEIC ACID PROBES

1.1. Introduction

Study of interactions of small molecules with nucleic acids has assumed great significance over the past few decades because of their importance in biochemical and medicinal applications. Such studies not only give insight into the molecular hasis of nucleic acid interactions, development and analysis of drugs targeted to nucleic acids but also in the design of new highly specific agents whose DNA sequence-recognition properties can be selected as desired.[1] Besides this, there has also been great interest in understanding the natural process of DNA recognition by biomolecules such as proteins and enzymes.[2] Research in these areas has led to the development of several probes, which are now used in a wide range of applications, including DNA detection and quantification[3], DNA damage analysis[4], real-time monitoring of polymerase chain reaction (PCR)[5], DNA hybridization[6] and in DNA microarrays.[7]

Though the double strand DNA plays a major role as the carrier of genetic information, much of the biological activity of DNA depends on the interactions of various biomolecules at the regions of DNA, which are single stranded or have unpaired nucleotides.[8] For example, the interaction between proteins and single

stranded DNA plays an important role in the regulation of critical biological processes such as telomeric-end protection,[9] DNA replication[10] and repair.[11] Also, tagged single stranded oligonucleotides are used in genetic applications such as microarrays, which make the study of interactions of probes with single stranded DNA important.[8,12] In this context, we have undertaken the design and study of interactions of a few substituted acridinium derivatives with single strand and double strand DNA. This chapter gives a brief description of the structure and constituents of DNA, with a particular emphasis on various ligand binding sites of DNA, examples of different nucleic acid probes and their mode of interactions with single strand and double strand DNA. The objectives of the present thesis are also described in this Chapter.

1.2. Structure of DNA

Nucleic acids of all organisms are made up of a number of nucleotides joined together by phosphodiester linkages. Each nucleotide comprises of a sugar, phosphate and a purine or pyrimidine base. Nucleic acids may be divided into two classes depending upon the nature of their sugar residues. Those that contain β-2'-deoxy-D-ribose are called the deoxyribonucleic acids (DNA), while those containing β-D-ribose are known as ribonucleic acid (RNA). The common heterocyclic bases present in DNA are adenine (A), guanine (G), cytosine (C) and thymine (T), whereas in RNA, the thymine is replaced by uracil (U). While adenine and guanine belong to the class of purines, the pyrimidine bases are the

cytosine, thymine and uracil (Figure 1.1). Combination of one of these bases (N-1 of C, T or U and N-9 of A or G) with a sugar residue via the C-1 carbon constitutes a nucleoside and phosphorylation at the 5'-hydroxyl group of the nucleoside results in a nucleotide, the monomeric unit of the nucleic acids (Figure 1.2). The primary structure of DNA has each nucleoside joined by a

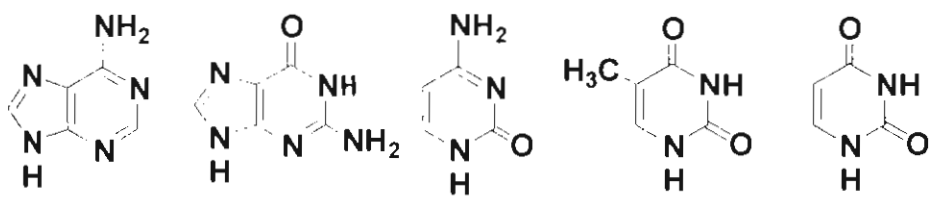

Figure 1.1. Structures of purine and pyrimidine bases present in nucleic acids.

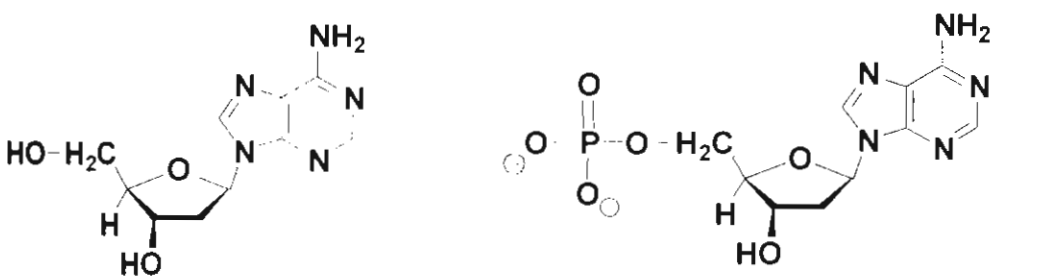

Figure 1.2. Structures of a representative nucleoside, 2'-deoxyadenosine (dA) and nucleotide, 2'-deoxyadenosine-5'-monophosphate (dAMP).

phosphodiester from its 5'-hydroxyl group to the 3'-hydroxyl group of one neighbor and by a second phosphodiester from its 3'-hydroxyl group to the 5'-hydroxyl of its other neighbor (Figure 1.3A). This 5'-3' linkage is maintained

throughout the entire length of DNA, which means that the uniqueness of a given DNA primary structure resides solely in the sequence of its bases.

DNA consists of two chains, which run in opposite directions and are coiled around each other to form a double helix. These two chains are linked together by a large number of weak hydrogen bonds formed between complementary bases (Figure 1.3B). The complementary base pairs are adenine-

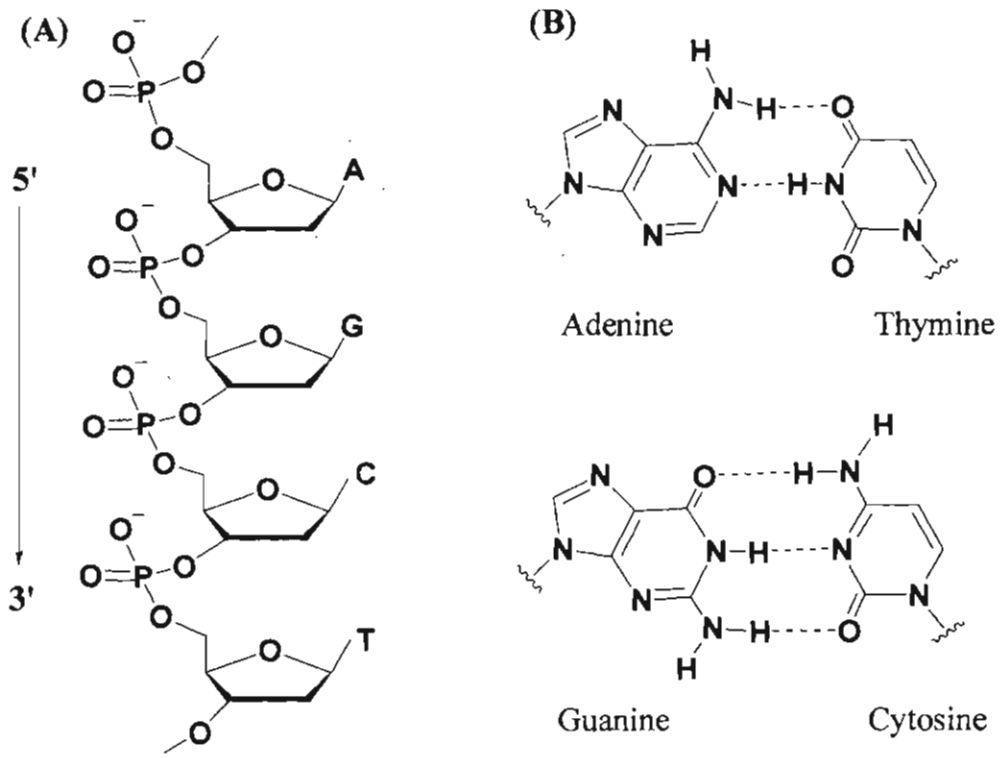

Figure 1.3. (**A**) Schematic representation of the primary structure of DNA and (**B**) Watson-Crick base pairing of adenine-thymine (A-T) and guanine-cytosine (G-C).

thymine and guanine-cytosine. The bases, which are hydrophobic and paired by hydrogen bonding lie inside and perpendicular to the helix axis, whereas the hydrophilic and negatively charged sugar and phosphate residues face out into the

aqueous medium. The double helical structure of DNA (dsDNA) is stabilized by hydrogen bonding between the complementary base pairs and also by hydrophobic interactions between the stacked bases. The hydrogen bonding in nucleic acids is vital not only in the maintenance of structure of DNA but also in the performance of its important biological functions such as the expression of genetic information, replication and transcription.[13] Most of these biological functions of the double strand DNA occurs by the unwinding of the duplex and formation of single stranded regions along the double helix as well as the formation of single strand DNA.[14] The single strand DNA (ssDNA) comprises of the same basic components as the double strand DNA (dsDNA), but, the bases in the strand are not H-bonded to their complementary base pairs. The base stacking interactions in ssDNA have been widely reported and are found to favor the parallel orientation of adjacent aromatic rings of the bases giving rise to rigid helical domains (Figure 1.4).[15-18]

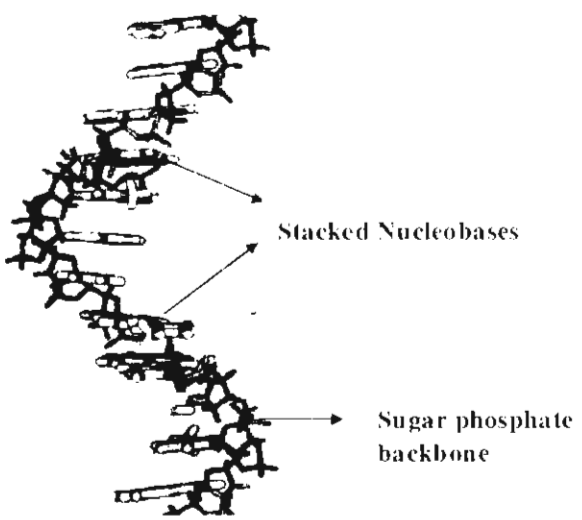

Figure 1.4. Helical structure of single strand DNA with stacked nucleobases.

The physical characteristics of ssDNA determine its secondary structure and dynamics that are essential for its biological functions. Therefore, the understanding of the physical basis underlying the formation of specific ssDNA conformations would be important in elucidating its biological functions. However, the available data are not sufficient to describe the extremely variable conformations of ssDNA in solution, which are affected by electrostatic, base pairing and stacking interactions.

Double strand DNA (dsDNA) is known to exist in several polymorphic forms, of which three polymorphs are important, namely, A, B and Z forms.[13] The existence of such conformations depends on factors such as humidity, salt concentration and the energetics of base stacking. A-DNA and B-DNA are the important standard DNA secondary structures with right-handed double helices and Watson-Crick base pairing (Figure 1.5). Table 1.1 summarizes the properties of these three morphological forms of DNA. B-form DNA is predominantly found under physiological conditions and was first observed from the X-ray fiber diffraction patterns of the paracrystalline DNA at a relative humidity of above 80%.[13d]

In B-DNA, the diameter of the helix is constant over the entire length and equals 20 Å. Each base pair is rotated approximately 36^0 relative to the one preceding it, resulting in a complete helical turn for every 10 base pairs. Since each base has a thickness of 3.4 Å, and the bases are perpendicular to the helix

axis, the helical pitch is 34 Å in B-DNA. Another important feature of the B-form of DNA is the presence of two distinct grooves, a major groove and a minor groove. These two grooves provide a very distinct surface with which proteins and certain chemicals can interact. At a relative humidity below 80 per cent or at a low

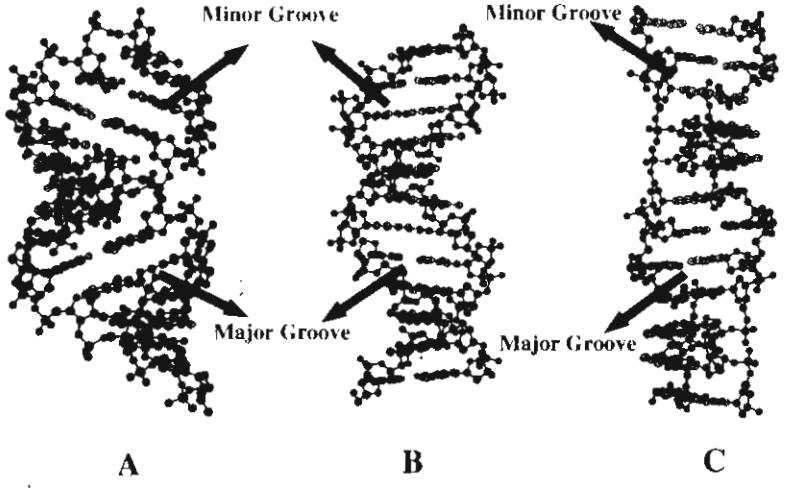

Figure 1.5. Structures of various forms of double strand DNA. (**A**) A-DNA, (**B**) B-DNA and (**C**) Z-DNA.

concentration of counter-ions in the sample, DNA exists in a crystalline form known as the A-DNA.[13d] It differs from the B-DNA in many ways. The grooves are not as deep as in B-DNA and the bases are neither normal to the axis of the helix (the angle with the perpendicular to the axis is about 20^0) nor coplanar within a pair. The helix rise per base pair in A-DNA is much smaller and equals 2.3-2.6 Å. Further, it has been found that sugar in the A-form of DNA has a C3'-*endo* conformation, as compared to the 2'-*endo*-conformation in B-form.

Oligo- and polynucleotides with alternating G and C sequences when crystallized from a solution with high concentration of salts, leads to the formation of the left-handed DNA, also known as Z-DNA.[19] It has remarkable features, namely, alternation of nucleotide conformation: the sugar moieties in 2'-deoxycytidine (dC) units have C2'-*endo* conformation and the base in an *anti*-conformation, whereas in the complementary base, dG units, the deoxyriboses are

Table 1.1. Characteristics of A, B and Z forms of DNA.[19c]

Property	A	B	Z
Relative humidity (%)	75	92	66
Pitch (Å)	28	34	31
Residues per turn	11	10	9.3
Inclination of base pair from horizontal	20°	0°	6°
Sugar ring conformation	C3'endo	C2'endo	C3'endo(syn)
Base conformation (rotated relative to sugar)	anti	anti	syn
Major groove	Fully hidden	Accessible (10 Å in width)	Accessible
Minor groove	Accessible	Accessible	Fully hidden

in the C3'-*endo* conformation and the base is in a *syn*-conformation. Thus, the repeating units in the Z form of DNA consists of two base pairs and not one as in the case of the B-form. As a result, the line connecting the phosphate groups takes a sharp turn and assumes a zig-zag shape. When compared to the B-DNA, the Z form of DNA is a higher energy conformation, where a considerable reorganization of the double helix takes place so that it is in the left-handed mode. A-DNA, on the other hand is a somewhat less stable conformation of B-DNA. Therefore, the energy required to go from B to A form is much less than that required going from B to Z form.

In addition to the A, B and Z forms, DNA can adopt a wide variety of so-called unusual structures, which are often limited to a particular base sequence. Examples include, self-complementary single stranded DNA formed into hairpins, single and multiple base bulges and quartet structures consisting of four DNA strands.[19c] Ligands such as, small organic and inorganic molecules, can undergo various types of covalent and non-covalent interactions with DNA. They can interact with both ssDNA and dsDNA, however, the complex formed with ssDNA will be weaker compared to those formed with dsDNA.[20] This is because of the lesser compact structure of ssDNA when compared to the dsDNA. The ligand-DNA non-covalent interactions and few examples of the probes developed for the detection of ssDNA and dsDNA are described in the following sections.

1.3. Ligand-DNA Interactions: Covalent and Non-Covalent Binding

There are two principal ways through which a molecule can bind with DNA. Molecules can form non-covalent complexes with DNA via non-covalent interactions such as hydrogen bonding and π- stacking or undergo covalent interactions through the formation of covalent bonds. Drugs which bind covalently to DNA are used to either add substituents onto the base residues or to form cross-links between different sections of DNA. An example is cis-platin, $[Pt(Cl)_2(NH_3)_2]$, a well known anti-cancer drug. The chlorine atoms of cis-platin are good leaving groups. When cis-platin enters cells with a low chlorine concentration, ligand exchange takes place forming an activated aqua complex, which is electrophilic. It has been shown that cis-platin preferentially react with the N7 of the purine bases and N3 of the pyrimidines bases.[19c] Being bifunctional it binds to two bases, which can be from two different strands of the dsDNA forming interstrand cross-links, preventing it from unwrapping during replication.

DNA can also undergo reversible or non-covalent interactions with a broad range of chemical species that include water, metal ions and their complexes, small organic molecules, drugs and proteins. All of the intricate nucleic acid conformations which exist are stabilized by and only possible because of these reversible interactions. The three primary types of non-covalent interactions are electrostatic, groove-binding and intercalative interactions (Figure 1.6), which are described in the following sections.

1.3.1. Electrostatic Interactions

DNA is a negatively charged polyelectrolyte, whose phosphate groups strongly affect its structure and interactions. Simple ions and positively charged molecules can 'condense' on to the anionic outer surface of DNA, which helps in maintaining the charge neutralization of DNA. This mode of binding is comparatively flexible and the bound molecules or ions can move freely along the nucleic acid chain. Metal cations such as Na^+, Mg^{2+}, Ca^{2+} and organic molecules bearing positive charge are known to bind with DNA through electrostatic mode.

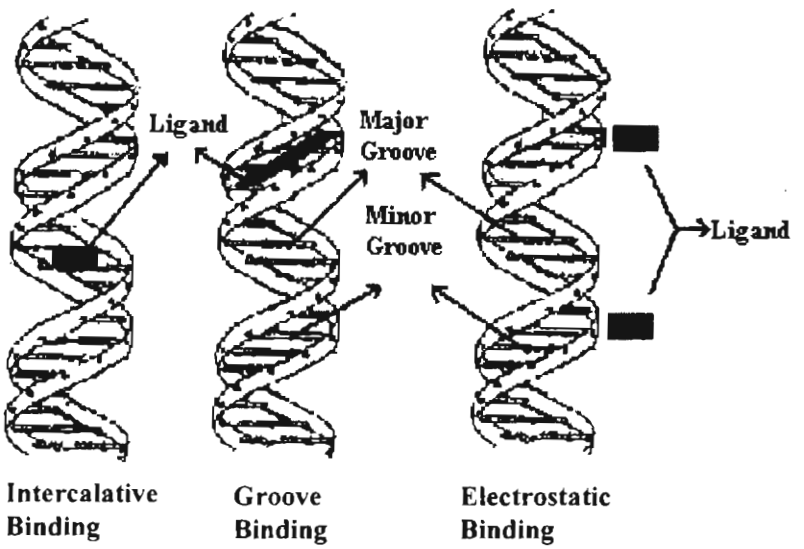

Figure 1.6. Schematic representation of different binding modes of ligands with DNA.

Multiple charged simple cations such as Mg^{2+} and cations of simple organic amines such as 1,3-diaminopropane interact with DNA more strongly than monovalent cations (Na^+, K^+ etc) and displace the monocations from DNA.[21] Non-specific outside stacking of cationic organic molecules on the surface of DNA

forms another mode of electrostatic interaction. Planar aromatic molecules can stack on each other to form dimers and higher aggregates, however, in the case of charged compounds, such as proflavine, they repel each other electrostatically. If the cations stack along the anionic DNA sugar-phosphate chain, the charge repulsion is decreased and this type of binding leads to non-specific outside stacking of planar cations along the double helix.[22]

1.3.2. Groove Binding

B-DNA possesses a wide major groove and a narrow minor groove through which small molecules can interact with the duplex (Figure 1.6). The major and minor grooves differ significantly in electrostatic potential, hydrogen bonding characteristics, steric effects and hydration. Many proteins exhibit binding specificity primarily through major groove interactions, while small molecules in general prefer the minor groove of DNA. Minor groove binding molecules have several simple aromatic rings such as pyrrole, furan, or benzene connected by bonds with torsional freedom. This helps the compounds to fit into the helical curve of the minor groove, with appropriate twist of the bonds and thus displace water from the groove. The DNA minor groove is generally not as wide as in A.T-rich relative to G.C-rich regions and hence can accommodate aromatic molecules better at A.T than at G.C sequences. Inside the grooves, molecules can undergo van der Waals contacts with the helical chains, which define the 'wall' of the

groove. The contact between the bound molecule and the edges of the base pairs gives additional stability and specificity for the groove interactions. An important feature of the groove binding interaction not seen in other interactions is that such molecules can be extended to fit over many base pairs along the groove and hence can have high sequence specific recognition of nucleic acids. Antibiotics such as netropsin and distamycin (**1** and **2**, Chart 1.1) are typical examples of molecules which interact with DNA by this mechanism.[23,24]

Dickerson and co-workers[24] obtained a crystal structure of netropsin bound to the DNA duplex d(CGCGAATTCGCG) (Figure 1.7) which has provided considerable structural details of the complex formation in the minor groove. Netropsin binds at the AATT region of the duplex and displaces the spine of

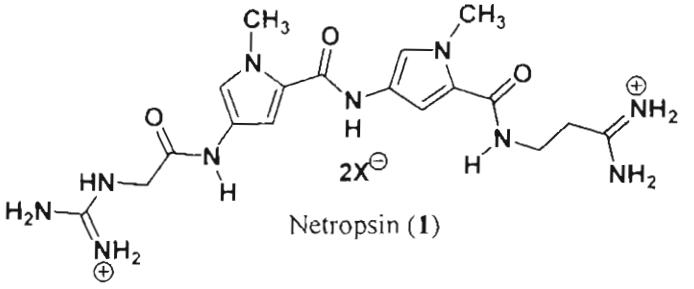

Netropsin (**1**)

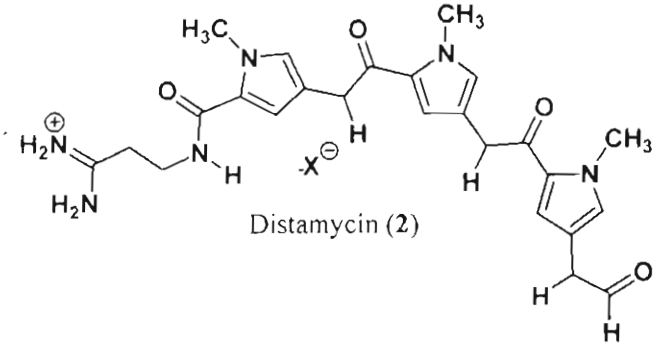

Distamycin (**2**)

Chart 1.1

hydration seen in that region of the free oligomer. The three amide NH groups point inward and form bifurcated hydrogen bonds with N-3 of adenine and O-2 of thymine. The molecule is held in the centre of the groove by van der Waals contacts with the atoms of DNA which form the walls of the groove. These contacts hold the pyrrole rings approximately parallel to the walls of the groove and as a consequence of the helical twist of the groove, the two pyrrole rings are twisted by approximately 33^0 with respect to one another. The two cationic ends of netropsin are also centred in the minor groove. Steric interactions between the pyrrole-CHs and the DNA bases prevent netropsin from moving more deeply into the groove. Binding of netropsin causes a slight widening of the minor groove in the AATT region and a bending of the helix axis away from the site of binding. No other characteristic helical parameters are significantly changed in the complex. As

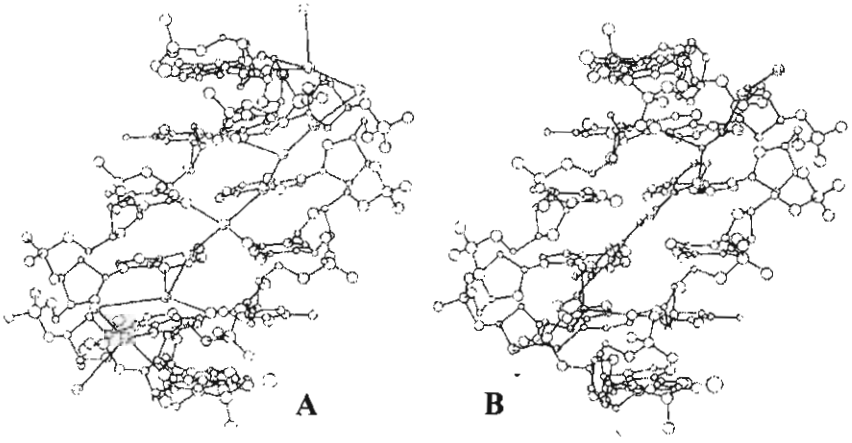

Figure 1.7. Stereoviews of B-DNA minor groove interactions of (**A**) the spine of hydration and (**B**) the netropsin molecule (**1**). In each case, only the central six base pairs are drawn for the dodecamer of sequence: CGCGATAT-BrC-GCG, as established through single crystal X-ray structural analysis.[25]

indicated above, the amino group of guanosine prevents molecules of this type from sliding deeply into the minor groove and forming hydrogen bonds with the bases. Netropsin binding to G.C-rich regions of DNA is thus weaker than to A.T sequences.[23,24] Factors such as water and counter-ion release contribute to the overall free energy of binding of netropsin, but have little effect on binding specificity. Other important examples for minor groove binding interactions are given in Chart 1.2, which include the aromatic diamidines **3** and **4**, methyl viologen (**5**) and SN 6999 (**6**).[26,27] All these molecules exhibit A.T specific minor groove binding interactions. Among these, SN 6999 is an interesting example, where the quinolinium ring can undergo intercalation in addition to groove binding interactions.

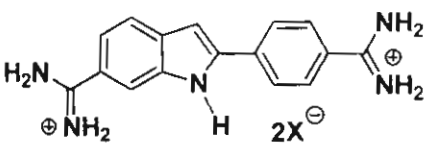

4,6'-diamidino-2-phenylindole (DAPI, 3)

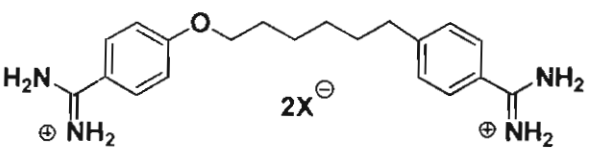

Pentamidine (**4**)

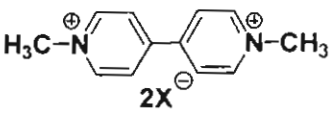

Methyl viologen (**5**)

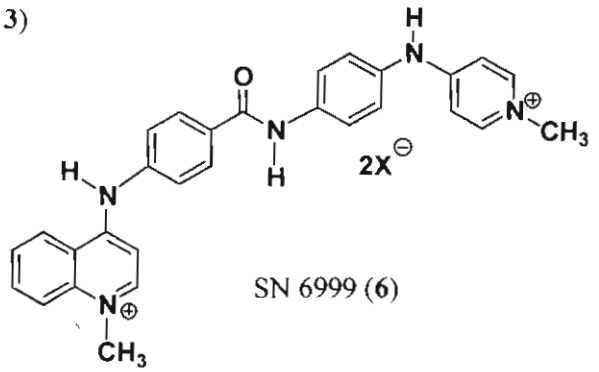

SN 6999 (**6**)

Chart 1.2

1.3.3. Intercalative Interactions

Many of the DNA-binding agents have been shown to associate with DNA by inserting between two base pairs, a process described as intercalation and was first described by Lerman.[25] Usually such association causes elongation of the DNA and local helix unwinding. This local distortion of DNA is commonly spread over several base pairs and induces conformational changes in the adjacent sequences, which result in a pronounced alteration of the DNA structure. Lerman's classical model of DNA intercalation has the following features: (i) the structure and hydrogen bonding of B-form of DNA is retained; (ii) two adjacent base pairs are separated to create a planar vacancy (intercalation site) for intercalation; (iii) a local unwinding of the double helix is required; and (iv) the planar polycyclic moiety of the intercalator is inserted between and parallel to the base pairs to fit into the intercalation site created by extension and local unwinding of the double helix.[25,28] The width of the intercalation site is close to that required to insert an anthracene or acridine ring or any other similar aromatic system. Chart 1.3 shows typical examples of classical intercalators. Creation of an intercalation site causes separation of base pairs with a lengthening of the double helix and a decrease in the helical twist at the intercalation site. In the classical model, the helix is lengthened by 3.4 Å, which is equivalent to the thickness of typical aromatic ring systems. However, in practice, the observed increase in length is generally less than 3.4 Å because of the bending of the helix at the intercalation

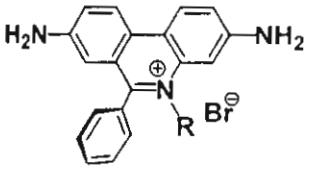

Ethidium bromide (R = C_2H_5, 7)
Propidium bromide (R = $(CH_2)_3\overset{\oplus}{N}MeEt_2$, **8**)

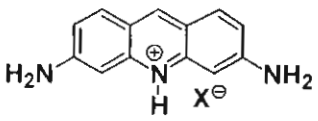

Proflavine (**9**)

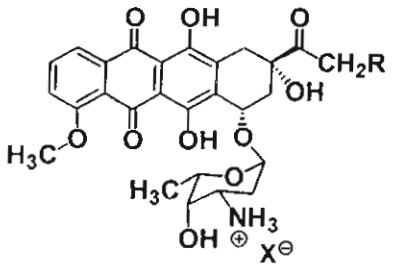

Daunomycin (R = H, **10**)
Adriamycin (R = OH, **11**)

Chart 1.3

site. The helix is unwound at the site of an intercalation complex and the normal approximately 36^0 rotation of one base pair with respect to the next is decreased as a result of intercalation. The amount of unwinding varies considerably with the intercalator structure and DNA sequence. Of the compounds shown in Chart 1.3, ethidium (7) and propidium (**8**) unwind DNA by 26^0, while proflavine (**9**) and related acridines by 17^0. In contrast, significantly decreased unwinding (11^0) was observed with anthracycline drugs, daunomycin (**10**) and adriamycin (**11**).

The intercalation model has been extended to describe the interaction of different classes of molecules with DNA. These include mono-, bis-, poly- and cyclic-intercalators, threading intercalators as well as propeller twisted intercalators.[29-35] Bis-intercalators have two intercalating units connected by a rigid or flexible chain, whereas polyintercalators contain many such systems capable of undergoing intercalation in a polymeric fashion.[36-39] In most of these complexes, the neighbor exclusion principle holds good. According to this

principle, the intercalator can at most bind at alternative possible base pair sites in DNA duplex giving a maximum of one intercalator between every second site.[40] Figure 1.8 schematically represents the intercalation and bis-intercalation processes in DNA duplex. A few examples of bis-intercalators with flexible and rigid linkers based on acridine moiety (**12** and **13**) are given in Chart 1.4.

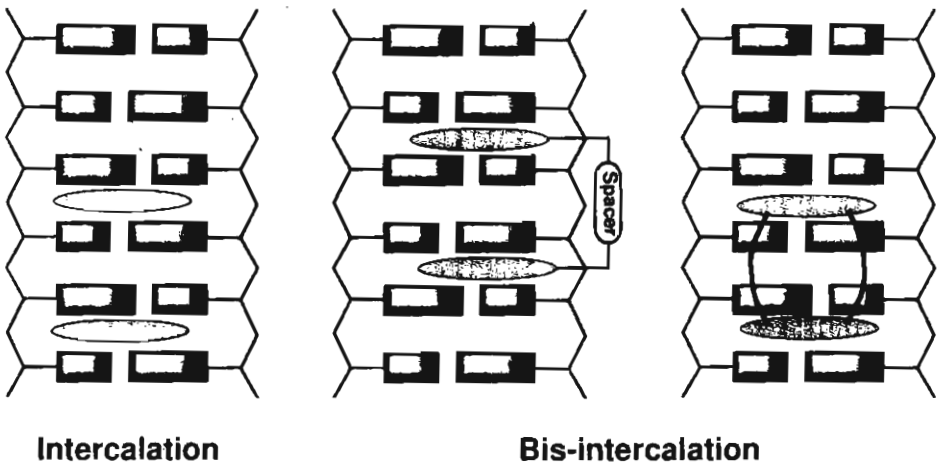

Figure 1.8. Schematic representation of intercalation and bisintercalation of planar molecules between the DNA base pairs.

In the case of the bisacridine derivatives with flexible spacer groups, the alkyl chain length is found to be a deciding factor in the observation of mono- or bis-intercalation.[41] When the spacer length is $n < 4$, the molecule binds to DNA with only one acridine moiety intercalated while in molecules with $n > 6$ bis-intercalation was observed. In the case of **13**, where the two intercalating moieties are connected by a rigid spacer, bis-intercalation with the violation of neighbor exclusion principle due to steric constraints was observed.[41]

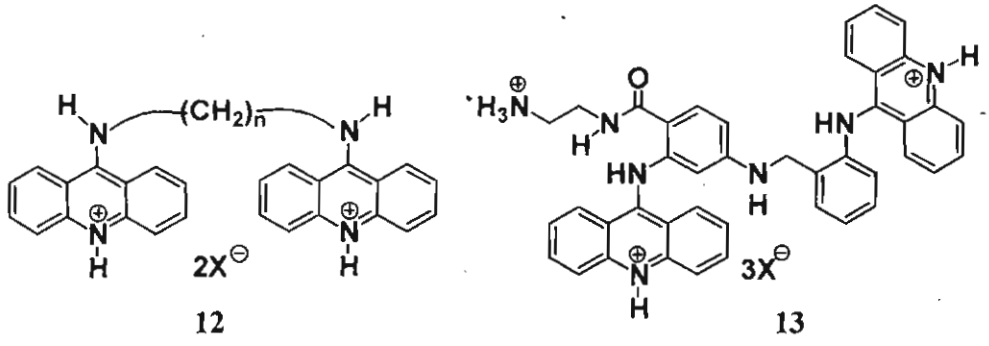

12 **13**

Chart 1.4

The anti-cancer drugs such as ditercalinium (**14**, Chart 1.5) and the quinoxaline antitumor antibiotics, echinomycin (**15**) and triostin A (**16**, Chart 1.6) are known to interact with DNA through bisintercalation.[41c,42] Ditercalinium exhibits partial rigidity because of the linker and binds to DNA with the aromatic rings intercalated at the G-C sites with the linker placed in the major groove.[41c] This molecule is one of the few examples of intercalators with major parts of the molecule lying in the major groove. The aromatic parts of ditercalinium stack well with the base pairs at the intercalation site with the long axes of the aromatic groups roughly parallel to the base pair axes. Very little of the drug protrudes into the minor groove, when viewed from the minor groove making the drug molecule resemble a DNA base pair. The rigidity of the linker causes an approximately 15° bend in the DNA double helix and hence unwinding of DNA occurs as in the case of intercalation complexes. The greater biological activity of this drug has been attributed to its efficiency in inducing kinks in DNA and its resemblance to a base pair from the minor groove side that mimic the structural distortion produced by

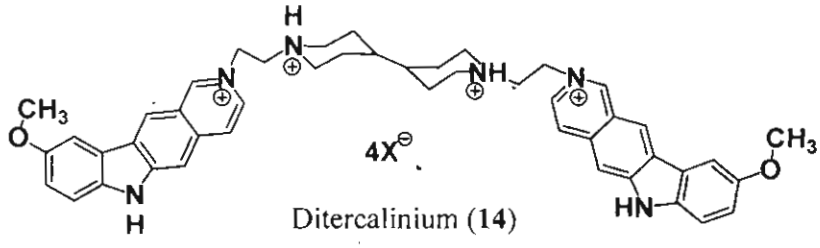

Ditercalinium (**14**)

Chart 1.5

many DNA lesions and could account for the ability of ditercalinium to induce DNA repair.

In the case of echinomycin (**15**) and triostin A (**16**), the cross linked cyclic peptides form a relatively rigid plate with two quinoxaline rings perpendicular to the plate. These rings are parallel to each other on the same side, but at opposite ends of the plate[42] and are oriented in optimum configuration for bis-intercalation. These molecules were found to unwind the duplex by 40-50° and produce a length increase of approximately twice that of the monointercalators.

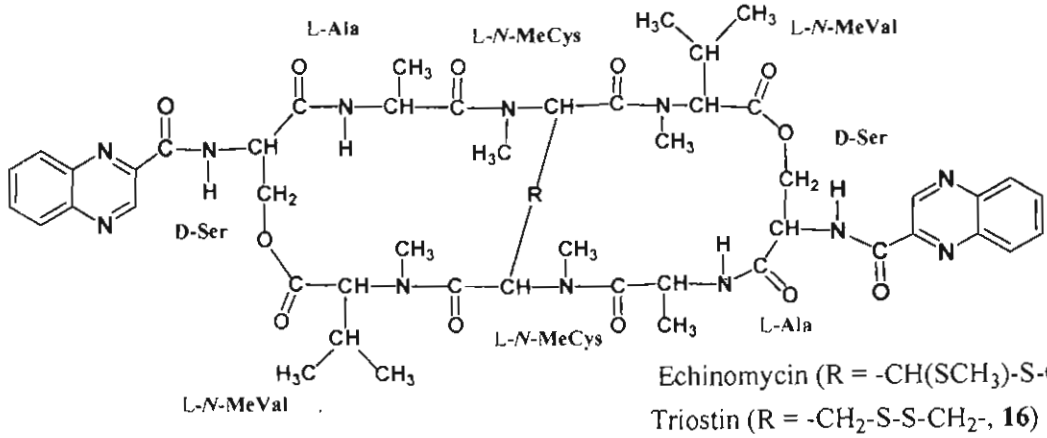

Echinomycin (R = -CH(SCH$_3$)-S-CH$_2$-, **15**)

Triostin (R = -CH$_2$-S-S-CH$_2$-, **16**)

Chart 1.6

Intercalators with substituents on opposite sides of the intercalating aromatic system must thread one of the substituents between the base pairs at the intercalation site during binding. Examples of intercalators of this type are, naphthalene bisimide (**17**), cationic porphyrins (**19**) having a planar cyclic unit with bulky substituents and the antibiotic nogalamycin (**18**) (Chart 1.7). An interesting class of non-classical intercalators is the propeller-twisted intercalators, which possesses the necessary characteristics of a groove binder, but interact with

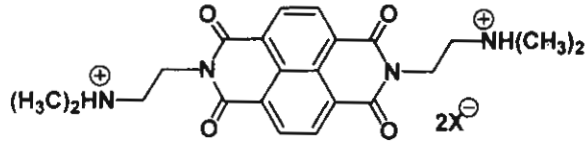

17

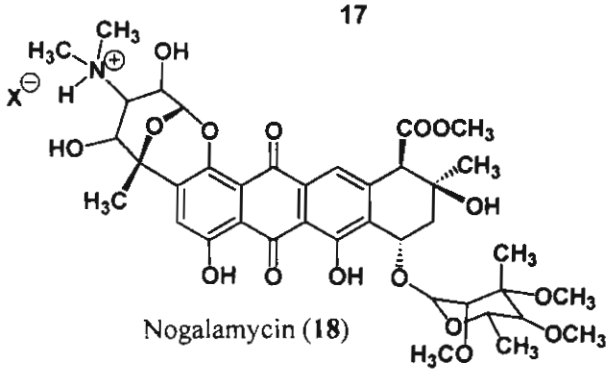

Nogalamycin (**18**)

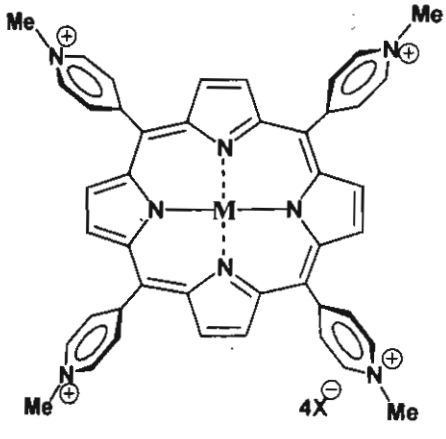

19 (M = 2H, Zn(II), Ni(II) or Cu(II))

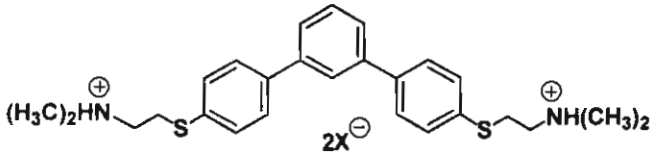

20

Chart 1.7

DNA through intercalation. Although the Watson-Crick model for DNA has planar base pairs, it is now well established that these base pairs can have significant propeller-twist that could reduce π stacking energy with planar

intercalators.[43] However, an unfused aromatic system can match the base pair propeller-twist to create a more optimally stacked complex. A typical example for this type of interaction is shown by the molecule **20** given (Chart 1.7). It was found that this molecule could unwind supercoiled DNA, lengthen linear DNA and show characteristics, which undoubtedly establish it as an efficient intercalator.

1.4. Probes for Double Strand and Single Strand DNA

Nucleic acids, especially ssDNA and dsDNA, are used in numerous molecular biological experiments that involve its quantification and selective staining in vivo and in vitro. As a result various dyes have been developed for the qualitative and quantitative analysis of nucleic acids. Few examples of dyes currently used as probes for ssDNA and dsDNA along with their interactions are described in the following sections.

1.4.1 Cyanine Dyes

Cyanine dyes have recently become important as nucleic acid stains, particularly for dsDNA.[3,44] Cationic cyanine dyes exhibit very large degrees of fluorescence enhancement on binding to nucleic acids. In addition, the covalent linkage of two cyanine dyes to form a bichromophore increases the nucleic acid binding affinity by approximately 2 orders of magnitude.[45] These characteristics of fluorescence enhancement and high binding affinity are crucial for high sensitivity

nucleic acid detection applications. TO-PRO-1 (**21**) and TOTO-1 (**22**) (Chart 1.8) are representative examples of the cyanine dyes.[46,47] Both these dyes bind to ssDNA as well as dsDNA, however, with marginal fluorescence enhancement

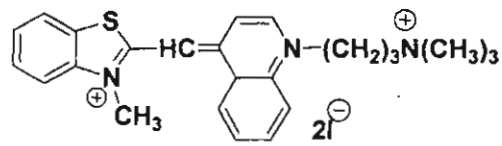

TO-PRO-1 (**21**)

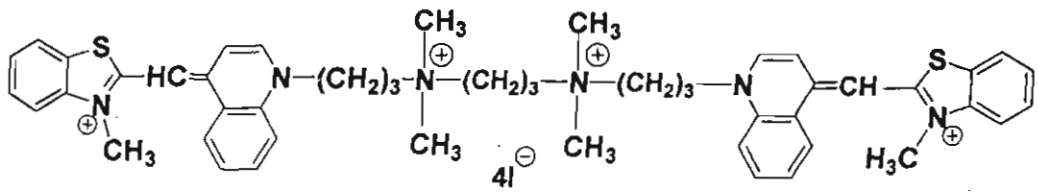

TOTO (**22**)

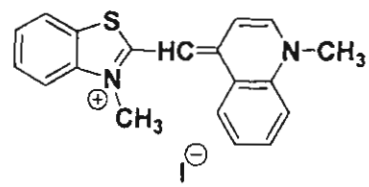

PicoGreen (**23**)

Chart 1.8

with ssDNA. The TOTO-1 dye is capable of undergoing bis-intercalation, although it reportedly interacts with dsDNA and ssDNA with similarly high affinity.[48] NMR studies of interactions of **22** with a double stranded 8-mer indicate that it acts as a bis-intercalator, with the aromatic units intercalating between the bases and the linker region undergoing interactions with the minor groove of DNA (Figure 1.9).[49] Binding of this dye partially unwinds the DNA thereby, distorting

and elongating the helix. However, studies using fluorescence polarization measurements suggest that an external binding mode, where the dipole of the dye molecules is aligned with the DNA grooves is more important for its efficient interaction. The molecule was found to exhibit some sequence selectivity for the site 5'-CTAG-3', although it can bind to almost any sequence in dsDNA. Pico-Green (**23**) is another example of a cyanine dye,[50] where its binding to dsDNA preferentially occurs by intercalation between alternating GC base pairs. Intercalation is also the most important association mode for other base-pair configurations, but in many cases, binding to the exterior of DNA efficiently competes with intercalation. Intercalated Pico-Green molecules in calf thymus

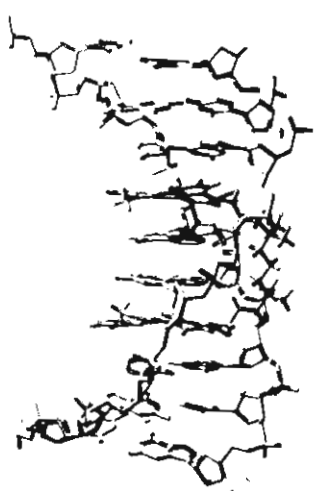

Figure 1.9. NMR solution structure of the TOTO-1 (**22**) dye bound to DNA.[20]

dsDNA are characterized by a monoexponential fluorescence decay, which is independent of the base pairs surrounding the dye.[51] However, it exhibited multiexponential decay in all types of ssDNA indicating that it binds to the calf

thymus ssDNA as a monomer, further, the dominant mode of binding of this dye was found to be intercalation between two different bases, one of them being G or T. These dyes have found important applications as ultra sensitive reagents for solution quantitation and stain of DNA in electrophoresis and blots.[52]

1.4.2 Phenanthridine and Acridine Dyes

Ethidium bromide (**7**), propidium bromide (**8**), hexidium iodide (**24**) dihydroethidium (**25**), ethidium monoazide (**26**), ethidium homodimer-1 (**27**) and ethidium homodimer-2 (**28**) (Chart 1.9) are some of the phenanthridium dyes used as nucleic acid stains. These dyes exhibit ca. 20 to 30 fold enhancement in fluorescence emission when bound to nucleic acids. The mode of binding is intercalation with no sequence specificity. Ethidium bromide currently is the most commonly used general nucleic acid gel stain, while propidium iodide is commonly used as a nuclear or chromosome counterstain and as a stain for dead cells. However, both ethidium bromide and propidium bromide are potent mutagens. Hexidium iodide, on the other hand, is a moderately lipophilic phenanthridium dye that is permeant to mammalian cells. Ethidium homodimers-1 and 2 bind strongly to dsDNA, ssDNA and RNA with significant increase in fluorescence yields.[53] Interestingly, the ethidium homodimer-1 shows high affinity to triplex nucleic acid structures when compared to other DNA structures.[54] One

molecule of it binds per four base pairs in dsDNA without any sequence selectivity. It was originally reported that only one of the two phenanthridium

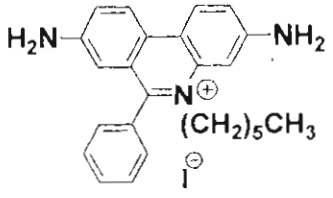

Hexidium iodide (**24**)

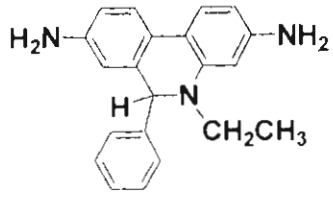

Dihydroethidium (**25**)

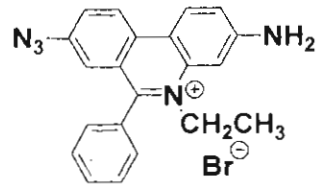

Ethidium monoazide (**26**)

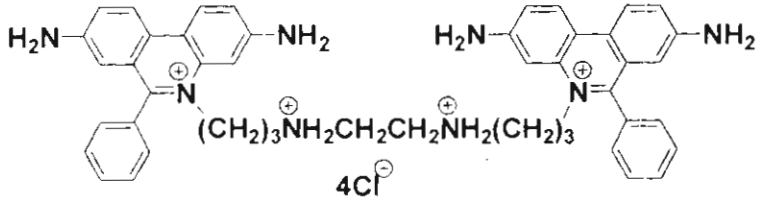

Ethidium homodimer-1 (**27**)

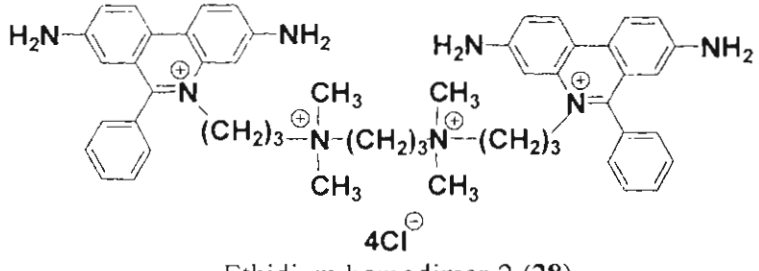

Ethidium homodimer-2 (**28**)

Chart 1.9

rings of ethidium homodimer-1 is bound at a time, however the subsequent reports indicate that bis-intercalation appears to be involved in staining both double strand and triplex DNA. The spectra and other properties of ethidium homodimers are almost identical. However, the DNA affinity of the homodimer-2 is found to be twice than that of the homodimer-1. The ethidium homodimer dyes, **27** and **28**, are impermeant to cells with intact membranes making them useful as dead cell indicator. Dihydroethidium (**25**) is a chemically reduced ethidium derivative and

exhibits blue fluorescence when located in the cytoplasm.[55] Many viable cells oxidize it to ethidium, which then fluoresces red upon DNA intercalation.[56] Ethidium monoazide (**26**), on the other hand, has found application as an efficient photocrosslinking agent. It is used as a fluorescent photoaffinity label that, after photolysis, binds covalently to nucleic acids.[57] The quantum yield for covalent photolabeling by ethidium monoazide was found to be unusually high (>0.4).

Acridine orange (**29**) belongs to the class of acridine dyes that binds with DNA by intercalation and electrostatic interactions[58] and is used as flow cytometric dye. The acridine-homodimer (**30**) is an example of acridine dimer that has extremely high affinity for A.T rich regions of nucleic acids, making it particularly useful for chromosome banding.[59] It emits blue-green fluorescence when bound to DNA, yielding fluorescence that is proportional to the fourth power of the AT base pair content. 9-Amino-6-chloro-2-methoxyacridine (ACMA, **31**) is a DNA intercalator[60] that selectively binds to polyd(A-T) with an association constant of $2 \times 10^5\ M^{-1}$.

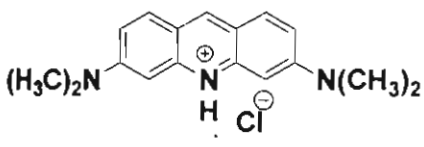

Acridine orange (**29**)

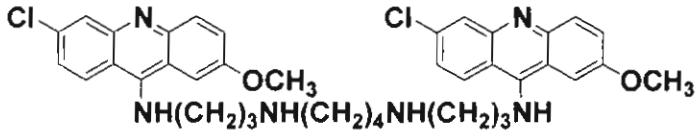

Acridine homodimer (**30**)

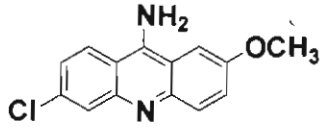

31

Chart 1.10

1.4.3 Indole and Imidazole Dyes

The bisbenzimide dyes-Hoechst 33258 (**32**)[61], Hoechst 33342 (**33**)[62] and Hoechst 34580 (**34**)[63] (Chart 1.11) are minor groove binding DNA stains that fluoresce blue upon binding to DNA. These dyes show a wide spectrum of sequence dependent DNA affinities and bind with polyd(A-T) sequences with high association constants. They also exhibit multiple binding modes and distinct fluorescence emission spectra that are dependent on dye:base pair ratios. Hoechst 33258 is an antibiotic and chromosome stain and binds to AT minor groove sequences of DNA.[64] This molecule has a crescent shape with hydrogen bond

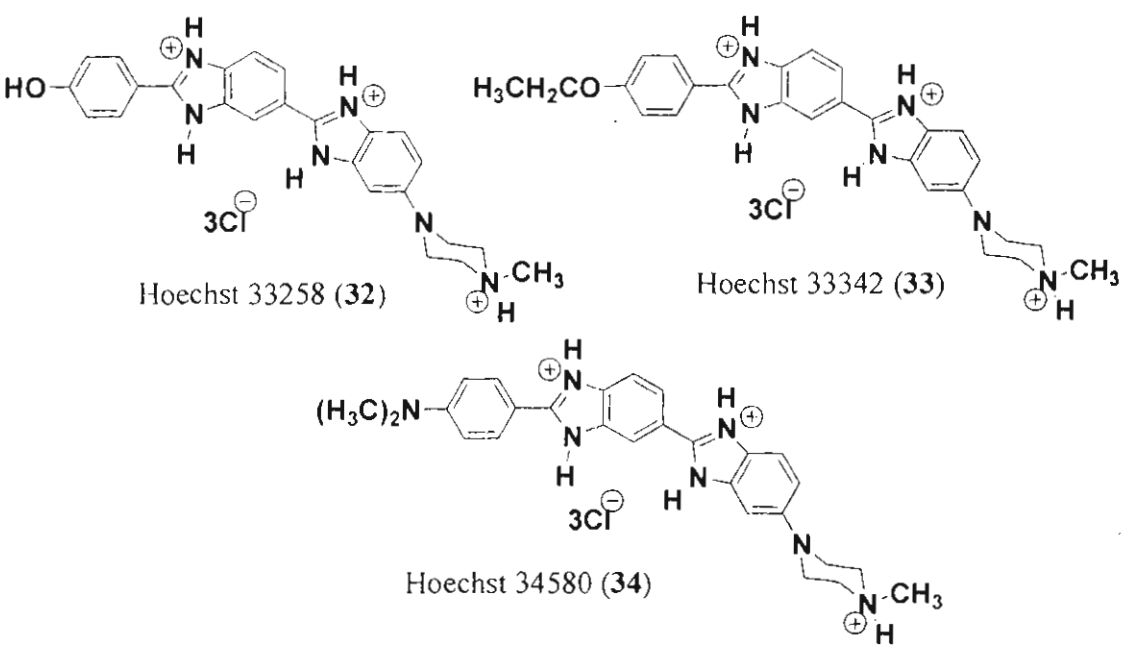

Chart 1.11

donating groups on the inner face. The binding involves both hydrogen bonds from the benzimidazole-NH groups to O-2 of thymine and N-3 of adenine and

electrostatic interaction of the cationic dye with the anionic oligomer. The phenol ring of Hoechst 33258 makes an angle of 8^0 with the benzimidazole ring to which it is attached, while the two benzimidazole ring planes are twisted 32^0 with respect to each other. The piperazine moiety in this case is only slightly puckered and lies almost in the plane of the benzimidazole moiety to which it is attached. The dye maintains van der Waals contact with the walls of the minor groove, thus, placing itself in a favorable position so that its π-electron system can interact with the $O^{4'}$ atoms of deoxyribose in the minor groove.

Similar to the imidazole based Hoechst dyes, the indole based DNA stain, DAPI (**3**) (Chart 1.2), associates with the minor groove of DNA preferentially binding to AT clusters.[65] DAPI is also reported to bind to DNA sequences that contain as few as two consecutive AT base pairs employing a different binding mode. Figure 1.10 shows the X-ray crystal structure of DAPI bound to DNA.[66]

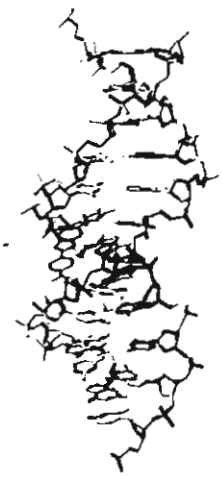

Figure 1.10. X-ray crystal structure of DAPI (**3**) bound to DNA.

Binding of DAPI to dsDNA produces a 20 fold fluorescence enhancement, apparently due to the displacement of water molecules from both DAPI and the minor groove of DNA. In the presence of high salt concentrations, it exhibits negligible interactions with ssDNA and GC pairs.

1.4.4 Other Nucleic Acid Dyes

Hydroxystilbamidine (**35**), a trypanocidal drug is an interesting probe of nucleic acid conformations with high staining properties.[67] It is a non-intercalating dye that exhibits AT-selective binding and favors regions of nucleic acids that have secondary structure. Methylene blue (**36**), a phenothiazine dye, is another well known nucleic acid stain which interacts with DNA through intercalation. Azure B (**37**), toluidine blue O (**38**) and thionin (**39**) are other methylene blue homologues (Chart 1.12) widely used as biological stains.[68] These dyes undergo intercalative interactions with DNA along with the formation of H-bonds between the exocyclic amines and the sugar phosphates of the DNA conferring extra stability to the complex.[69] Nile blue (**40**), is a cationic phenoxazine dye, which binds with DNA through intercalation and exhibits quenching in fluorescence in the presence of DNA.[70]

Small molecular mimics of DNA-binding proteins have been shown to be useful as synthetic nucleases, inhibitors of protein interactions and transcriptional

activators.[71] Recent studies have indicated that thiazole orange-peptide bioconjugates can act as synthetic nucleases.[72] The functionality responsible for

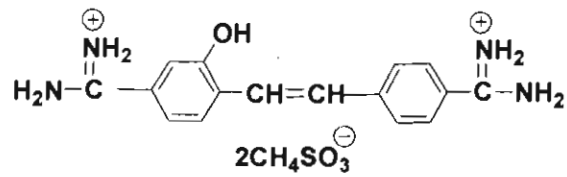

Hydroxystilbamidine (**35**)

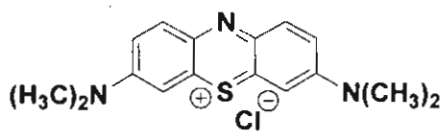

Methylene blue (**36**)

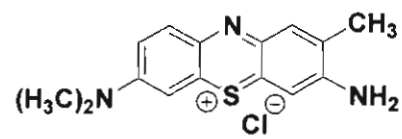

Azure B (**37**)

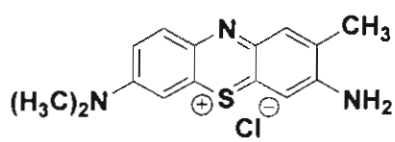

Toluidine blue O (**38**)

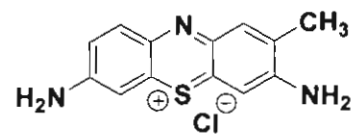

Thionin (**39**)

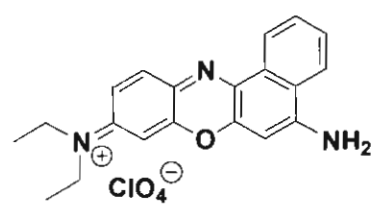

Nile blue (**40**)

Chart 1.12

nucleic acid targeting in such systems is derived from a segment of a DNA-binding protein comprising the protein-DNA interface. The drawback of such systems is that they alone bind with DNA, but with low affinity. This is because many of the protein-DNA contacts of such short peptides will be different from those of the native protein from which it is obtained. Therefore, many of the electrostatic interactions between backbone phosphate groups and positively

charged side chains of the proteins otherwise located in nearby regions of the native-protein are lost. To act as molecular probes for a particular DNA sequence and structure, these peptide-dye bioconjugates need to be highly sequence-specific due to the low ratio of specific to nonspecific sites in genomic DNA and bind with sufficiently high affinity.

Oxazole yellow-peptide bioconjugate (**41**) (Chart 1.13), is an example of a peptide-bioconjugate that has the molecular recognition features of the polypeptide from a DNA-binding protein and the dsDNA-dependent fluorescence of an intercalating dye. This bioconjugate exhibits DNA recognition and binding affinity comparable to the native Hin recombinase protein.[72] Fluorescence studies have shown that this probe is useful to determine the presence of a given DNA target sequence since negligible fluorescence emission was observed in the absence of a given target site. Another example is 7-actinomycin D (**42**) which is a fluorescent intercalator that undergoes spectral shift upon association with DNA. It binds selectively to GC regions of DNA and this property has been exploited for chromosome banding studies.[73]

Examples of reagents for selective detection of ssDNA are very few in literature. OliGreen is a ssDNA quantitation reagent patented by the Molecular Probes. This reagent exhibits significant base selectivity showing a large fluorescence enhancement when bound to poly(dT) sequence while relatively negligible fluorescence enhancement was observed with poly(dG), poly(dA) and

poly(dC).[67] The unsymmetrical cyanine dye thiazole orange homodimer (TOTO) (Chart 1.8) also binds to both ssDNA and dsDNA to form stable fluorescent complexes. However, at ionic strengths greater than 50 mM of Na^+ or Mg^{2+}, the dye-dsDNA complex found to undergo dissociation as compared to the dye-ssDNA complex indicating thereby its potential as a probe for ssDNA at high ionic strengths.[48b]

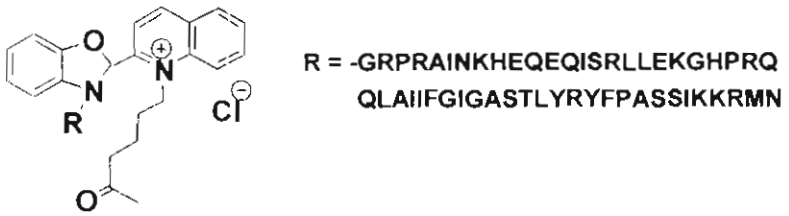

Oxazole Yellow-HIN (**41**)

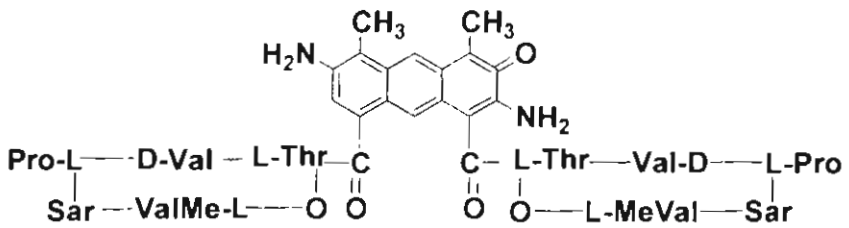

7-Actinomycin D (**42**)

Chart 1.13

1.5. *Objectives of the Present Investigation*

Development of organic molecules that exhibit selective interactions with different nucleic acid structures has immense significance in biochemical and medicinal applications. In this context, our interest has been to design novel fluorescent molecules that bind with DNA through non-covalent interactions and

can act as effective probes for nucleic acids. Our main objective has been to investigate the influence of steric effects on ligand-DNA binding through intercalative interactions and thus develop fluorescent probes for efficient discrimination between various nucleic acid structures, namely single strand (ssDNA) and double strand DNA (dsDNA). Another objective was to develop efficient DNA oxidizing agents through electron transfer mechanism so that they can be used as DNA cleaving agents that functions through electron transfer mechanism.

In this context, we were interested in the DNA binding interactions of substituted acridinium and bisacridinium derivatives which can, in principle, undergo mono-intercalative and bis-intercalative interactions with DNA. Our strategy involves the design of molecules in which the 9^{th}-position of the acridinium fluorophore is systematically varied with sterically hindered substituents and investigate the role of steric factors in controlling their intercalative interactions. The interactions of these derivatives with dsDNA, ssDNA and various oligonucleotides have been investigated through photophysical, chiroptical and microscopic techniques. Our results indicate that the steric factors had a significant effect in the intercalative properties of these derivatives. Subtle changes in the substitution pattern resulted in changing the binding preferences of the acridinium moiety making it selective for ssDNA as compared to the dsDNA. Furthermore, we observed that spacer length and ion

strength control the mono- and/or bis-intercalative interactions of the bisacridinium derivatives. As characterized by theoretical calculations and laser flash photolysis studies, these molecules depending on the substitution, were found to oxidize ssDNA or dsDNA, thereby indicating their potential use as efficient DNA photo-oxidizing agents.

1.6. References

1. (a) Dervan, P. B. *Science* **1986**, *232*, 464-471. (b) In *Molecular aspects of anticancer drug-DNA interactions*; Neidle, S. N, Waring, M. J., Eds.; The Macmillan Press, Ltd, 1993, Vol. 2. (c) Waring, M. J. *Annu. Rev. Biochem.* **1981**, *50*, 159-192. (d) Tomasz, M. In *Molecular Aspects of Anticancer-Drug Interactions*; Neidle, S., Waring, M. J., Eds.; Macmillan Press: Boca Raton, FL, 1994, Vol. 2, pp 312-349. (e) Tidd, D. M. In *Molecular Aspects of Anticancer Drug-DNA Interactions*; Neidle, S., Waring, M. J., Eds.; CRC: Boca Raton, FL, 1993, Vol. 1, pp 272-300.

2. (a) Harrison, S. C.; Saeur, R. T. *Curr. Opinion Struc. Biol.*, **1994**, *4*, 1-66. (b) Philips, S. E. V.; Moras, D. *Curr. Opinion Struc. Biol.*, **1992**, *2*, 69-149. (c) Churchill, M. E. A.; Travers, A. A. *Trends Biochem. Sci.*, **1991**, *16*, 92-97.

3. (a) Rye, H. S.; Yue, S.; Wemmer, D. E.; Quesada, M. A.; Haugland, R. P.; Mathies, R. A.; Glazer, A. N. *Nucleic Acids Res.*, **1992**, *20*, 2803-2812. (b) Glazer, A. N.; Rye, H. S. *Nature*, **1992**, *359*, 859-861. (c) Rye, H. S.;

Quesada, M. A.; Peck, K.; Mathies, R. A.; Glazer, A. N. *Nucleic Acids Res.*, **1991**, *19*, 327-333. (d) Figeys, D.; Arriaga, E.; Renborg, A.; Dovichi, N. J. *J. Chromagr. A.*, **1994**, *669*, 205-216.

4. (a) Rogers, K. R.; Apostol, A.; Madsen, S. J.; Spencer, C. W. *Anal. Chem.* **1999**, *71*, 4423-4426. (b) Elmendorff-Dreikorn, K.; Chauvin, C.; Slor, H.; Kutzner, J.; Batel, R.; Muller, W. E.; Scroder, H. C. *Cell. Mol. Biol.*, 1999, *45*, 211-218. (c) Cosa, G.; Focsaneanu, K. –S.; McLean, J. R. N.; Scaiano, J. C. *Chem. Comm.*, **2000**, 689-690. (d) Cosa, G.; Vinette, A. L.; McLean, J. R. N.; Scaiano, J. C. *Anal. Chem.*, **2002**, *74*, 6163-6169.

5. (a) Ishiguro, T.; Saitoh, J.; Yawata, H.; Yamagishi, H.; Iwasaki, S.; Mitoma, Y. *Anal. Biochem.* **1995**, *229*, 207-213. (b) Rajeevan, M. S.; Ranamukhaarachchi, D. G.; Vernon, S. D.; Unger, E. R. *Methods,* **2001**, *25,* 443-451.

6. Privat, E.; Melvin, T.; Merola, F.; Schweizer, G.; Prodhomme, S.; Asseline, U.; Vigny, P. *Photochem. Photobiol.,* **2002**, *75* , 201-210.

7. (a) Chee, M.; Yang, R.; Hubbell, E.; Berno, A.; Huang, X. C.; Stern, D.; Winkler, J.; Lockhart, D. J.; Morris, M. S.; Fodor, S. P. *Science* **1996**, *274*, 610-614. (b) Jaccoud, D.; Peng, K.; Feinstein, D.; Kilian, A. *Nucleic Acids Res.* **2001**, *29*, e25.

8. Bloomfield, V. A.; Crothers, D. M.; Tinoco, I. In *Physical chemistry of nucleic acids;* Harper and Row: NewYork, 1974.

9. (a) Butterfield, S. M.; Cooper, W. J.; Waters, M. L. *J. Am. Chem. Soc.* **2004**, *216*, 475-485. (b) Classen, S.; Ruggles, J. A.; Schultz, S. C. *J. Mol. Biol.* **2001**, *314*, 1113-1125. (c) Mitton-Fry, R.; Anderson, E. M.; Hughes, T. R.; Lunblad, V.; Wuttke, D. S. *Biochemistry* **2003**, *42*, 3751-3758.

10. Bocharey, A.; Pfuetzner, R. A.; Edwards, A. M.; Frappier, L. *Nature,* **1997**, *385,* 176-181.

1. Kloks, C. P. A. M.; Sponk, C. A. E. M.; Lasonder, E.; Hoffman, A.; Vuister, G. W.; Grzesiek, S.; Hilbers, C. W. *J. Mol.Biol.* **2002**, *16,* 317-326.

2. Record, M. T., Jr.; Lohman, T. M.; deHaseth, P. *J. Mol. Biol.* **1976**, *107*, 145-158.

3. (a) Watson, J. D.; Hopkins, N. H.; Roberts, J. W.; Steitz, J. A.; Weiner, A. M. *Molecular biology of the gene*; 4th Ed.; Benzammin / Cumings: Menlo Park, CA, 1987. (b) Crick, F. H. C. *Nature*, **1970**, *227*, 561-563. (c) Lehninger, A. L. In *Principles of Biochemistry*; CBS Publishers and Distribution: New Delhi, 1984. (d) Saenger, W. In *Principles of Nucleic Acid Structure*; Springer Verlag: New York, 1984.

4. Booth, C.; Griffith, E.; Brady, G.; Lydall, D. *Nucleic Acids Res.* **2001**, *29*, 4414-4422.

5. (a) Buhot, A.; Halperin, A. *Phys. Rev. E.* **2004**, *70*, 020902(R). (b) Buhot, A.; Halperin, A. *Macromolecules* **2002**, *35*, 3238-3242.

16. Ansari, A.; Kuznetsov, S. V.; Shen, Y. *Proc. Natl. Acad. Sci. USA* **2001**, *98*, 7771-7774.

17. Goddard, N. L.; Bonnet, G.; Krichevsky, O.; Libchaber, A. *Phys. Rev. Leti.* **2000**, *85*, 2400-2403

18. Smith, S. B.; Cui, Y.; Bustamante, C. *Science* **2004**, *271*, 795-796.

19. (a) Dickerson, R. E.; Drew, H. R. *J. Mol. Biol.* **1981**, *152*, 723-736. (b) Dickerson, R. E. *J. Mol. Biol.* **1983**, *166*, 419-441. (c) In *Nucleic acids in chemistry and biology*; Blackburn, G. M.; Gait, M. J. Eds.; Oxford University Press: Oxford, 1996, 2nd Edition, Friedman, R. A. G.; Manning, G. S. *Biopolymers* **1984**, *23*, 2671-2714.

20. Schweitzer, C.; Scaiano, J. C. *Phys. Chem. Chem. Phys.* **2003**, *5*, 4911-4917.

21. Friedman, R. A. G.; Manning, G. S. *Biopolymers* **1984**, *23*, 2671-2714.

22. Record, M. T.; Lohman, T. M.; deHaseth, P. *J. Mol. Biol.*, **1976**, *105*, 145-158.

23. Pelton, J. S.; Wemmer, D. E. *J. Am. Chem. Soc.* **1990**, *112*, 1393-1399.

24. Kopka, M. L.; Yoon, C.; Goodsell, D.; Pjura, P.; Dickerson, R. E. *Proc. Nat. Acad. Sci. USA*, **1985**, *82*, 1376-1380.

25. Wang, A. H. –J. *Curr. Opinion Struc. Biol.*, **1992**, *2*, 361-368.

26. Jenkins, T. C.; Lane, A. N.; Neidle, S.; Brown, D. G. *Eur. J. Biochem.* **1993**, *213*, 1175-1184.

27. Lavery, R.; Zakrzrewska, K.; Pullman, B. *J. Biomol. Str. Dyn.* **1986**, *3*, 1155-1170.

28. Address, K. J.; Gilbert, D. E.; Olsen, R. K.; Feigon, J. *Biochemistry* **1992**, *31*, 339-350.

29. (a) Waring, M. *J. Mol. Biol.* **1970**, *54*, 247-279. (b) Wilson, W. D. In *DNA and Aspects of Molecular Biology*; Kool, E. T., Ed.; Series on *Comprehensive Natural Products Chemistry*; Barton, D, Nakanishi, K., Eds.; 1999, Vol. 7, Chapter 8. (c) Lerman, L. S. *J. Mol. Biol.* **1961**, *3*, 18-30. (d) Pindur, U.; Haber, M.; Sattler, K. *J. Chem. Ed.* **1993**, *70*, 263-272.

30. Assa-Munt, N.; Denny, W. A.; Leupin, W.; Kearns, D. R. *Biochemistry* **1985**, *24*, 1441-1449.

31. Atwell, G. J.; Stewart, G. M.; Leupin, W.; Denny, W. A. *J. Am. Chem. Soc.* **1985**, *107*, 4335-4337.

32. Chaires, J. B.; Fox, K. R.; Herrera, J. E.; Britt, M.; Waring, M. J. *Biochemistry* **1987**, *26*, 8227-8236.

33. Egli, M.; Williams, L. D.; Frederick, C. A.; Rich , A. *Biochemistry* **1991**, *30*, 1364-1372.

34. Wakelin, L. P. G. *Med. Res. Rev.* **1986**, *6*, 275-340.

35. Wilson, W. D.; Krishnamoorthy, C. R.; Wang, Y. –H.; Smith, J. C. *Bioploymers* **1985**, *24*, 1941-1961.

36. Marzilli, L. G.; Banville, D. L.; Zon, G.; Wilson, W. D. *J. Am. Chem. Soc.* **1986**, *108*, 4188-4192.

37. Strekowski, L.; Wilson, W. D.; Mokrosz, J. L.; Strekowska, A.; Koziol, A. E.; Palenik, G. J. *Anti-Cancer Drug Design* **1988**, *2*, 387-398.

38. Tanious, F. A.; Yen, S. –F.; Wilson, W. D. *Biochemistry* **1991**, *30*, 1813-1819.

39. Wilson, W. D.; Tanious, F. A.; Barton, H. J.; Jones, R. L.; Fox, K.; Wydra, R. L.; Strkowski, L. *Biochemistry* **1990**, *29*, 8452-8461

40. Pelton, J. S.; Wemmer, D. E. *J. Am. Chem. Soc.* **1990**, *112*, 1393-1399.

41. (a) Assa-Munt, N.; Denny, W. A.; Leupin, W.; Kearns, D. R. *Biochemistry* **1985**, *24*, 1441-1449. (b) Atwell, G. J.; Stewart, G. M.; Leupin, W.; Denny, W. A. *J. Am. Chem. Soc.* **1985**, *107*, 4335-4337. (c) Gao, Q.; Williams, L. D.; Egli, M.; Rabinovich, D.; Chen, S. –L.; Quigley, G. J.; Rich, A. *Proc. Natl. Acad. Sci. USA* **1991**, *88*, 2422-2426.

42. Wang, A. H. –J.; Ughetto, G.; Qiigley, G. J.; Hakoshima, T.; van der Marcel, G. A.; van Boom, J. H.; Rich, A. *Science* **1984**, *225*, 1115-1121.

43. (a) Neidle, S. In *DNA Structure and Recognition*; Rickwood, D., Male, D., Eds.; Oxford University Press: New York, 1994. (b) Yanagi, K.; Prive, G. G.; Dickerson, R. E. *J. Mol. Biol.* **1991**, *217*, 201-214.

44. Cosa, G.; Focsaneanu, K. -S.; McLean, J. R. N.; McNamee, J. P.; Scaiano, J. C. *Photochem. Photobiol.* **2001**, *73*, 585-599.

45. Rye, H. S.; Yue, S.; Wemmer, D. E.; Quesada, M. A.; Haugland, R. P.; Mathies, R. A.; Glazer, A. N. *Nucleic Acids Res.* **1992**, *20*, 2803-2812.

46. (a) Larsson, A.; Carlsson, C.; Jonsson, M.; Albinsson, B. *J. Am. Chem. Soc.* **1994**, *116*, 8459-8465. (b) Carlsson, C.; Larsson, A.; Jonsson, M.; Albinsson, B.; Norden, B. *J. Phys. Chem.* **1994**, *98*, 10313-10321.

47. Rye, H. S.; Quesada, M. A.; Peck, K.; Mathies, R. A.; Glazer, A. N. *Nucleic Acids Res.* **1991**, *19*, 327-333.

48. (a) Carisson, C.; Johnson, M.; Åkerman, B. *Nucleic Acids Res.* **1995**, *23*, 2413-2420. (b) Rye, H. S.; Glazer, A. N. *Nucleic Acids Res.* **1995**, *23*, 1215-1222.

49. (a) Spielmann, H. P.; Wemmer, D. E.; Jacobsen, J. P. *Biochemistry* **1995**, *34*, 8542-8553. (b) Spielmann. H. P. *Biochemistry* **1998**, *37*, 16863-16876.

50. Singer, V. L.; Jones, L. J.; Yue, S. T.; Haugland, R. P. *Anal. Biochem.* **1997**, *249*, 228-238.

51. Berman, H. M.; Westbrook, J.; Feng, Z.; Gilliland, G.; Bhat, T. N.; Weissig, H.; Shindyalov, I. N.; Bourne, P. E. *Nucleic Acids Res.* **2000**, *28*, 235-242.

52. Romppanen, E. L. ; Savolainen, K. ; Mononen, I. *Anal. Biochem.* **2000**, *279*, 111-114.

53. Gaugain, B.; Barbet, J.; Capelle. N.; Roques, B. P.; Le Pecq, J. B.; Bret, M. L. *Biochemistry* **1978**, 17, 5078-5088.

54. Tuite, E. ; Norden, B. *Bioorg. Med. Chem.* **1995**, *3*, 701-711.

55. Perticarari, S.; Presani, G.; Banfi, E. *J. Immunol. Met.* **1994**, *170*, 117-124.

56. Bucana, C.; Saiaki, I.; Nayar, R. *J. Histochem. Cytochem.* **1986**, *34*, 1109-1115.

57. (a) McMurray, C. T.; Small, E. W.; van Holde, K. E. *Biochemistry* **1991**, *30*, 5644-5652.

58. Delic, J.; Coppey, J.; Magdelenat, H.; Copey-Moisan, M. *Exp. Cell. Res.* **1991**, *194*, 147-153.

59. (a) Capelle, N.; Barbet, J.; Dessen, P.; Blanquet, S.; Roques, B. P.; Le Pecq, J. B. *Biochemistry* **1979**, *18*, 3354-3362. (b) Le Pecq, J. B.; Le Bret, M.; Barbet, J.; Roques, B. *Proc. Natl. Acad. Sci. USA* **1975**, *72*, 2915.

60. Markovits, J.; Garbay-Jaureguebeberri, C.; Roques, B. P.; Le Pecq, J. B. *Eur. J. Biochem.* **1989**, *180*, 359-366.

61. Loonteins, F. G.; Regenfuss, P.; Zechel, A.; Dumortier, L.; Cleg, R. M. *Biochemistry* **1990**, *29*, 9029-9039.

62. Görner, H. *Photochem. Photobiol.* **2001**, *73*, 339-348.

63. Shapiro, H. M.; Perlmutter, N. G. *Cytometry* **2001**, *44*, 133-136.

64. (a) Searle, M. S.; Embrey, K. J. *Nucleic Acids Res.* **1990**, *18*, 3753-3762. (b) Teng, M. –K.; Wahnert, U. *Nucleic Acids Res.* **1988**, *16*, 2670-2690.

65. (a) Kubista, M.; Åkerman, B.; Norden, B. *Biochemistry* **1987**, *26*, 4545-4553. (b) Wilson, W. D.; Tanious, F. A.; Barton, H. J.; Jones, R. L.; Fox, K.; Wydra, R. L.; Strekowski, L. *Biochemistry* **1990**, *29*, 8452-8461.

66. Berman, H. M.; Westbrook, J.; Feng, Z.; Gilliland, G.; Bhat, T. N.; Weissig, H.; Shindyalov, I. N.; Bourne, P. E. *Nucleic Acids Res.* **2000**, *28*, 235-242.

67. Haugland, R. P. In *Handbook of fluorescent probes and research products*; Gregory, J., Ed.; 2002.

68. Kelly, J. M.; Tuite, E. *Biopolymers* **2004**, *35*, 419-433.

69. Chen, Q.; Li, D.; Zhao,Y.; Yang, H.; Zhu, Q.; Xu, J. *Analyst* **1999**, *124*, 901-906.

70. (a) Sluka, J. P.; Horvath, S. J.; Bruist, M. F.; Simon, M. I.; Dervan, P. B. *Science* **1987**, *238*, 1129-1132. (b) Gearhart, M.; Dickinson, L.; Ehley, J.; Melander, C.; Dervan, P. B.; Wright, P.; Gottesfeld, J. *Biochemistry* **2005**, *44*, 4196-4203.

71. Thompson, M.; Woodbury, N. W. *Biochemistry* **2000**, *39*, 4327-4338.

72. Thompson, M. *Bioconjugate Chem.* **2006**, *17*, 507-513.

73. (a) Chiao, Y. C.; Rao, K. G.; Hook, J. W.; Krugh, T. R.; Sengupta, S. K. *Biopolymers* **1979**, *18*, 1749-1762. (b) Loborg, H.; Lindén, E.; Lönn, A.; Skoglund, P.; Rundquist, I. *Cytometry* **1995**, *20*, 296-306.

Chapter 2

SYNTHESIS OF SUBSTITUTED ARYLACRIDINIUM DERIVATIVES AND STUDY OF THEIR INTERACTIONS WITH SINGLE STRAND AND DOUBLE STRAND DNA

2.1. Abstract

A few novel acridinium derivatives **1-8**, wherein steric factors have been varied systematically through substitution at the 9th position of the acridinium ring, were synthesized and their interactions with single strand and double strand DNA have been investigated through photophysical, biophysical and microscopic techniques. These compounds were synthesized in good yields by the quarternization of the corresponding acridines with iodomethane. All the derivatives exhibited characteristic absorption of the acridinium chromophore that extends upto 470 nm. The acridinium derivatives **1, 2** and **6** exhibited quantitative fluorescence yields ($\Phi_f \cong 1$) and long lifetimes of 35, 34 and 25 ns respectively, while significantly lower fluorescence yields ($\Phi_f \leq 0.13$) and lifetimes (< 4 ns) were observed for **3-5** and **7-8**. DNA binding studies indicated that the derivatives **1-5** exhibited significant interactions with double strand DNA (dsDNA) with association constants (K_{dsDNA}) in the range 10^4-10^5 M^{-1}, while the derivatives **6-8** having *ortho* substituents on the phenyl moiety at the 9th position of the acridinium

ring showed negligible interactions with dsDNA. However, the derivatives **6** and 7 showed selective interactions with single strand DNA (ssDNA) with association constants of K_{ssDNA} = 6.3-6.6 × 10^4 M^{-1}, while, the derivative **8** exhibited negligible interactions with both ssDNA and dsDNA. The results reveal the importance of steric factors in determining the efficiency of DNA binding of various ligands. These derivatives with high water solubility and the ability to distinguish between ssDNA and dsDNA can be used as fluorescent probes for understanding the role of ssDNA in various biological processes and to study various DNA-ligand interactions.

2.2. Introduction

DNA-Ligand interactions have been the subject of intense investigations for the past several years. Studies in this aspect has helped in understanding various factors that govern the binding mode of ligands with DNA, which in turn has provided critical insight into the design of drugs targeted to DNA and in the development of probes for nucleic acids.[1-2] Development of strategies to control the DNA binding modes of ligands has enormous potential in the area of DNA recognition. Small molecules which can undergo sequence selective interactions with DNA and can recognize specifically, different DNA structures such as the double strand DNA, single strand DNA, abasic sites, base bulges and G-quadruplex and different DNA polymorphs such as the A, B and Z DNA has wide applications in medical and biological research.[3-6]

Different strategies have been reported in the literature, where the ligand structure has been tailored to bring about the required selectivity in the DNA-ligand binding interactions. One such strategy involves the design of chiral ligands, where one enantiomer can selectively bind to left or right handed DNA duplex structures by intercalation, whereas the other enantiomer can bind to the DNA grooves or remain free in solution.[7-8] Design of dye-peptide conjugates forms another strategy wherein a peptide chain is linked to a DNA intercalator to modify its DNA binding properties. An example is the thiazole orange-peptide conjugate, in which, the peptide unit is linked to the thiazole orange through its endocyclic nitrogens.[9] The peptide chain when linked through the benzothiazole nitrogen of the thiazole orange inhibits intercalation of the thiazole orange, while the linkage through the quinoline nitrogen results in vastly different photophysical and DNA binding properties of the conjugate.

Selective recognition of either single strand DNA (ssDNA) or double strand DNA (dsDNA) by small molecules is a challenging task because most of the reported molecules can interact with both dsDNA and ssDNA through similar mode of binding. Comparing the structures of the ssDNA and dsDNA, the nucleobases in the dsDNA are situated well inside the double helix while those of the ssDNA are more exposed to the external media.[10] Hence, the extent of binding of ligands with different substitutions to ssDNA and dsDNA will be different. It was of our interest to understand the influence of steric and conformational factors

on the extent of binding of the acridinium derivatives to dsDNA and ssDNA.[11] We chose acridines since they were the first chromophore to be extensively studied for its non-covalent DNA interactions and these studies had led to the concept of intercalation.[12] However, the study of the steric and conformational effects on the DNA binding properties of the acridine chromophore has received less attention.[13] In this context, we have designed a series of acridinium derivatives **1-8** (Chart 2.1),

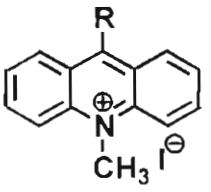

1-8

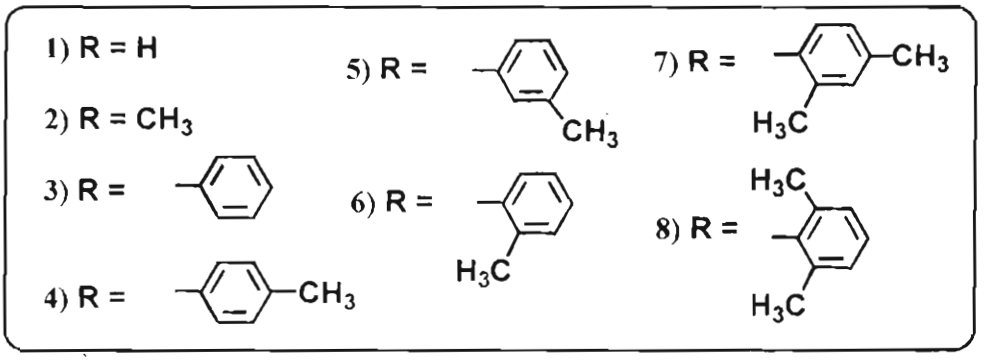

Chart 2.1

wherein we have systematically varied the steric factors through substitution at the 9 position of the acridinium ring to assess the energetics and nature of their DNA binding interactions. The results of these investigations indicate that the substituent group at the 9th position of the acridinium ring has a strong influence and controls the photophysical and DNA binding properties of these simple and potential probes for nucleic acids.

2.3. Results and Discussion

2.3.1. Synthesis

The acridine derivatives were synthesized by a modified Bernthsen procedure as shown in Scheme 2.1. The condensation reaction of diphenylamine with the corresponding carboxylic acid in the presence of anhydrous $ZnCl_2$ yielded the acridine derivatives in 50-60% yields. [27] The quarternization of these acridine derivatives with methyl iodide gave the corresponding acridinium derivatives (**1-8**) in quantitative yields. All these compounds were characterized on the basis of spectral data and analytical results.

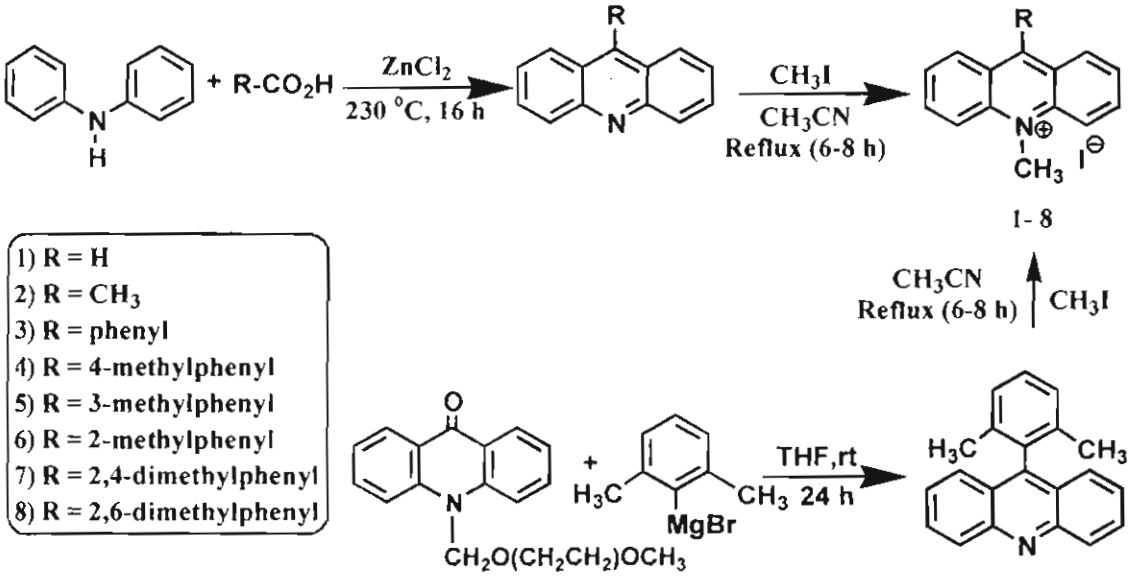

Scheme 2.1

For example, the ^{1}H NMR spectrum of the *ortho*-tolylacridinium derivative **6** showed a peak at δ 1.87 corresponding to the CH_3 protons of the tolyl group, whereas the $N^{\oplus}$-CH_3 protons appeared as a singlet at δ 4.97. The ^{13}C NMR

spectrum of **6**, showed thirteen signals in the aromatic region (seven for the acridinium ring and six for the aryl group), whereas the peaks corresponding to the $-CH_3$ of the tolyl group and $N^{\oplus}-CH_3$ carbons appeared at δ 19.75 and 39.45, respectively. The ^1H NMR spectrum of 2,6-dimethylphenyl acridinium derivative **8** on the other hand showed a peak at δ 1.71 corresponding to the two $-CH_3$ protons. As in the case of the derivative **6**, the $N^{\oplus}-CH_3$ protons appeared as a singlet at δ 4.95. The ^{13}C NMR spectrum of **8**, showed thirteen signals in the aromatic region (seven for the acridinium ring and six for the aryl group), whereas the peaks corresponding to the two $-CH_3$ substituents and $N^{\oplus}-CH_3$ carbons appeared at δ 19.75 and 39.39, respectively. Similarly, all compounds exhibited characteristic $N^{\oplus}-CH_3$ signals in the ^1H and ^{13}C NMR spectra with small shifts in their peaks.

2.3.2. Absorption Properties

Figure 2.1 shows the absorption spectra of the representative acridinium derivatives in aqueous medium. The absorption maxima and the molar extinction coefficients of all these acridinium derivatives are summarized in Table 2.1. All the derivatives exhibited characteristic acridinium moiety absorption that extends upto 470 nm and obeyed the Beer-Lambert's law under our experimental conditions. All the derivatives showed absorption maxima in the range 358-361 nm and at 425 nm. While the molar extinction coefficients of the derivatives at

358-361 nm are in the order of 1.5-2 × 10^4 $M^{-1}cm^{-1}$, the molar extinction coefficients of the substituted arylacridinium derivatives at 425 nm are in the range 5-7 × 10^3 $M^{-1}cm^{-1}$. The unsubstituted and the methyl substituted derivatives exhibited relatively low molar extinction coefficients of the order 3.5-3.6 × 10^3 $M^{-1}cm^{-1}$.

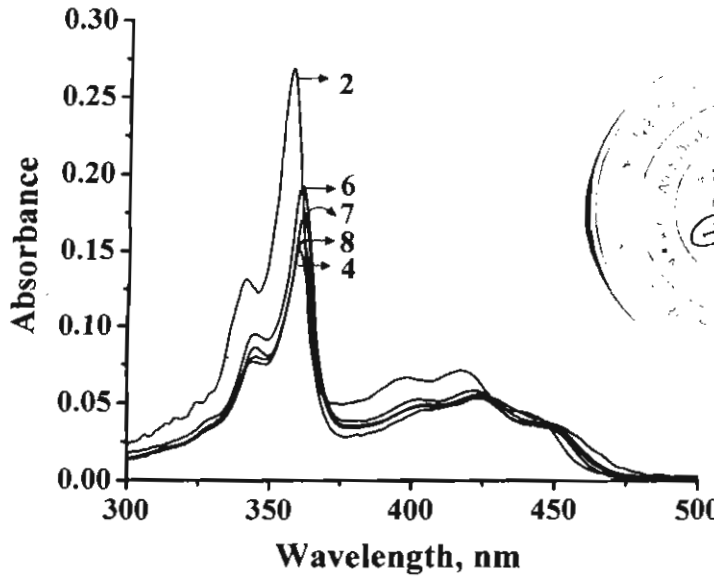

Figure 2.1. Absorption spectra of the representative acridinium derivatives **2-8** in water.

2.3.3. Fluorescence Properties

Figure 2.2 shows the fluorescence emission spectra of the acridinium derivatives **1-8**. The acridinium derivatives **1, 2** and the *ortho*-tolylacridinium derivative **6** exhibited quantitative fluorescence quantum yields ($\Phi_f \cong 1$) with an emission maximum around 500 nm. In contrast, the fluorescence quantum yields of the arylacridinium derivatives **3-5** (Φ_f = 0.09, 0.05 and 0.1, respectively) and **7-8** (Φ_f = 0.11 and 0.02, respectively), with emission maxima in the range 500-510 nm,

Table 2.1. Photophysical properties of the acridinium derivatives **1-8** in water.[a]

Compd	λ_{abs}, nm (ε, $M^{-1}cm^{-1}$)	λ_{em} nm	Φ_f[b]	τ, ns	k_r $\times 10^7$ s^{-1}	k_{nr} $\times 10^8$ s^{-1}
1	358 (20220) 415 (3600)	491	1	35	2.86	c
2	358 (18800) 415 (3500)	493	1	34	2.96	c
3	357 (20200) 425 (6000)	508	0.09	1.3	6.9	7
4	361 (20000) 427 (6900)	508	0.05	0.6	8.3	15.8
5	361 (15500) 425 (5100)	508	0.11	1.7	7.6	5.1
6	361 (19250) 425 (5900)	501	1	25	4.03	c
7	361 (18300) 425 (6200)	501	0.11	3.6	3	2.47
8	361 (17300) 424 (5200)	499	0.02	1.2	0.6	8.1

[a]Average of more than two experiments. [b]Fluorescence quantum yields were calculated using **1** as the standard ($\Phi_f = 1$),[15] error ca. ±10%. [c]The non-radiative decay rates equals to zero, since these derivatives showed quantitative fluorescence yields.

were found to be significantly quenched when compared to other derivatives. The acridinium derivatives **1** and **2** exhibited single exponential decay with a lifetime of 35 ns, whereas the *ortho*-derivative **6** showed a reduced lifetime of 25 ns.

When compared to **1**, **2** and **6**, unusually low lifetimes were observed for the arylacridinium derivatives **3**, **4**, **5**, **7** and **8** (1.3, 0.6, 1.7, 3.6 and 1.2 ns, respectively). The quenched fluorescence and reduced lifetimes for the acridinium derivatives can be attributed to either fast non-radiative relaxation of the excited

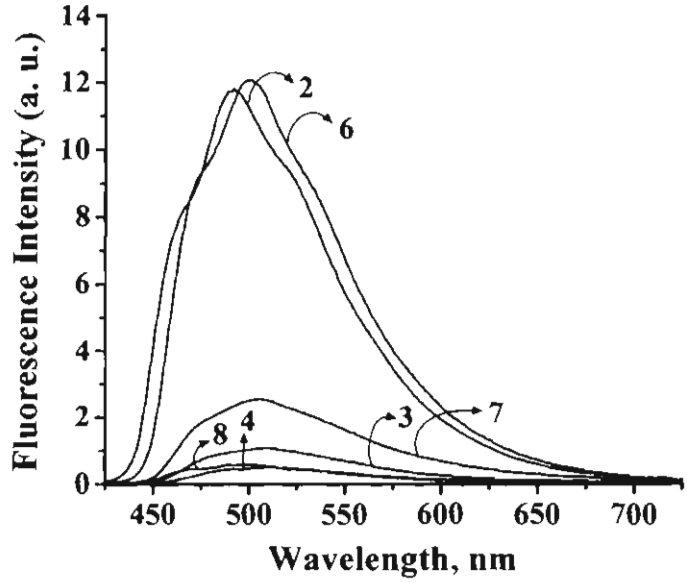

Figure 2.2. Fluorescence emission spectra of the acridinium derivatives **2-8** in water. Excitation wavelength, 366 nm.

state of the aryl derivatives by the rotation between the acridinium and the aryl ring or due to the quenching of the singlet excited state of the acridinium moiety by the aryl group through electron transfer mechanism. The radiative (k_r) and non-radiative (k_{nr}) rate constants for the decay of the singlet excited states of these molecules were evaluated from the fluorescence quantum yields (Φ_f) and lifetimes (τ_f), using equations 2.1 and 2.2,

$$k_r = \Phi_f / \tau_f \qquad (2.1)$$

$$k_{nr} = (1-\Phi_f) / \tau_f \qquad (2.2)$$

and the values obtained are summarized in Table 2.1. The non-radiative decay rate constant k_{nr} includes both the decay rates corresponding to the processes such as rotational relaxation and the electron transfer reaction. The involvement of the rotational relaxation pathway in the present case may be considered as marginal, since the 9,10-dimethylacridinium derivative **2**, where such an efficient relaxation is possible, exhibited quantitative fluorescence yield with significantly longer lifetime of 34 ns (Table 2.1).

In support of the fluorescence quenching by the electron transfer mechanism in the case of the arylacridinium derivatives **3-5**, we have calculated the change in free energy for the electron transfer process (ΔG_{el}) from the corresponding aryl groups to the acridinium moiety, using the Rehm-Weller[16] equation 2.3,

$$\Delta G_{el} = E_{ox} - E_{red} - w_p - E_{0,0} \qquad (2.3)$$

where, $E_{(0,0)}$ is the singlet excitation energy in eV, w_p is the work term, which was taken as 0.056 eV in acetonitrile,[17] E_{ox} is the oxidation potential of the donor and E_{red} is the reduction potential of the acceptor. Based on the oxidation potentials of phenyl (2.3 eV *vs* SCE) and tolyl (1.98 eV *vs* SCE) groups[18] and reduction potential (-0.57 eV *vs* SCE)[18] and singlet excitation energy (2.75 eV)[19] of the acridinium moiety, the change in free energies were calculated and were found to be 0.06 and –0.26 eV, for the electron transfer processes from the phenyl and tolyl groups, respectively. This indicates that the acridinium fluorescence can be

intramolecularly quenched by these groups through an electron transfer mechanism.

The fluorescence with quantitative quantum yield in the case of the acridinium derivative **6** originates from the locally excited acridinium singlet state. While in the case of the derivatives, **7** and **8** having *ortho*-substituents, the significantly quenched fluorescence is attributed to be from locally excited state which arises from a charge-transfer state in which the aryl group acts as the donor and the acridinium moiety as the acceptor. Such electron transfer mechanism in the case of the substituted acridinium derivatives was based on literature reports[20-22] and the evidence obtained through the laser flash photolysis and time-resolved fluorescence studies.

2.3.4. Double Strand DNA Binding Properties

The acridinium derivatives **1-8**, should in principle interact with double strand DNA (dsDNA) through intercalation and/or electrostatic modes. Figure 2.3 shows the change in the absorption spectra of the acridinium derivative **2** with increasing dsDNA concentrations. The addition of CT DNA to a solution of **2** results in a strong decrease in the absorption of the acridinium chromophore, along with a red shift of around 3 nm. Furthermore, with the increase in DNA concentration, a strong quenching of the acridinium fluorescence emission was observed. Similar changes in absorption and fluorescence emission spectra were

observed for the acridinium derivatives **1** and **3-5**. Among all the acridinium derivatives, the *ortho*- substituted acridinium derivatives **6-8** showed interesting variation. Figures 2.4 and 2.5 show the changes in the absorption and fluorescence emission spectra of **6** and **7**, respectively with increasing concentration of dsDNA, while Figure 2.6 shows the absorption and fluorescence changes of the derivative **8** in the presence of dsDNA.

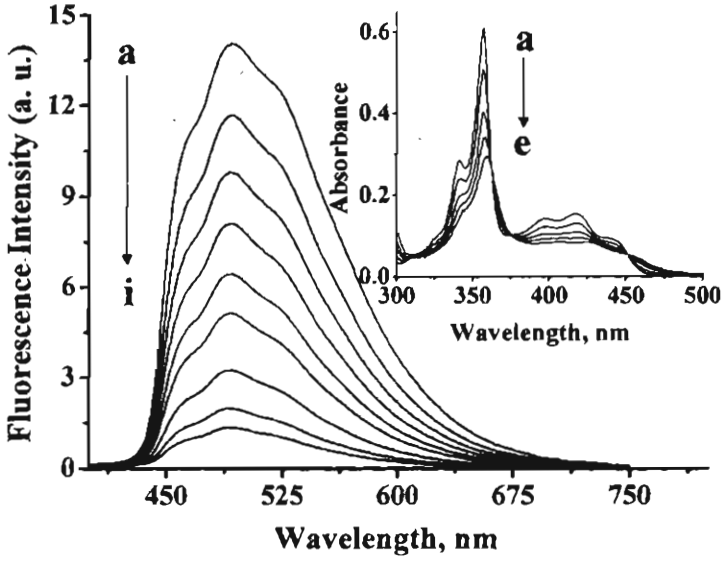

Figure 2.3. Change in fluorescence spectra of **2** (32 μM) in phosphate buffer (10 mM; pH 7.4) with increasing concentration of dsDNA. [dsDNA] (a) 0, (b) 0.05, (c) 0.09, (d) 0.12, (e) 0.16, (f) 0.19, (g) 0.26, (h) 0.34 and (i) 0.42 mM. Inset shows the change in absorption spectra of **2** (32 μM) with increasing concentration of dsDNA. [dsDNA] (a) 0, (b) 0.05, (c) 0.12, (d) 0.19 and (e) 0.34 mM. Excitation Wavelength, 366 nm.

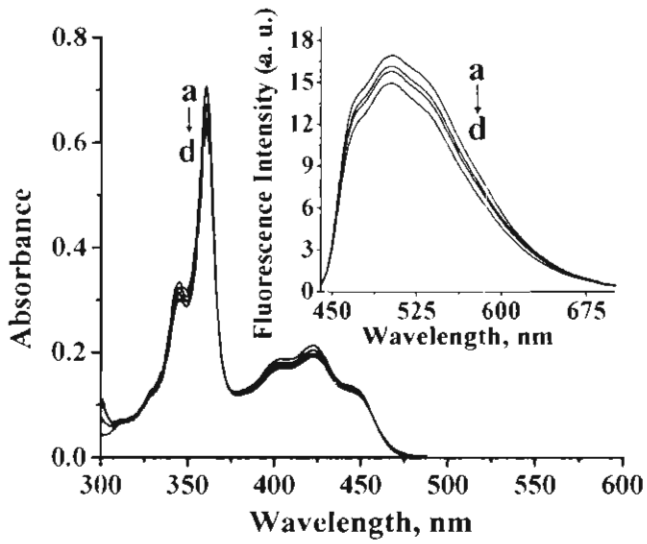

Figure 2.4. Change in absorption spectra of **6** (42.5 μM) in phosphate buffer (10 mM; pH 7.4) with increasing concentration of dsDNA. [dsDNA] (a) 0, (b) 0.17, (c) 0.34 and (d) 0.42 mM. Inset shows the change in fluorescence spectra of **6** with increasing concentration of dsDNA. [dsDNA] (a) 0, (b) 0.17, (c) 0.34, and (d) 1 mM. Excitation wavelength, 366 nm.

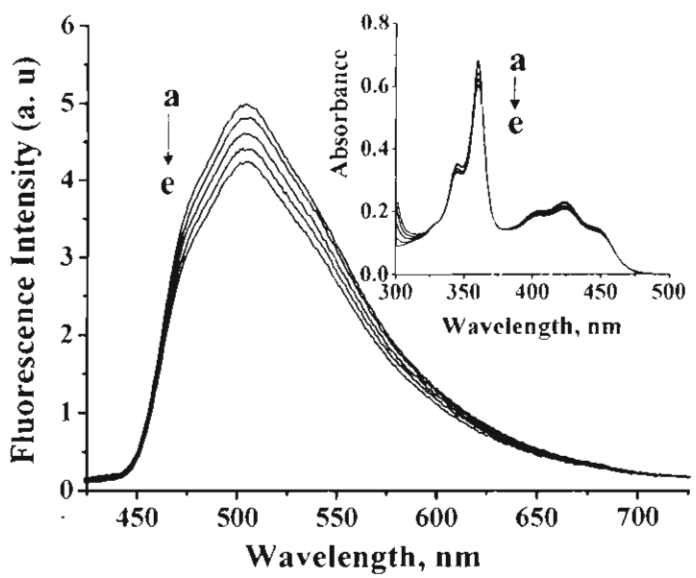

Figure 2.5. Change in fluorescence spectra of **7** (32 μM) in phosphate buffer (10 mM; pH 7.4) with increasing concentration of ds DNA. [dsDNA]] (a) 0, (b) 0.17, (c) 0.34, (d) 0.42 and (e) 1 mM. Inset shows the change in absorption spectra of **7** under similar conditions. Excitation wavelength, 363 nm.

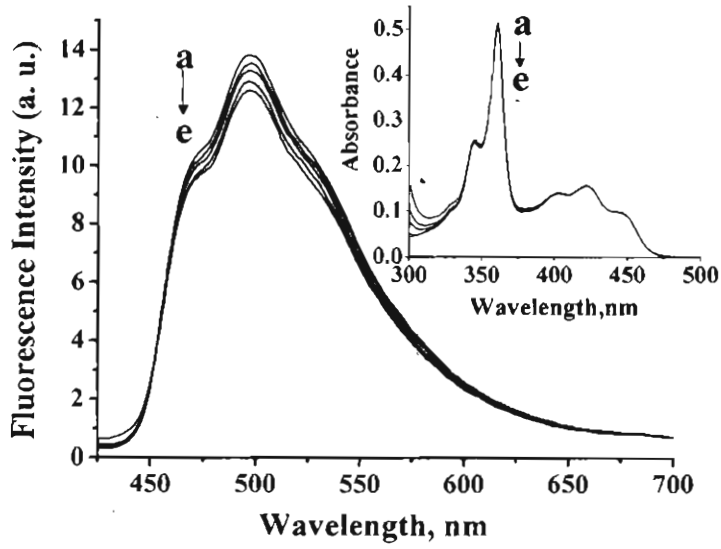

Figure 2.6. Change in fluorescence spectra of **8** (28 μM) in phosphate buffer (10 mM; pH 7.4) with increasing concentration of CT dsDNA. [dsDNA] (a) 0 and (e) 1 mM. Inset shows the change in absorption spectra of **8** under similar conditions. Excitation wavelength, 366 nm.

Both the absorption and fluorescence studies indicate that the *ortho*-substituted derivatives **6-8** exhibit negligible interactions with DNA. To understand the sequence selective interactions of the derivatives, we have investigated the changes in absorption and fluorescence properties in the presence and absence of polyoligonucleotides of different sequences such as poly(dG).poly(dC) and poly(dA).poly(dT). Figures 2.7 and 2.8 show the changes in fluorescence emission of the derivative **2** with increasing concentration of oligonucleotides poly(dG).poly(dC) and poly(dA).poly(dT) while the insets show the corresponding absorption changes. The poly(dG).poly(dC) which is rich in

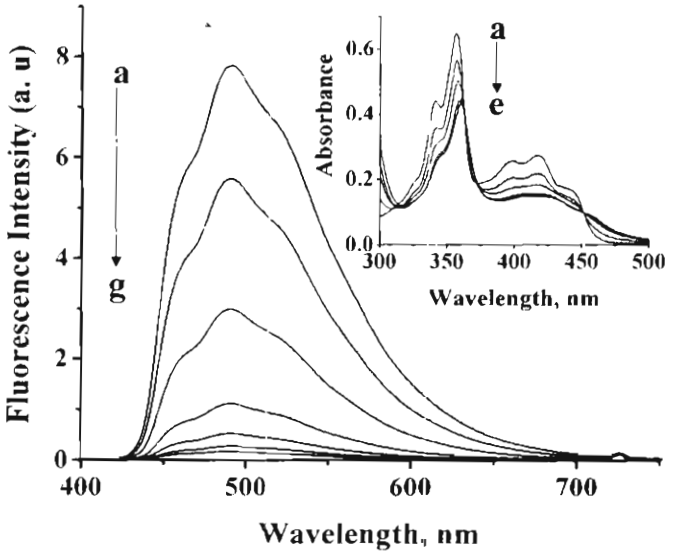

Figure 2.7. Change in fluorescence spectra of **2** (32 μm) in phosphate buffer (10 mM; pH 7.4) with increasing concentration of poly(dG).poly(dC). [poly(dG).poly(dC)] (a) 0, (b) 0.08, (c) 0.16, (d) 0.24, (e) 0.30, (f) 0.38 and (g) 0.5 mM. Excitation wavelength, 363 nm. Inset shows the change in absorption spectra of **2** under similar conditions.

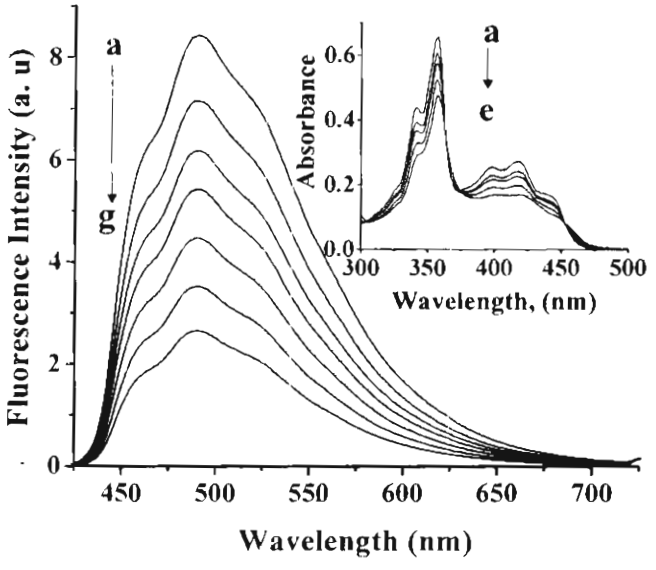

Figure 2.8. Change in fluorescence spectra of **2** in phosphate buffer (10 mM; pH 7.4) with increasing concentration of poly(dA).poly(dT). [poly(dA).poly(dT)] (a) 0, (b) 0.08, (c) 0.17, (d) 0.25, (e) 0.33, (f) 0.48 and (g) 0.63 mM. Excitation wavelength, 363 nm. Inset shows the change in absorption spectra of **2** under similar conditions.

guanosine base content showed an efficient quenching in fluorescence emission of the acridinium derivative **2** when compared to poly(dA).poly(dT). The absorption changes shows strong hypochromicity as well as a red shift of 3 nm in the presence of poly(dG).poly(dC) and poly(dA).poly(dT), which indicates intercalative interaction as reported for several known intercalators.[2d]

Picosecond time-resolved fluorescence studies in the presence and absence of DNA indicate that the acridinium derivative **2**, exhibits a single exponential decay in buffer with a fluorescence lifetime of 34 ns (Figure 2.9), while in the presence of DNA it shows triexponential decay with lifetimes of 45 ps, 0.8 ns and 33 ns. The short lifetimes observed (45 ps and 0.8 ns) may be attributed to the

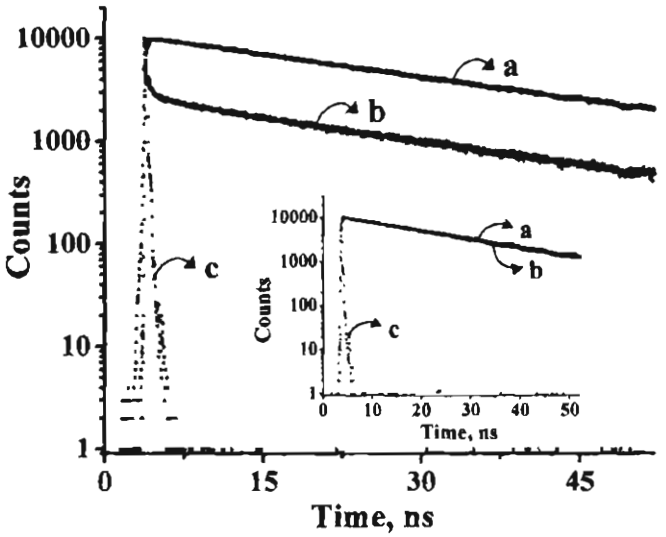

Figure 2.9. Fluorescence decay profiles of **2** (32 μM) in the presence and absence of DNA in phosphate buffer (10 mM; pH 7.4). [dsDNA] (a) 0 and (b) 0.34 mM, (c) Lamp profile. Inset shows the fluorescence decay profiles of **6** in the presence and absence of DNA under similar conditions. [dsDNA] (a) 0 and (b) 0.34 mM. Excitation wavelength, 401 nm.

intercalative binding of the acridinium chromophore at two different base sequence environments, whereas the third lifetime could be due to the unbound molecules. On the other hand, the *ortho*-derivative **6**, having a fluorescence lifetime of 25 ns in buffer, exhibited negligible changes in presence of DNA (inset of Figure 2.9). These observations confirm that the acridinium chromophore in the case of **6** undergoes neither intercalative nor groove binding interactions with DNA.

The DNA association constants (K) of the complexes formed between the acridinium derivatives **1-5** and DNA were determined based on fluorescence titration experiments, according to the method of McGhee and von Hippel by using the data points of the Scatchard plot[23,24] and are reported in Table 2.2. For example, 10-methylacridinium (**1**) and the 9,10-dimethylacridinium derivative (**2**) showed binding constants of 7.7×10^5 M^{-1} and 7.3×10^5 M^{-1}, respectively, whereas, relatively lower values of DNA association constants were observed for the arylacridinium derivatives **3-5**. Interestingly, the binding site size (n) was found to be greater for the arylacridinium derivatives **3-5** (n = 6-7), than the acridinium derivatives **1** and **2** (n = 2.5). Thus, a comparison of the DNA binding constants indicate that the acridinium derivatives **1** and **2** bind to DNA by nearly one order more efficiently when compared with the arylacridinium derivatives **3-5**. In the case of the aryl-substituted derivatives, the efficiency was found to be in the order, phenyl > 4-methylphenyl > 3-methylphenyl >>>> 2-methlphenyl ≈ 2,4-dimethylphenyl > 2,6-dimethylphenyl, wherein the increase in

Table 2.2. Photophysical and DNA binding properties of the acridinium derivatives **1-8**.[a]

Compound	K (M^{-1})[b]	n[c]	k_{DNA} (s^{-1})[d]
1	7.7×10^5	2.5	1.2×10^{10}
2 [e]	7.3×10^5	2.5	1.1×10^{10}
3	1.1×10^5	6	5×10^{10}
4	7.1×10^4	7	6.5×10^{10}
5	6.9×10^4	6.5	3×10^{10}
6	f	f	f
7	f	f	f
8	f	f	f

[a] Average of more than two experiments and error ca. ±5%; [b]The DNA binding properties were examined in phosphate buffer (10 mM, pH 7.4). DNA association constants determined by the Scatchard analysis of fluorescence titration data.[23,24] [c] Number of nucleotides occluded by a bound ligand. [d] Rate of static quenching by DNA calculated as reported earlier.[25] [e] For compound **2**, (i) $K_{p(dG)(dC)} = 8.5 \times 10^5$ M^{-1} and $k_{p(dG)(dC)} = 3.8 \times 10^{10}$ s^{-1}. (ii) $K_{p(dA)(dT)} = 4.12 \times 10^5$ M^{-1} and $k_{p(dA)(dT)} = 0.24 \times 10^{10}$ s^{-1}. [f] Negligible binding.

steric factors around the acridine ring hinders the DNA binding interactions and finally leads to the negligible binding as observed in the case of the *ortho*-substituted acridinium derivatives **6-8**. The association constant of the acridinium derivative **2** with poly(dG).poly(dC) was found to be 8.5×10^5 M^{-1}, which is 1.2 times greater than that observed with CT DNA (7.3×10^5 M^{-1}) while nearly ca. 2-fold larger value was observed for poly(dA).poly(dT) (4.12×10^5 M^{-1}).

3.5. Characterization of Double Strand DNA Binding Interactions

The double strand DNA (dsDNA) viscosity measurement is an efficient ethod to differentiate the intercalative mode of binding from other interactions.[26] ntercalation of the planar aromatic molecules proceeds by unwinding of the double elix to accommodate the molecule between the DNA base pairs. As a result, there is net increase in the length of the DNA, which is reflected in the increase in the iscosity of DNA. No other process, such as the electrostatic or the groove binding interactions can bring about effective increase in the DNA contour length.[26] Figure 2.10 shows the results of the viscometry studies of representative examples, which indicate that the viscosity of dsDNA increases proportionally with the binding affinity of the acridinium derivatives **2** and **4**, whereas negligible viscosity changes were observed for the *ortho*-derivative **6**. The change in viscosity could be attributed to the π-stacking of the acridinium derivatives between DNA base pairs, which results in the increase in the viscosity of dsDNA. On the other hand, the

ortho-derivative **6** shows negligible binding with dsDNA by intercalation as observed from the physical and spectroscopic studies.

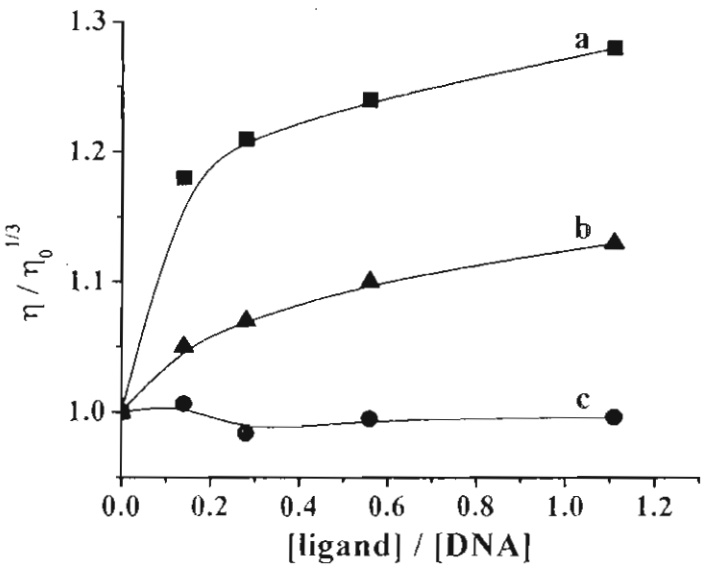

Figure 2.10. Effect of increasing concentration of the acridinium derivatives (a) **2**, (b) **4** and (c) **6** on the relative viscosity of CT dsDNA (0.7 mM) at 26 ± 0.2 ^{0}C in phosphate buffer (10 mM; pH 7.4).

The circular dichroic (CD) studies of dsDNA in the presence and absence of the acridinium derivatives could provide additional information regarding their mode of binding. Location of an achiral molecule in a chiral environment can result in the induced optical activity of the bound species. The free acridinium derivative (**4**) being achiral did not show any CD signal, however, when bound to dsDNA, it showed an induced CD signal at the chromophore absorption region characteristic of the intercalative interaction (Figure 2.11).[27,28] On the other hand, the *ortho*-substituted tolyl acridinium derivative **6**, did not show any CD signal in the presence of dsDNA, indicating its negligible interactions.

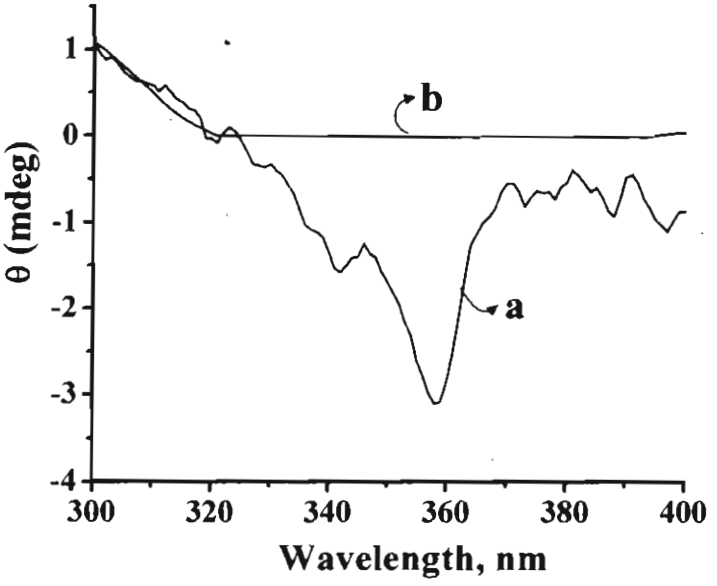

Figure 2.11. Circular dichroism (CD) spectra of (a) **4** (40 μM) and (b) **6** (40 μM) in the presence of dsDNA (1 mM) in phosphate buffer (10 mM, pH 7.4).

The differences observed in DNA binding affinity of these acridinium derivatives could be rationalized in terms of the steric effects offered by the substituents. The structural analysis of the arylacridinium derivatives reveals that the acridinium as well as the aryl substituent are out of plane to each other and the dihedral angle (φ) according to the minimum energy conformations for **3-8** are 64.8^0, 64^0, 64.7^0, 77.5^0, 83.1^0 and 88.5^0, respectively (Figure 2.12A and 2.12B).[29] In order to achieve an effective intercalation of the acridinium chromophore, the aryl group has to undergo a rotation during the process of intercalation. The feasibility of this rotation is the deciding factor in effective binding of these molecules to DNA. In the case of the *ortho*-derivatives **6-8**, the rotation of the

tolyl group is sterically hindered and hence no significant binding with DNA was observed.

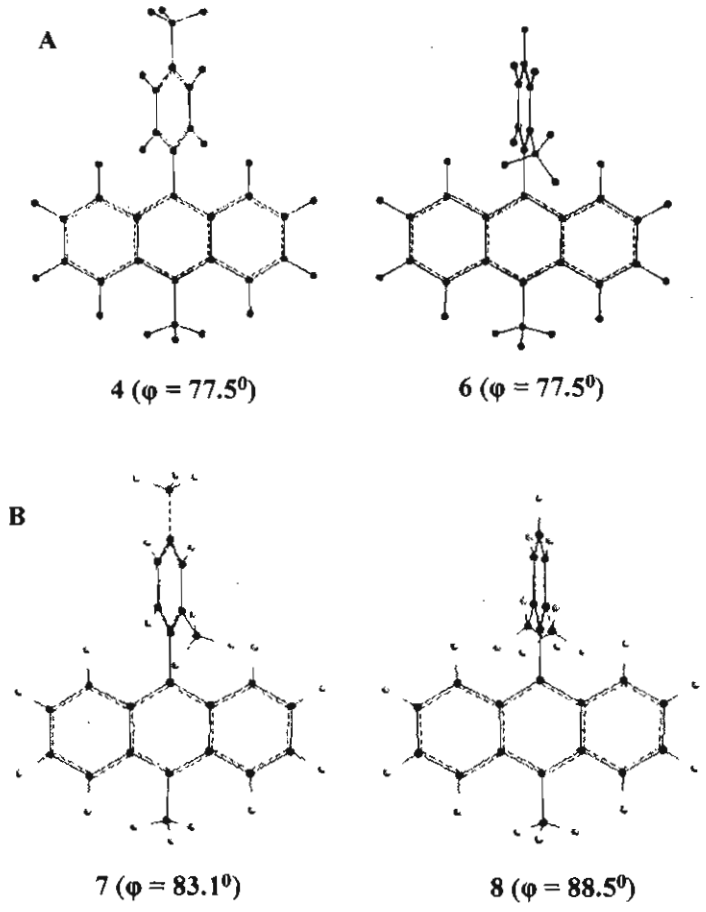

Figure 2.12. Minimum energy conformations of (**A**) 4-methylphenyl and 2-methylphenyl and (**B**) 2,4-dimethylphenyl and 2,6-dimethylphenyl acridinium derivatives obtained by AM1 calculations.

2.3.5. Single Strand DNA Binding Properties

The presence of *ortho*-substitution prevents the intercalation of the acridinium moiety between the dsDNA base pairs. However, since the bases in the ssDNA are more exposed to the external medium, the interaction of these

derivatives through intercalation between the ssDNA bases, should in principle, be favorable. Figure 2.13 shows the changes in absorption and fluorescence spectra of the acridinium derivative **6** with the addition of ssDNA. As shown in the figure, we observed decrease in absorption of the acridinium chromophore along with significant quenching of the fluorescence emission at 500 nm, with the increase in addition of ssDNA. Similar changes in the absorption and fluorescence emission spectra were observed for the acridinium derivative **7** (Figure 2.14).

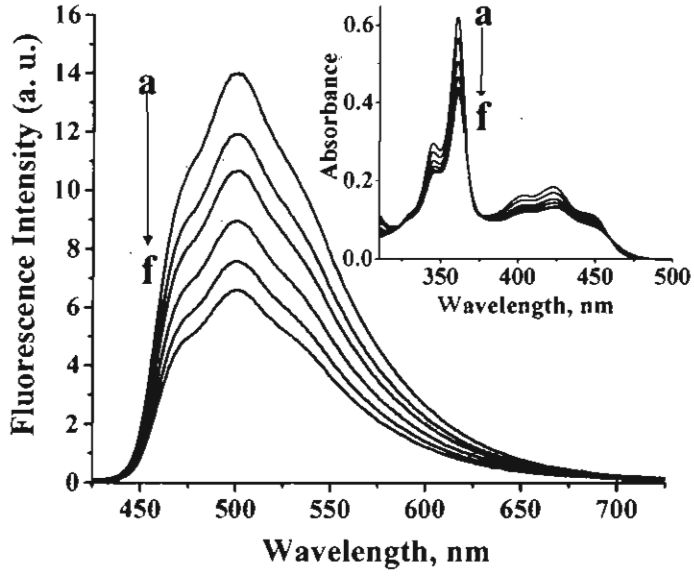

Figure 2.13. Change in fluorescence spectra of **6** (30 μM) with increasing concentration of single strand CT DNA in phosphate buffer (10 mM; pH 7.4). [ssDNA] (a) 0, (b) 0.20, (c) 0.43, (d) 0.63, (e) 0.82 and (f) 1 mM. Inset shows the corresponding changes in the absorption spectra of **6** with the gradual addition of ssDNA. Excitation wavelength, 366 nm.

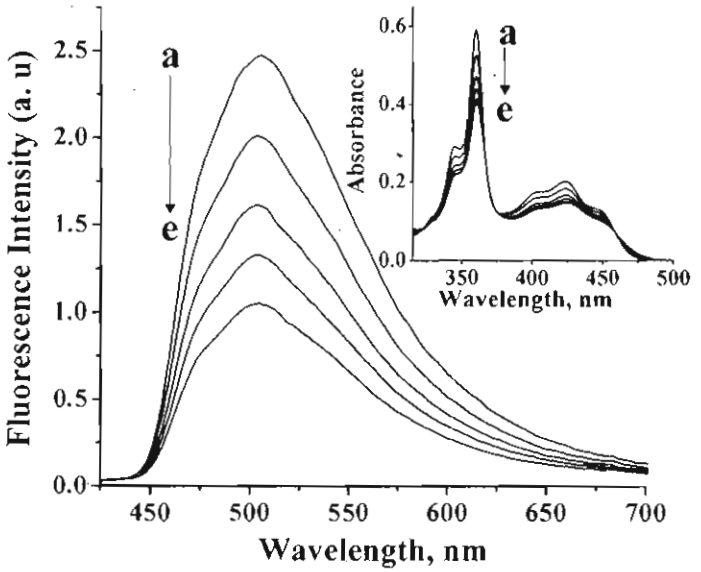

Figure 2.14. Change in fluorescence spectra of **7** (30 μM) in phosphate buffer (10 mM, pH 7.4) with increasing concentration of CT ssDNA. [ssDNA] (a) 0 and (e) 1 mM. Inset shows the change in absorption spectra of **7** under similar conditions. [ssDNA] (a) 0 and (e) 1 mM. Excitation wavelength, 366 nm.

An interesting variation was observed in the case of the derivative **8** which showed negligible changes in the absorption and fluorescence spectra in the presence of both ssDNA and dsDNA (Figure 2.15). The extent of quenching in fluorescence emission was observed to be greater in the presence of shorter oligonucleotides. When compared to the 65% fluorescence quenching observed in the presence of CT ssDNA, the short stranded random sequence oligonucleotide $(dN)_{19}$ showed >85% quenching under similar conditions (Figure 2.16). The long ssDNA with random base sequence shows a greater elastic nature, when compared to short ssDNA and has a tendency to form loops which leads to the formation of

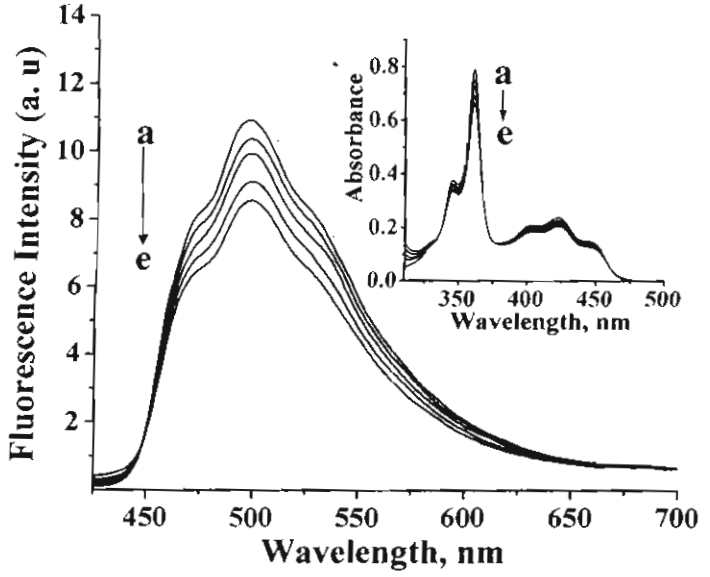

Figure 2.15. Change in fluorescence spectra of **8** (30 μM) in the presence of single strand CT DNA in phosphate buffer (10 mM, pH 7.4). [ssDNA] (a) 0, (b) 0.20, (c) 0.43, (d) 0.63 and (e) 1 mM. Inset shows the corresponding changes in the absorption spectra of **8** in the presence of ssDNA. Excitation wavelength, 366 nm.

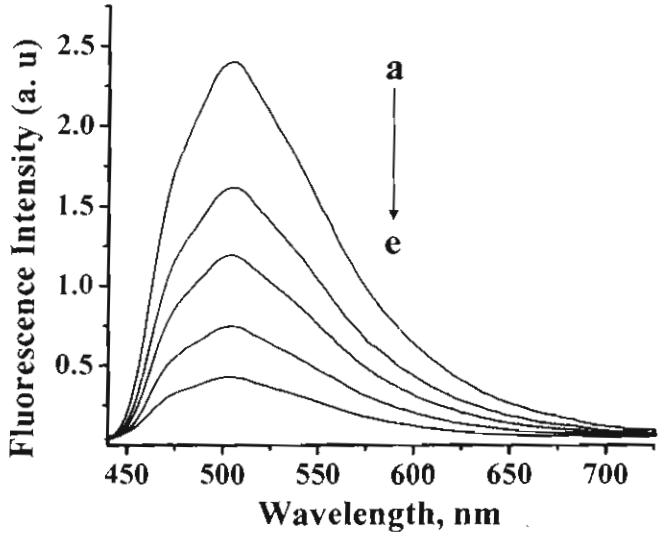

Figure 2.16. Change in fluorescence spectra of **7** (30 μM) with increasing concentration of 19-mer oligonucleotide, $(dN)_{19}$ in phosphate buffer (10 mM, pH 7.4). [ssDNA] (a) 0, (b) 0.20, (c) 0.43, (d) 0.63 and (e) 0.82 mM. Excitation wavelength, 366 nm.

double stranded regions. The lesser extent of quenching observed in the case of CT ssDNA could be attributed to the existence of such loops, which prevents the efficient intercalation of these derivatives at such regions when compared to the oligonucleotides of shorter length.

The association constants (K_{ssDNA}) of the complexes formed between the acridinium derivatives **6-7** and ssDNA were determined based on fluorescence titration experiments, according to the method of McGhee and von Hippel by using the data points of the Scatchard plot.[23,24] The acridinium derivative **6** shows a binding constant of 6.3×10^4 M^{-1} with ssDNA, while it was 6.6×10^4 M^{-1} for the derivative **7**, indicating that substitution at the *para*-position of the phenyl group has negligible effect on the ssDNA binding properties of the acridinium derivatives (Table 2.3).

Table 2.3. Photophysical and ssDNA binding properties of the acridinium derivatives **6-8**.[a]

Entry	Acridinium derivatives	K_{DNA} (M^{-1})[b]	k (s^{-1})[c]
1	**6**	6.3×10^4	0.5×10^8
2	**7**	6.6×10^4	3.6×10^8
3	**8**	d	d

[a] Average of more than two experiments. [b]DNA association constants were determined by the Scatchard analysis of the fluorescence titration data.[23,24] [c]Rate of static quenching by DNA calculated as reported earlier.[25d] Exhibits negligible binding interactions.

However, upon increasing the steric factors near the acridinium ring by the introduction of another *ortho*-substitution as in the case of the derivative **8**, results in negligible binding with ssDNA. The rate constants for the static quenching of the singlet excited state of the acridinium chromophore by DNA (k) were calculated and were found to be in the order of 10^7-10^8 s^{-1} (Table 2.3).

2.3.7. Characterization of Single Strand DNA Binding Interactions

To understand the mode of interaction of the acridinium derivatives with ssDNA, the changes in the viscosity and circular dichroism (CD) spectra have been investigated under different conditions. The CD spectra recorded for the *ortho*-tolyl acridinium derivative **6** is shown in Figure 2.17. A weak biphasic CD signal was observed at the chromophore absorption region of 300-475 nm, with a

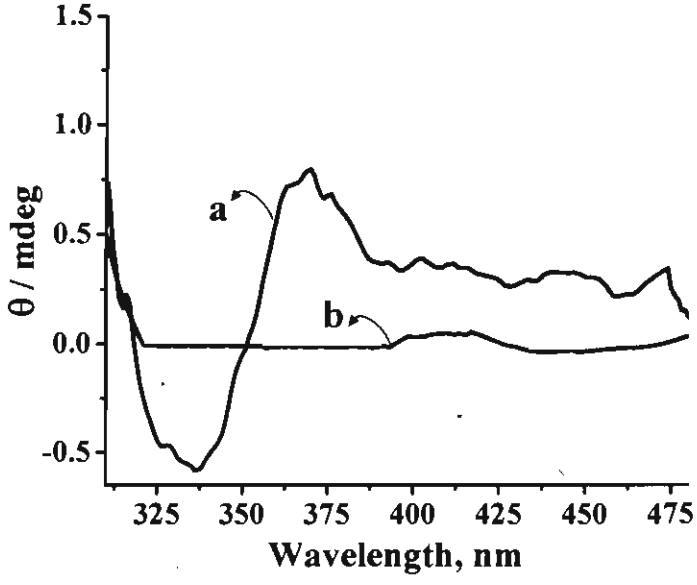

Figure 2.17. Circular dichroism (CD) spectra of **6** (80 μM) in the presence of (a) ssDNA (1 mM) and (b) dsDNA (1 mM) in phosphate buffer (10 mM; pH 7.4).

positive band at 370 nm and a negative band at 340 nm. In contrast, no CD signal corresponding to the chromophore was observed in the presence of dsDNA. The biphasic CD signal observed at the chromophore absorption region is attributed to the induced chirality in the probe when bound to ssDNA.[27,28]

Similarly, it was observed that the viscosity of dsDNA remains unchanged in the presence of **6**, while it decreased drastically for ssDNA (Figure 2.18), indicating that the acridinium derivative **6** undergoes selective interactions with ssDNA. In ssDNA, the repulsive columbic forces between the negatively charged phosphate groups maintain its highly coiled structure.[29] These forces are altered when a molecule with positive charge interacts with ssDNA, leading to the partial

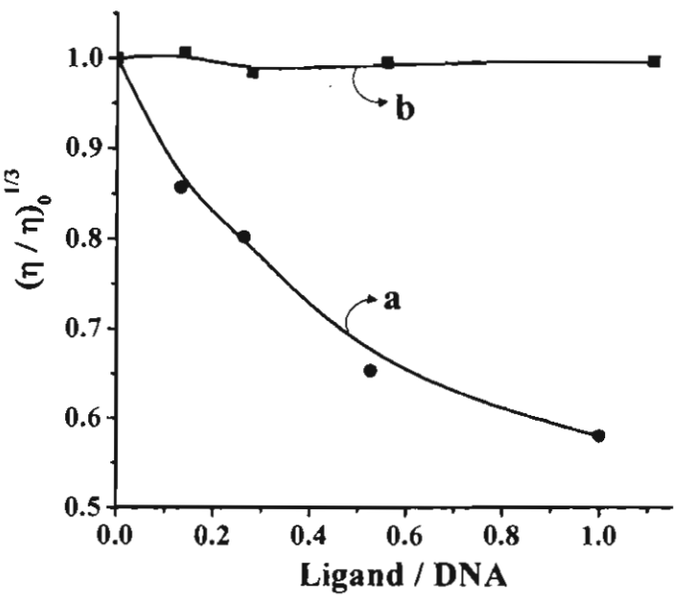

Figure 2.18. Effect of increasing in concentration of **6** on the relative viscosity of (a) ssDNA (0.7 mM) (b) dsDNA (0.7 mM) in phosphate buffer (10 mM; pH 7.4) at 26 ± 0.2 ^{0}C.

uncoiling of the coiled secondary structure and hence the observed reduction in scosity of ssDNA in the presence of the acridinium derivative **6**. Moreover, such partial uncoiling of ssDNA is supported by the observation of weak induced CD gnal in the presence of **6**. The absence of such intercalative interactions of **6** with sDNA leads to the negligible enhancement in the viscosity of dsDNA as ompared to the ssDNA.

Electrostatic contribution in the binding process was estimated by nonitoring the absorbance and fluorescence emission changes of these derivatives with increasing concentrations of ssDNA at different ionic strengths of the buffer. The quenching in fluorescence intensity was found to be considerably lower (45%), at an ionic strength of 100 mM NaCl, when compared to that observed at lower ionic strengths of 2 mM NaCl (Figure 2.19). When the ionic strength of the medium is increased from 2 mM to 100 mM NaCl, the association constant of **6** for ssDNA decreases by one order and the logK vs. $-\log[Na^+]$ gave a linear fit with a slope of 1.1 (Figure 2.20). This indicates the release of one Na^+ ion per bound ligand and confirms the role of electrostatic interactions in the binding process, which occurs prior to the intercalation of the planar acridinium ring between the ssDNA bases.[30]

The observed preference of the acridinium derivatives for ssDNA can be ationalized in terms of the steric effects of the substituents. Figure 2.12 shows the

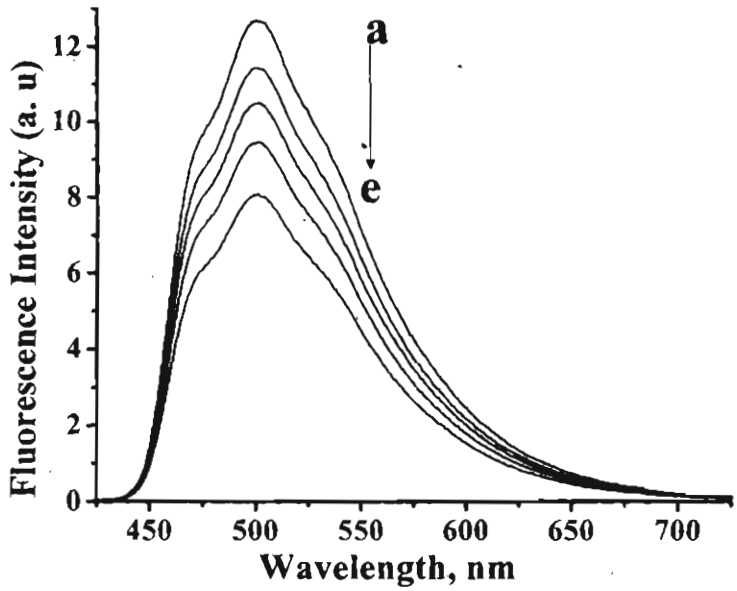

Figure 2.19. Change in fluorescence spectra of **6** (30 μM) in phosphate buffer (10 mM, pH 7.4) containing 100 mM NaCl, with increasing concentration of CT ssDNA. [DNA] (a) 0 and (e) 1 mM. Excitation wavelength, 366 nm.

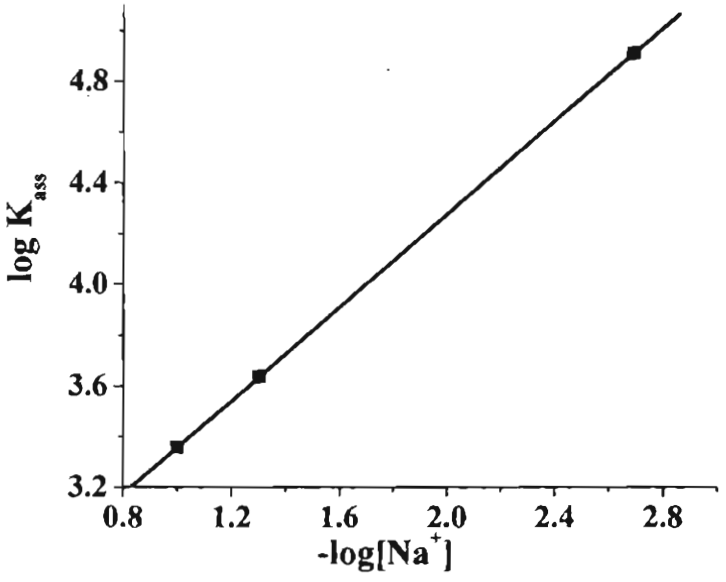

Figure 2.20. Change in log of association constants with negative log of the salt concentrations for the interaction of **6** with ssDNA.

minimum energy conformations for **6-8** with the dihedral angles of 77.5^0, 83.1^0 and 88.5^0 respectively. The quenching in the acridinium fluorescence in the

presence of ssDNA occurs due to the free energetically favorable electron transfer from the nucleobases to the excited states of the acridinium chromophore. However, for an efficient electron transfer process to occur the acridinium chromophore should π-stack between the nucleobases. This is possible only in the case of the acridinium derivatives **6** and **7**, with only one *ortho*- substitution, which offers lesser steric hindrance for the approach of the derivatives near the bases. In contrast, the derivative **8** with two *ortho*-substitutions behaves identically with both ssDNA and dsDNA because of the larger dihedral angle value of 88.5^0 which hinders its intercalation between the nucleobases in both ssDNA and dsDNA.

2.3.8. Microscopic Characterization of DNA Binding Interactions

Apart from the spectroscopic observation of the selective interactions of various acridinium derivatives, the morphological evidence for the DNA association was obtained through the atomic force microscopic (AFM) analysis. Figure 2.21A shows the AFM image obtained for a 20 μM solution of calf thymus dsDNA drop casted on mica surface. The AFM image shows a uniform cross-linked network like structure which arises from the self-assembly of the dsDNA strands on the mica surface.[31] This ordered structure was found to be disrupted and formation of aggregates was observed when calf thymus dsDNA was treated with the acridinium derivative **4**. Figure 2.21B shows the AFM image obtained for a 20 μM solution of calf thymus dsDNA incubated with 20 μM acridinium derivative **4**.

The observation confirms the experimental results described in the previous sections, wherein, the derivative was found to exhibit strong intercalative interactions with dsDNA. Intercalation leads to the unwinding of dsDNA and hence to structural distortions which in turn results in the observed breakage of the DNA self-assembly. Interestingly, the network like structure of calf thymus dsDNA is maintained in the presence of the derivative **6** (Figure 2.21C) which was earlier proven to be a non-intercalator by spectroscopic techniques. However, the

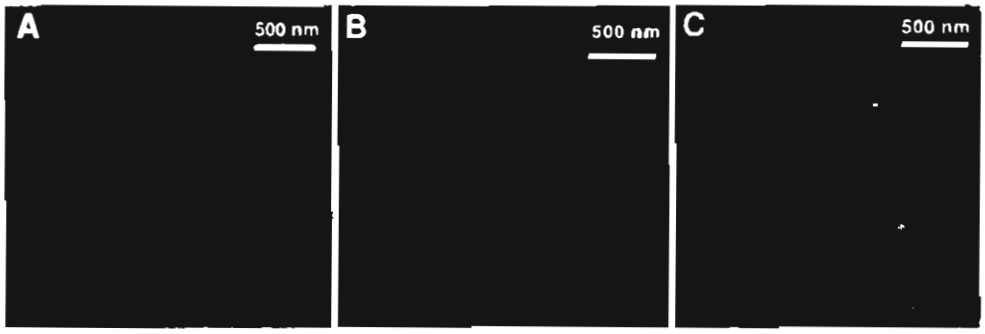

Figure 2.21. (A) AFM image of calf thymus dsDNA (20 μM) alone (B) in the presence of 20 μM **4** and (C) in the presence of 20 μM **6**.

morphological features of ssDNA change drastically in the presence of derivative **6**. It has been reported that the analysis of ssDNA through AFM gives concentration dependent compact network structures on HOPG surface.[32] Figure 2.22 shows the AFM images of ssDNA (20 μM) drop casted on mica surface in the presence and absence of **6** (20 μM). The AFM image of ssDNA alone (Figure 2.22A) exhibits randomly spaced voids of 300 ± 10 nm width having features with a height of 1 ± 0.5 nm. However, on interaction of ssDNA with **6**, in the place of

the voids, we observed features with an average height of 10 ± 2 nm and width of 300 ± 10 nm (Figure 2.22B). Similar studies with dsDNA showed negligible changes in the morphological features, thus confirming the selectivity of **6** for ssDNA. The ssDNA alone showed highly condensed globular structures. However, interaction of **6** with ssDNA leads to unwinding of the coiled structure due to the reduction in columbic repulsions between the phosphate groups of the ssDNA strands. This results in the formation of aggregates with average height of 10 ± 2 nm on mica.

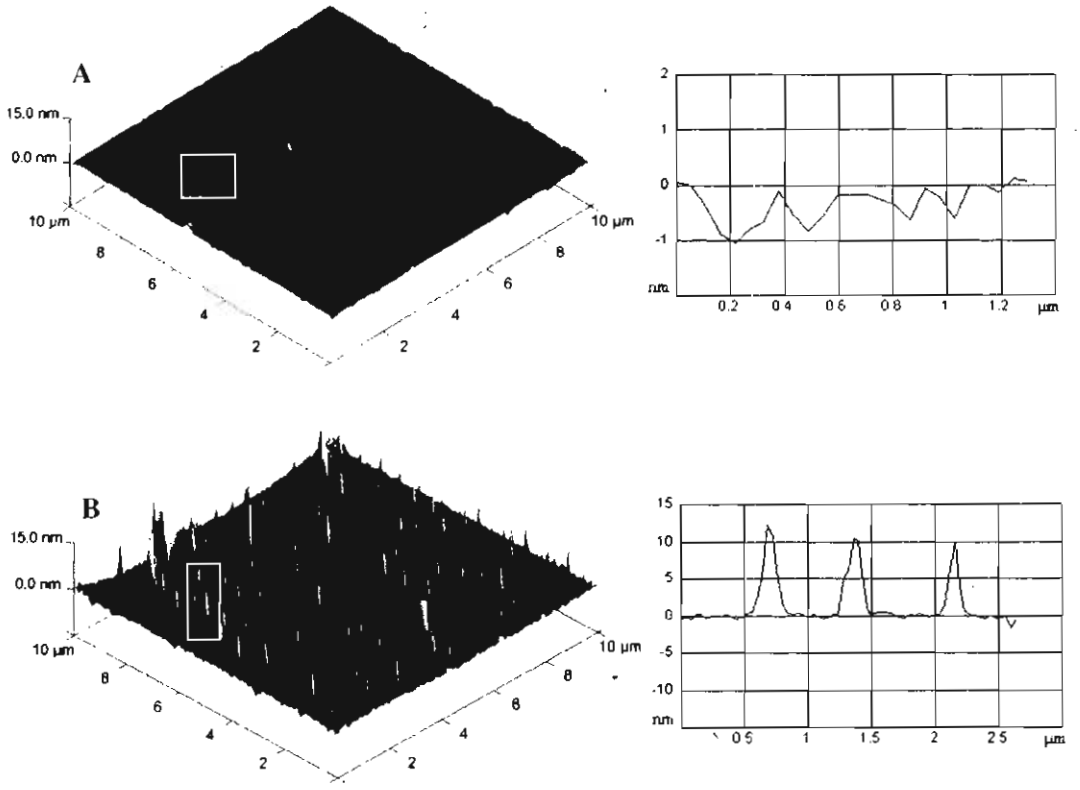

Figure 2.22. (A) AFM image of calf thymus ssDNA (20 µM) alone and (B) in the presence of **6** (20 µM).

2.4. Conclusions

In conclusion, we have demonstrated that variations in the substitution patterns can bring about extreme changes in the complexation preferences of the acridinium derivatives for the double strand or single strand DNA. It was observed that the unsubstituted and methylacridinium derivatives **1** and **2** bind with DNA by nearly one order more efficiently when compared to the bulky arylacridinium derivatives **3-5**. Furthermore, it was observed that the presence of one *ortho*-substituent, as in the case of the derivatives **6** and **7**, results in negligible interactions of the acridinium moeity with dsDNA, while they exhibited significant association with ssDNA. However, the introduction of another *ortho*-substituent, as in the case of **8**, results in negligible binding interactions with both ssDNA and dsDNA. The results indicate that the acridinium derivatives, which exhibit high solubility in buffer medium, can efficiently distinguish between ssDNA and dsDNA through changes in fluorescence intensity and hence can have applications as fluorescent probes.

2.5. Experimental Section

2.5.1. General Techniques

All melting points are uncorrected and were determined on a Mel-Temp II melting point apparatus. ^{1}H and ^{13}C NMR spectra were recorded on a Brucker DPX-300 MHz NMR spectrometer using tetramethylsilane as the internal standard.[33-34] CHN analyses were done using a Perkin-Elmer Series-II 2400 CHN

analyzer. The electronic absorption spectra were obtained using a Shimadzu UV-3101PC UV-VIS-NIR scanning spectrophotometer. The fluorescence spectra were recorded on a SPEX-Fluorolog F112X spectrofluorimeter.[33] The fluorescence lifetimes were measured on an IBH picosecond single photon counting system using a 401 nm IBH NanoLED source and a Hamamatsu C4878-02 MCP detector. The fluorescence decay profiles were deconvoluted using IBH Data Station software V2.1, fitted with a mono-, bi- or tri-exponential decay and minimizing the χ^2 values of the fit to 1 ± 0.1.[34] The fluorescence quantum yields were measured by the relative methods using optically dilute solutions, with 10-methylacridinium trifluoromethane sulphonate in water (Φ_f = 1) as the standard.[11,15,34a] Circular dichroism (CD) spectra were recorded on Jasco Corporation, J-810 spectropolarimeter. Atomic Force Microscopy (AFM) images were recorded under ambient conditions using a Digital Instrument Multimode Nanoscope IV operating in the tapping mode regime. Micro-fabricated silicon cantilever tips (MPP-11100-10) with a resonance frequency of 299 kHz and a spring constant of 20-80 Nm^{-1} were used. The scan rate varied from 0.5 to 1 Hz.[34d]

2.5.2. Materials

Polyoligonucleotides such as poly(dG).poly(dC) and poly(dA).poly(dT) and *calf thymus DNA* were obtained from Amersham Pharmacia Biotech Inc. Commercially available starting materials and solvents were purified and distilled before use. Petroleum ether used was the fraction boiling at 60-80 ^0C. The

acridinium derivatives **1-8** were prepared from the corresponding acridines, which were synthesized by the modified Bernthsen procedure[14] and/or the reaction between N-protected acridone and substituted phenylmagnesium bromide.[20]

2.5.2.1. Preparation of the acridine derivatives. The acridine derivatives were synthesized by a modified Bernthsen procedure as shown in Scheme 2.1. The condensation reaction of diphenylamine with the corresponding carboxylic acid in the presence of anhydrous $ZnCl_2$ yielded the acridine derivatives in 50-60% yields. 9-Methylacridine, mp 114-115 °C (lit. mp 116-117 °C),[14] 9-phenylacridine, mp 181-182, 9-(3-methylphenyl)acridine, mp 215-216 °C, 9-(2-methylphenyl)acridine, mp 212-213 °C (lit. mp 214 °C)[14b] and 9-(2,4-dimethylphenyl)acridine, mp 222-223 °C (lit. mp 224 °C).[14a]

Synthesis of 9-(2,6-dimethylphenyl)acridine. 10 mL of 2,6-dimethylphenyl magnesium bromide (1 M solution in THF) was added over a period of 15 min to a solution of N-(2-methoxyethoxymethyl)-9-acridone (1g, 3.53 mmol) in anhydrous THF (120 mL) at 0 °C under argon atmosphere. The mixture was stirred at room temperature for 24 h and then heated at 50 °C for 12 h. A solution of HCl (50 mL) and water (50 mL) was poured into the brown suspension. The resultant clear yellow solution was stirred overnight at room temperature. The mixture was neutralized with K_2CO_3 (aqueous) and extracted with ethyl acetate. The organic layer was washed with brine and dried over anhydrous sodium sulphate. The solvent was removed and the crude product was chromatographed over silica gel

Elution with a mixture (1:9) of ethyl acetate and petroleum ether gave 9-(2,6-dimethylphenyl)acridine in 45% yield, mp 219-220 °C, after recrystallization from a mixture (1:1) of petroleum ether and ethyl acetate. ^{1}H NMR (300 MHz, $CDCl_3$) δ 1.74 (6H, s), 7.26 (2H, d, J = 7.5 Hz), 7.39 (3H, m), 7.49 (2H, d, J = 8.5 Hz), 7.78 (2H, m), 8.30 (2H, d, J = 8.7 Hz); ^{13}C NMR (75 MHz, $CDCl_3$) δ 149.23, 146.79, 137.02, 136.33, 135.18, 130.37, 130.07, 128.61, 127.79, 126.16, 126.14, 125.01, 20.22. FAB-MS (m/z): Calcd for $C_{21}H_{17}N$: 283.37; Found: 284.49 (M+1).

2.5.2.2. General procedure for the synthesis of the acridinium derivatives 1-8.

To a stirred solution of the corresponding acridine derivative (1 mmol) in dry acetonitrile, excess methyl iodide (20 mmol) was added at room temperature. The reaction mixture was refluxed for 6-8 h, while circulating with cold water. The precipitated product was filtered, washed with dry acetonitrile and recrystallized from a mixture (1:1) of dichloromethane-ethyl acetate to give **1-8** in good yields.

10-Methylacridinium iodide (1): 79%; mp 230-232 °C; ^{1}H NMR (300 MHz, DMSO-d_6) δ 4.87 (3H, s), 8.05 (2H, t, J = 7.5 Hz), 8.48 (2H, t, J = 8 Hz), 8.63 (2H, d, J = 8.4 Hz), 8.79 (2H, d, J = 9.2 Hz), 10.21 (1H, s); ^{13}C NMR (75 MHz, DMSO-d_6) δ 150.96, 141.69, 139.43, 131.98, 128.15, 126.60, 119.36, 39.44. Anal. Calcd.for $C_{14}H_{12}IN$: C, 52.36; H, 3.77; N, 4.36. Found: C, 52.36; H, 3.51; N, 4.53.

9,10-Dimethylacridinium iodide (2): 76%, mp 248-249 °C; ^{1}H NMR (300 MHz, DMSO-d_6) δ 3.48 (3H, s), 4.77 (3H, s), 8.01 (2H, t, J = 7.2 Hz), 8.41 (2H, t, J = 7.4 Hz), 8.72 (2H, d, J = 9.2 Hz), 8.89 (2H, d, J = 8.2 Hz); ^{13}C NMR (75 MHz,

DMSO-d_6) δ 149.76, 138.85, 136.22, 127.42, 125.55, 124.71, 120.51, 39.59, 15.36. Anal. Calcd. for $C_{15}H_{14}IN$: C, 53.75; H, 4.21; N, 4.18. Found: C, 53.87; H, 4.07; N, 4.18.

*9-Phenyl-10-methylacridinium iodide (**3**)*: 71%; mp 201-202 °C; ^{1}H NMR (300 MHz, DMSO-d_6) δ 4.93 (3H, s), 7.54-7.56 (2H, m), 7.75-7.80 (3H, m), 7.92 (4H, d, J = 3.7 Hz), 8.44-8.49 (2H, m), 8.88 (2H, d, J = 9.2 Hz); ^{13}C NMR (75 MHz, DMSO-d_6) δ 160.95, 141.76, 138.97, 133.66, 130.67, 130.35, 130.06, 129.41, 128.49, 126.08, 119.81, 39.52. Anal. Calcd. for $C_{20}H_{16}IN$: C, 60.47; H, 4.06; N, 3.53. Found: C, 60.55; H, 4.03; N, 3.27.

*9-(4-Methylphenyl)-10-methylacridinium iodide (**4**)*: 71%; mp 228-230 °C; ^{1}H NMR (300 MHz, DMSO-d_6) δ 2.54 (3H, s), 4.93 (3H, s), 7.47 (2H, d, J = 8 Hz), 7.58 (2H, d, J = 7.9 Hz), 7.90-7.99 (4H, m), 8.46 (2H, t, J = 7.7 Hz), 8.85 (2H, d, J = 9.3 Hz). ^{13}C NMR (75 MHz, DMSO-d_6) δ 161.26, 141.67, 140.41, 138.88, 130.66, 130.40, 130.11, 129.92, 128.35, 126.09, 119.75, 39.62, 21.54. Anal. Calcd. for $C_{21}H_{18}IN$: C, 61.33; H, 4.41; N, 3.41. Found: C, 61.60; H, 4.39; N, 3.48.

*9-(3-Methylphenyl)-10-methylacridinium iodide (**5**)*: 68%; mp 220-222 °C; ^{1}H NMR (300 MHz, DMSO-d_6) δ 1.86 (3H, s), 4.95 (3H, s), 7.36 (1H, d, J = 7.5 Hz), 7.57 (1H, t, J = 7.3 Hz), 7.63-7.72 (2H, m), 7.78 (2H, d, J = 8.6 Hz), 7.95 (2H, t, J = 7.6 Hz), 8.48 (2H, t, J = 7.9 Hz), 8.90 (2H, d, J = 9.2 Hz); ^{13}C NMR (75 MHz, DMSO-d_6) δ 160.72, 141.76, 139.04, 136.33, 133.30, 131.16, 130.72,

129.92, 129.40, 128.75, 126.78, 125.96, 120.03, 39.63, 19.76. Anal. Calcd. for $C_{21}H_{18}IN$: C, 61.33; H, 4.41; N, 3.41. Found: C, 61.08; H, 4.18; N, 3.51.

*9-(2-Methylphenyl)-10-methylacridinium iodide (**6**)*: 60%; mp 224-225 °C; ^{1}H NMR (300 MHz, DMSO-d_6) δ 1.87 (3H, s), 4.97 (3H, s), 7.36 (1H, d, J = 7.5 Hz), 7.57 (1H, t, J = 7.3 Hz), 7.63-7.72 (2H, m), 7.78 (2H, d, J = 8.6 Hz), 7.95 (2H, t, J = 7.6 Hz), 8.48 (2H, t, J = 7.9 Hz), 8.90 (2H, d, J = 9.2 Hz); ^{13}C NMR (75 MHz, DMSO-d_6) δ 160.72, 141.76, 139.04, 136.33, 133.30, 131.16, 130.72, 129.92, 129.40, 128.75, 126.78, 125.96, 120.03, 39.63, 19.76. Anal. Calcd. for $C_{21}H_{18}IN$: C, 61.33; H, 4.41; N, 3.41. Found: C, 61.55; H, 4.17; N, 3.62.

9-(2,4-Dimethylphenyl)-10-methylacridinium iodide (7): 65%; mp 242-245 °C; ^{1}H NMR (300 MHz, DMSO-d_6) δ 1.82 (3H, s), δ 2.49 (3H, s), 4.92 (3H, s), 7.23 (1H, d, J = 7.5 Hz), 7.35 (1H, d, J = 7.8 Hz), 7.44 (1H, s), 7.80 (2H, d, J = 8.4 Hz), 7.92 (2H, t, J = 7.2 Hz), 8.46 (2H, t, J = 7.5 Hz), 8.86 (2H, d, J = 9 Hz); ^{13}C NMR (DMSO-d_6, 75 MHz) δ 160.71, 141.24, 139.79, 138.51, 135.71, 131.28, 129.95, 129.45, 129.06, 128.17, 126.90, 125.65, 119.44, 39.79, 20.94, 19.21. FAB-MS (m/z): Calcd for $C_{22}H_{20}N$: 298.40; Found: 298.23; Anal. Calcd. for $C_{22}H_{20}IN$: C, 62.28; H, 4.51; N, 3.30. Found: C, 62.31; H, 4.41; N, 3.63.

*9-(2,6-Dimethylphenyl)-10-methylacridinium iodide (**8**)*: 63%; mp 255-257 °C; ^{1}H NMR (300 MHz, DMSO-d_6) δ 1.71 (6H, s), 4.95 (3H, s), 7.44 (2H, d, J = 7.5 Hz), 7.56 (1H, m), 7.73 (2H, m), 7.94 (2H, m), 8.47 (2H, m), 8.91 (2H, d, J = 9.2 Hz); ^{13}C NMR (75 MHz, DMSO-d_6) δ 160.23, 141.57, 138.85, 135.87, 132.60,

130.25, 128.83, 128.29, 128.18, 125.32, 120.02, 39.95, 19.75. FAB-MS (m/z): Calcd for $C_{22}H_{20}N$: 298.40; Found: 298.58.

2.5.3. DNA Binding Studies

DNA binding studies with various probes were carried out in 10 mM phosphate buffer (pH 7.4) containing either 2 mM or 100 mM NaCl. [26b-c,34a] Solution of calf thymus DNA (CT DNA) was filtered through a 0.45 μM Millipore filter. The concentrations of CT DNA solutions were determined by using the average extinction coefficient value of 6600 M^{-1} cm^{-1} for a single nucleotide at 260 nm.[35] The absorption and fluorescence titrations with DNA were carried out by adding small aliquots of DNA solution containing the same concentration of the compound as that in the test solution. The concentrations of the polyoligonucleotides such as poly(dG).poly(dC) and poly(dA).poly(dT) were determined by using the average extinction coefficient value of 7400 M^{-1} cm^{-1} at 253 nm for poly(dG).poly(dC) and 6000 M^{-1} cm^{-1} at 260 nm for poly(dA).poly(dT). For the single strand DNA, all conditions were the same except that the CT DNA solution was heated in a boiling water bath for 30 min in order to denature the DNA. Complete denaturation was confirmed by comparing the absorption ratio at 260 nm for the heated (ssDNA) and non-heated (dsDNA) samples. A value of 1.32 was obtained in good agreement with the literature value.[36] DNA association constants were calculated using fluorescence quantum

yields, and according to the method of McGhee and von Hippel by using the data points of the Scatchard plot.[23-24]

The rate constant for the static quenching of the singlet excited state[37] of the acridinium chromophore by DNA (k) was evaluated using equation 2.4,

$$I_o/I = 1 + k/k_{SI} \qquad (2.4)$$

where, I_o and I are the fluorescence intensities in the absence and presence of ssDNA and k_{SI} is the sum of rate constants ($k_r + k_{nr}$) of the singlet excited state deactivation. The counterion release that accompanies the binding of a ligand to DNA can be obtained from the slope of log K_{ass} versus $-\log[Na^+]$ according to the equation 2.5,

$$\frac{-\delta \log K_{ass}}{\delta \log [Na^+]} = -Z\psi \qquad (2.5)$$

where Z is charge of the ligand and ψ represents the average number of condensed and screened sodium ions associated with the DNA phosphate group.

References

a) Waring, M. J. *Annu. Rev. Biochem.* **1981**, *50*, 159-192. (b) Tomasz, M. In *Molecular Aspects of Anticancer-Drug Interactions*; Neidle, S., Waring, M. J., Eds.; Macmillan Press: Boca Raton, FL, 1994, Vol. 2, pp 312-349. (c) Bischofberger, N.; Shea, R. G. In *Nucleic Acid Targeted Drug Design*; Propst, C. L., Perun, T. J., Eds.; Dekker: New York, 1992, pp 579-612.

2. (a) Wilson, W. D.; Jones, R. L. In *Intercalator Chemistry*, Whittingham, M. S., Jacobson, A. J., Eds.; Academic Press: New York, 1982, pp 445-474. (b) Sigman, D. S. *Acc. Chem. Res.* **1986**, *19*, 180-186. (c) Kumar, C. V.; Asuncion, E. H. *J. Am. Chem. Soc.* **1993**, *115*, 8547-8553.

3. Boon, E. M.; Barton, J. K. *Bioconjugate Chem.* **2003**, *14*, 1140-1147.

4. O' Neil, L. L.; Wiest, O. *J. Am. Chem. Soc.* **2005**, *127*, 16800-16801.

5. Han, H.; Langley, D. R.; Rangan, A.; Hurley, L. H. *J. Am. Chem. Soc.* **2001**, *123*, 8902-8913.

6. Xu, Y.; Zhang, Y. X.; Sugiyam, H.; Umano, T.; Osuga, H.; Tanaka, K. *J. Am. Chem. Soc.* **2004**, *126*, 6566-6567.

7. (a) Pindur, U.; Haber, M.; Sattler, K. *J. Chem. Ed.* **1993**, *70*, 263-272. (b) Gao, Q.; Williams, L. D.; Egli, M.; Rabinovich, D.; Chen, S. -L.; Quigley, G. J.; Rich, A. *Proc. Natl. Acad. Sci. USA* **1991**, *88*, 2422-2426.

8. (a) Sitlani, A.; Long, E. C.; Pyle, A. M.; Barton, J. K. *J. Am. Chem. Soc.* **1992**, *114*, 2303-2312. (b) Barton, J. K.; Lolis, E. *J. Am. Chem. Soc.* **1985**, *107*, 708-709. (c) Pyle, A. M.; Rehmann, J. P.; Meshoyrer, R.; Kumar, C. V.; Turro, N. J.; Barton, J. K. *J. Am. Chem. Soc.* **1989**, *111*, 3051-3058.

9. Carreon, J. R.; Mahon, K. P., Jr.; Kelley, S. O. *Org. Lett.* **2004**, *6*, 517-519.

10. Goldman, A. In *Nucleic acids in chemistry and biology: Interaction of proteins with nucleic acids*; Blackburn, G. M.; Gait, M. J., Eds.; Oxford University Press: Oxford, 1996, pp 380-381.

11. (a) Joseph, J.; Kuruvilla, E.; Achuthan, A. T.; Ramaiah, D.; Schuster, G. B. *Bioconjugate Chem.* **2004**, *15*, 1230-1235. (b) Kuruvilla, E.; Joseph, J.; Ramaiah, D. *J. Phys. Chem. B* **2005**, *109*, 21997-22002.

12. Lerman, L. S. *J. Mol. Biol.* **1961**, *3*, 18-30.

13. (a) Waring, M. J. *J. Mol. Biol.* **1970**, *54*, 247-279. (b) Eldho, N. V.; Joseph, J.; Ramaiah, D. *Chem. Lett.*, **2001**, 438-439. (c) Joseph, J.; Eldho, N. V.; Ramaiah, D. *J. Phys. Chem. B* **2003**, *107*, 4444-4450. (d) Joseph, J.; Eldho, N. V.; Ramaiah, D. *Chem. Eur. J.* **2003**, *9*, 5926-5935.

14. Bernthsen, A. *Justus Liebigs Ann. Chem.* **1884**, *224*, 1-56.

15. Weber, G.; Teale, F. W. J. *Trans. Faraday Soc.* **1957**, *53*, 646-655.

16. (a) Rehm, D.; Weller, A. *Ber. Bunsenges Phys. Chem.* **1969**, *73*, 834-839. (b) Weller, A. *Z. Phys. Chem.* **1982**, *133*, 93-98.

17. Kavarnos, G. J. In *Fundamentals of Photoinduced Electron Transfer*, VCH Publishers, Inc., New York, 1993, p. 39.

18. Mann, C. K.; Barnes, K. K. In *Electrochemical Reactions in Non-aqueous Systems*, Marcel Dekker, Inc., New York, 1970.

19. Murov, S. L.; Carmichael, I.; Hug, G. L. In *Handbook of Photochemistry*, II[nd] Edition, Marcel Dekker, Inc., New York, 1993.

20. Benniston, A. C.; Harriman, A.; Li, P.; Rostron, P. J.; van, Ramesdonk, H. J.; Groeneveld, M. M.; Zhang, H.; Verhoeven, J. W. *J. Am. Chem. Soc.* **2005**, *127*, 16054-16064.

21. Jones, G., II.; Farahat, M. S.; Greenfield, S. R.; Gosztola, G. J.; Wasielewski, M. R. *Chem. Phys. Lett.* **1994**, *229*, 40-46.

22. van Willigen, H.; Jones, G., II.; Farahat, M. S. *J. Phys. Chem. B* **1996**, *100*, 3312-3316.

23. Scatchard, G. *Ann. N. Y. Acad. Sci.* **1949**, *51*, 660-672.

24. McGhee, J. D.; Von Hippel, P. H. *J. Mol. Biol.* **1974**, *86*, 469-489.

25. Rogers, J. E.; Le, T. P.; Kelly, L. A. *Photochem. Photobiol.* **2001**, *73*, 223-229.

26. (a) Reinert, K. E. *Nucleic Acids. Res.* **1983**, *11*, 3411-3430. (b) Breslin, D. T.; Coury, J. E.; Anderson, J. R.; McFail-Isom, L.; Kan, Y.; Williams, L. D.; Bottomley, L. A.; Schuster, G. B. *J. Am. Chem. Soc.* **1997**, *119*, 5043-5044.

27. Ardhammar, M.; Kurucsev, T.; Nordén, B. (2000) In *Circular dichroism: principles and application*; Berova, N.; Nakanishi, K.; Woody, R. W., Eds.; Wiley-VCH, Chapter 26.

28. Becker, H.; Nordén, B. *J. Am. Chem. Soc.* **1997**, *119*, 5798-5803.

29. Rye, H. S.; Glazer, A. N. *Nucleic Acids Res.* **1995**, *23*, 1215-1222.

30. Petty, J. T.; Bordelon, J. A.; Robertson, M. E. *J. Phys. Chem. B* **2000**, *104*, 7221-7227.

31. Drirscoll, R. J.; Youngquist, M. G.; Baldeschwieler, J. D. *Nature* **1990**, *346*, 294.

32. Brett, A. M. O.; Chiorcea, A. *Langmuir* **2003**, *19*, 3830-3839.

33. (a) Avirah, R. R.; Jyothish, K.; Ramaiah, D. *Org. Lett.* **2007**, *9*, 121-124. (b) Jyothish, K.; Avirah, R. R.; Ramaiah, D. *Org. Lett.* **2006**, *8*, 111-114. (c) Jyothish, K.; Arun, K. T.; Ramaiah, D. *Org. Lett.* **2004**, *6*, 3965-3968.

34. (a) Neelakandan, P. P.; Hariharan, M.; Ramaiah, D. *J. Am. Chem. Soc.* **2006**, *128*, 11334-11335. (b) Jisha, V. S.; Arun, K. T.; Hariharan, M.; Ramaiah, D. *J. Am. Chem. Soc.* **2006**, *128*, 6024-6025. (c) Hariharan, M.; Joseph, J.; Ramaiah, D. *J. Phys. Chem. B* **2006**, *110*, 24678-24686. (d) Arun, K. T.; Ramaiah, D. *J. Phys. Chem. A* **2006**, *109*, 5571-5578.

35. Baguley, B. C.; Falkenhaug, E. M. *Nucleic Acids Res.* **1978**, *5*, 161-171.

36. Wolfe, A.; Shimer, G. H. Jr.; Meehan, T. *Biochemistry* **1987**, *26*, 6392-6396.

37. Rogers, J. E.; Le, T. P.; Kelly, L. A. *Photochem. Photobiol.* **2001**, *73*, 223-229.

Chapter 3

MONO- AND BIS-INTERCALATING ACRIDINIUM SYSTEMS AND STUDY OF THEIR PHOTOSENSITIZED OXIDATION OF NUCLEOTIDES AND DNA

3.1. Abstract

Novel bisacridinium derivatives **1** and **2** with varying polymethylene spacer group and the acridinium derivatives **3** and **4** were synthesized and their DNA binding interactions as well as DNA oxidation efficiencies have been investigated by various photophysical and biophysical techniques. The absorption spectra of these systems showed bands in the region 300-475 nm, corresponding to the acridinium chromophore. The bifunctional derivatives **1** and **2**, exhibited quantitative fluorescence yields (Φ_f = 0.91 and 0.98) and long lifetimes (τ = 38.9 and 33.2 ns). DNA binding studies through spectroscopic investigations, CD and viscosity measurements indicate that these systems interact with DNA preferentially through intercalation of the acridinium chromophore and exhibit significant DNA association constants (K_{DNA} = 10^5-10^7 M^{-1}). Among the bifunctional derivatives **1** and **2**, the former undergoes DNA mono-intercalation, whereas the latter exhibits bis-intercalation, however both these were found to undergo only mono-intercalation at higher ionic strength. Laser flash photolysis

studies of bisacridinium derivatives and the monoacridinium derivative **4** in buffer gave transients with absorption maxima in the range 480-500 nm having lifetimes 0.6-3 μs. These transients can be attributed to their triplet excited states based on the quenching studies with molecular oxygen. Excitation of these derivatives in presence of DNA and guanosine monophosphate (GMP) led to the formation of oxidized species like radical cations of DNA and GMP. The efficiency of oxidation of GMP and DNA by these derivatives was further increased in the presence of an efficient electron acceptor such as methylviologen. These results indicate that ionic strength has a profound influence on the DNA mono- and bis-intercalating properties of the novel bisacridinum derivatives and further demonstrate that depending on the spacer and substituents present, these molecules can act as efficient DNA photo-oxidizing agents.

3.2. Introduction

DNA is now seen as the prime target of most of the chemotherapeutical agents and research in this area has made evident the importance of developing molecules which can undergo efficient interactions with DNA.[1-6] Interactions with DNA are not the only the factors that determine the biological activity of these molecules, but their reactivity and selectivity are often correlated with their mode of binding with DNA.[5,6] Therefore, a better understanding of the factors, which govern the interactions of small molecules with DNA, has an important role in the

rational design of various DNA targeted drugs. Of these small molecules, the bifunctional derivatives that can undergo photoinduced electron transfer processes have attracted much attention in recent years for their use in DNA detection, analysis and cleavage.[6-12]

There has been widespread interest in bifunctional molecules joined by various linker groups, in order to obtain molecules of higher DNA binding affinity for use both as chemotherapeutic agents and as probes for nucleic acids.[2,13-21] These molecules can, in principle, bind with DNA through intercalation, bis-intercalation, groove binding and electrostatic interactions, depending on the nature of the chromophore and the spacer group present in them. Le Pecq and coworkers[2] have postulated that bisintercalative binding occurs in a molecule only when the linker chain length is more than 10.2 Å. Such molecules follow the neighbor exclusion principle wherein the DNA interacting chromophores occlude two base pairs between them (Figure 3.1 A). When the spacer group is rigid or insufficient to span two base pairs, such molecules prefer mono-intercalation as shown in Figure 3.1 B.[22-24] Very few examples are reported in the literature that exhibit bis-intercalation, with the violation of the neighbor exclusion principle as represented in Figure 3.1 C.[15, 24, 25]

Although the interactions of small molecules with DNA have been extensively investigated, the ionic strength dependent interactions of bifunctional molecules bearing two different DNA binding motifs have received less attention.

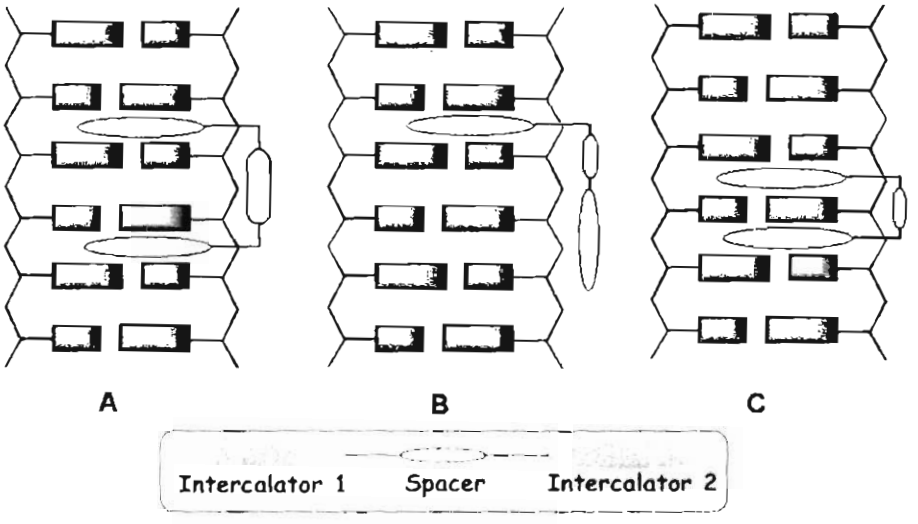

Figure 3.1. Schematic representation of DNA interactions of a small molecule bearing two intercalating motifs: (**A**) bis-intercalation (**B**) mono-intercalation and (**C**) bis-intercalation with the violation of neighbor exclusion principle.

In this context, we have designed novel acridine based bifunctional conjugates, not only because of their interesting chemical and physical properties, but due to their immense utility in the pharmaceutical and dye industries.[13-14,18-19,26] The derivatives of acridine exhibit a broad range of chemotherapeutic properties against prokaryotic and eukaryotic cells, because of their ability to interact with DNA. Although, the antitumor acridines are known to exert their activity through DNA intercalation,[5,6] their interaction with topoisomerase II and inhibition of DNA processing enzymes such as polymerases and telomerase might also contribute to the overall biological activity.[27-28] Our objectives were to study the ionic strength and spacer length dependent DNA binding properties of bisacridinium derivatives **1** and **2** (Chart 3.1) and also to investigate their

efficiency of DNA oxidation. These derivatives with polymethylene spacers linked directly to the 9-position of the acridine ring are easier to synthesize and are different from the previously reported bisacridines, where the spacers are linked

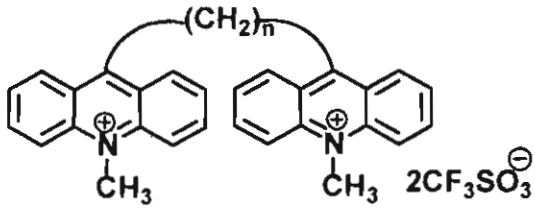

1) n = 5
2) n = 10

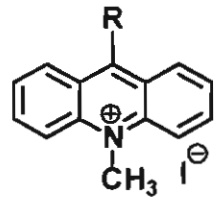

3) R = CH_3
4) R = 2,4 -dimethylphenyl

Chart 3.1

through the amino functionality.[14] The acridinium derivatives exhibit significant quenching in the fluorescence emission in the presence of DNA and the redox potentials and excited state properties of the derivatives indicate that the electron transfer from the DNA bases to the acridinium moiety is responsible for the quenching observed. Our results reveal that the bisacridinium derivatives **1** (r = 7.6 Å) and **2** (r = 12.6 Å) undergo mono- and bis-intercalation, respectively, at low ionic strength (2 mM NaCl), but exhibit only mono-intercalative interactions at the higher ionic strength (100 mM NaCl). These bifunctional systems which show quantitative fluorescence yields and exhibit chromophore selective and spacer length and ionic strength dependent interactions with DNA can have potential applications as fluorescent probes in biology.

3.3. Results and Discussion

3.3.1. Synthesis

The bisacridine derivatives with pentamethylene and decamethylene spacers were synthesized by a modified Bernthsen procedure as shown in Scheme 3.1.[29] The condensation reaction of diphenylamine (**5**) with the corresponding dicarboxylic acid in the presence of anhydrous $ZnCl_2$ yielded the acridine derivatives **6** and **7** in 50-60% yields. The quarternization of these acridine derivatives with methyl iodide or methyl trifluoromethanesulphonate gave the corresponding acridinium derivatives (**1-2**) in quantitative yields. All these compounds were characterized on the basis of spectral data and analytical results.

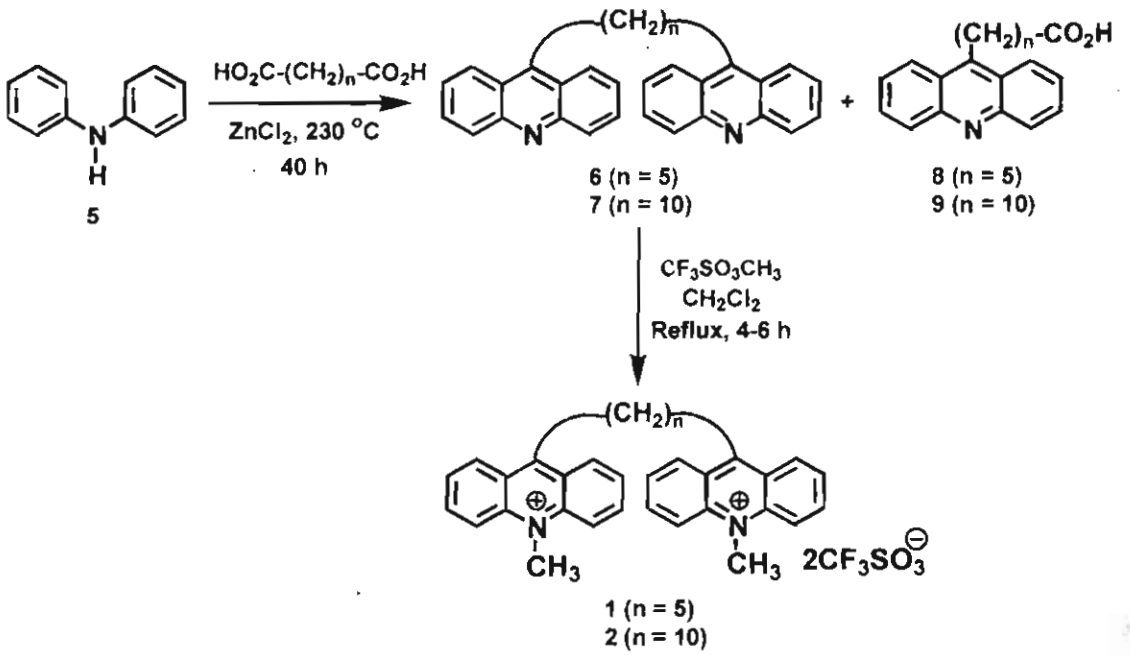

Scheme 3.1

For example, in the ^1H NMR spectrum of the bifunctional derivatives **1** and **2**, two methyl groups linked to two quaternary nitrogen of the acridinium moieties

appeared as singlet at δ 4.81, while the aliphatic protons of the spacer group appeared as multiplets in the region between δ 1.82–3.97 and δ 1.15–3.98, respectively. Characteristically, the bisacridinium derivatives exhibited symmetrical structure and hence we obtained peaks corresponding to 11 and 13 carbon, respectively for **1** and **2**, in their ^{13}C NMR spectra. These derivatives showed high solubility in aqueous medium as demonstrated by various photophysical experiments.

3.3.2. Absorption and Fluorescence Properties

Figures 3.2 and 3.3 show the absorption and fluorescence emission spectra, respectively of the bifunctional derivatives **1**, **2** and the model acridinium derivative **3** in aqueous medium, while their photophysical properties are summarized

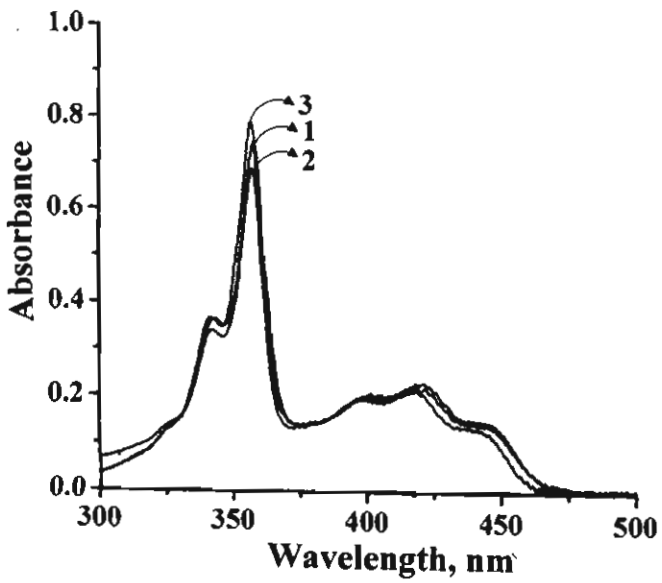

Figure 3.2. Absorption spectra of acridinium derivatives **1**, **2** and **3** in water.

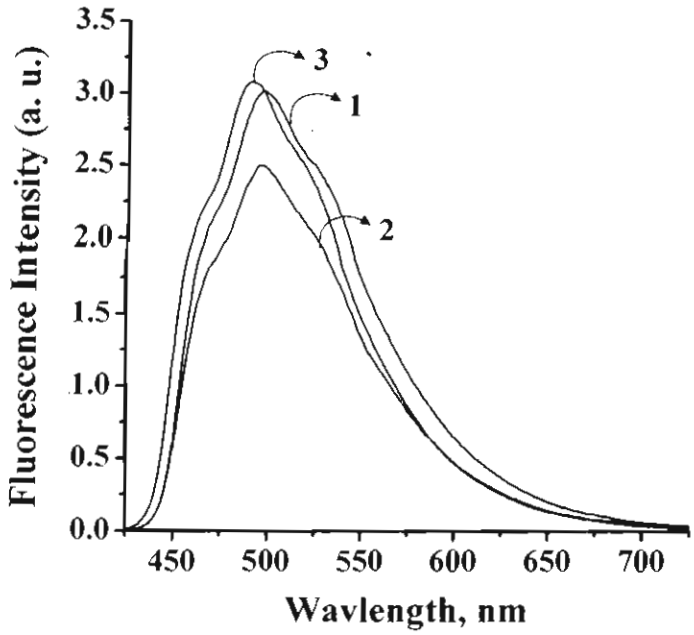

Figure 3.3. Fluorescence spectra of acridinium derivatives **1**, **2** and **3** in water.

in Table 3.1. In all these cases acridinium chromophore exhibits absorption in the region 300-470 nm. As shown in Figure 3.3, the bisacridinium derivatives **1** and **2** and the model compound, **3** exhibit fluorescence emission in the range 425-550 nm, with quantitative fluorescence quantum yields (ϕ_f = 0.91, 0.98 and 1.0, respectively). While the fluorescence emission maximum of the bisacridinium derivatives **1** and **2** were found to be 496 nm, the model acridinium derivative **3** showed an emission maximum at 490 nm. Nanosecond time resolved fluorescence studies indicate that the compounds **1** and **2** showed single exponential decays with lifetimes of 38.9 and 33.2 ns (Figure 3.4), respectively while the derivative **3** exhibited a lifetime of 33.8 ns (Table 3.1).

Table 3.1. Photophysical and DNA Binding Properties of the Bifunctional Derivatives **1**, **2** and **3**[a]

Compd	λ_{ab}, nm (ε, $M^{-1}cm^{-1}$)	λ_{em}, nm	Φ_f[b]	τ, ns	K_{DNA} (M^{-1})[c]	n[e]
1	358 (33200) 421 (9450)	496	0.91	38.9	4.3×10^6 (4.5×10^5)[d]	2.7
2	358 (33600) 418 (10100)	496	0.98	33.2	2.5×10^7 (4.31×10^5)[d]	2
3	357 (19100) 416 (5000)	490	1	33.8	7.31×10^5 (6.34×10^4)[d]	2.5

[a]Average of more than two experiments and error ca. ±5%. The photophysical and DNA binding properties were examined 10 mM phosphate buffer containing 2 mM and [d]100 mM NaCl (pH 7.4), respectively. [b]Fluorescence quantum yields were calculated using 10-methylacridinium trifluoromethane sulfonate as the standard (Φ_f = 1).[30] [c]DNA association constants determined by the Scatchard analysis of fluorescence titration data. [e] Number of nucleotides occluded by a bound ligand.[31]

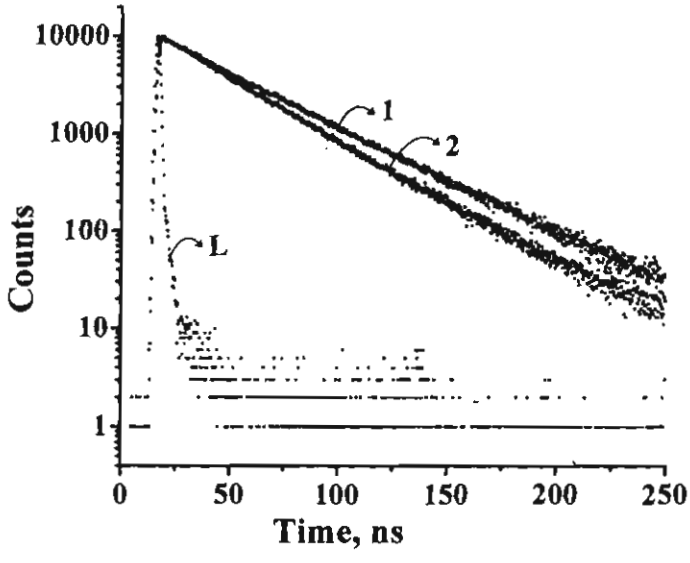

Figure 3.4. Fluorescence decay profiles of **1** and **2** in water along with the lamp profile (**L**). Excitation wavelength, 355 nm.

3.3.3. DNA Binding Properties

The change in the absorption and fluorescence emission properties of the bisacridinium derivatives **1** and **2** with added DNA concentrations are shown in Figures 3.5-3.7, respectively. The bisacridinium derivative **1** showed significant hypochromicity in the absorption spectrum upto a [DNA]/[Ligand] ratio of 12 (0.14 mM of DNA), after which a small increase in the absorption spectrum was observed (Inset of Figure 3.5). Similarly, a strong fluorescence quenching of **1** was observed upto a DNA concentration of 0.14 mM, thereafter the addition of DNA induced a negligible effect as shown in Figure 3.6. The changes observed in

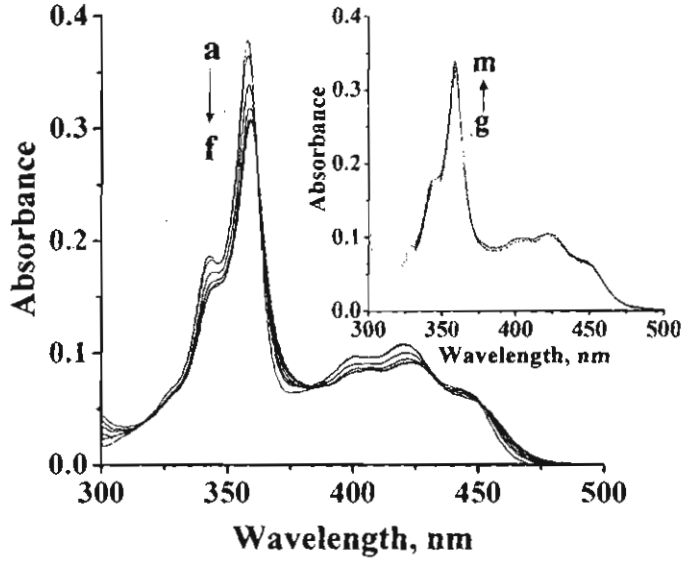

Figure 3.5. Change in absorption spectra of bisacridinium derivative **1** (11.4 μM), with increasing DNA concentrations in 10 mM phosphate buffer containing 2 mM NaCl. [DNA] (a) 0, (b) 0.024, (c) 0.048, (d) 0.072, (e) 0.096 and (f) 0.12 mM and in the inset (g) 0.14, (h) 0.17, (i) 0.19, (j) 0.24, (k) 0.28, (l) 0.38 and (m) 0.47 mM.

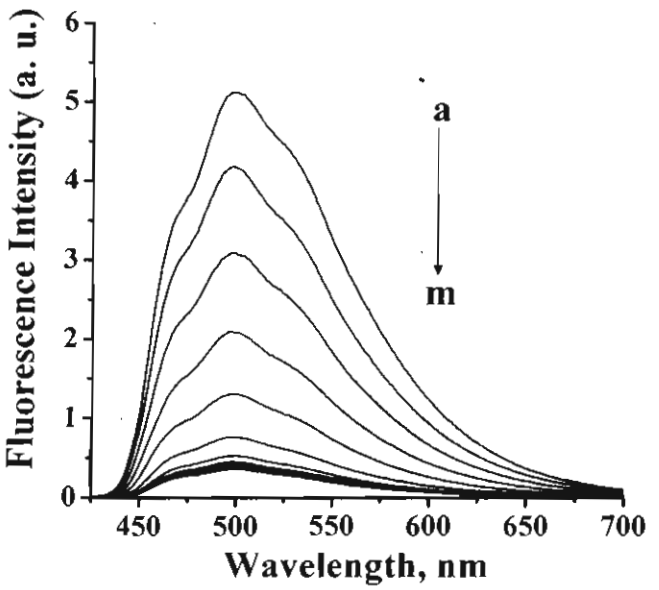

Figure 3.6. Change in fluorescence spectra of bisacridinium derivative **1** (11.4 μM), with increasing DNA concentrations in 10 mM phosphate buffer containing 2 mM NaCl. [DNA] (a) 0, (b) 0.024, (c) 0.048, (d) 0.072, (e) 0.096, (f) 0.12 mM, (g) 0.14, (h) 0.17, (i) 0.19, (k) 0.28 and (m) 0.47 mM. Excitation wavelength, 363 nm.

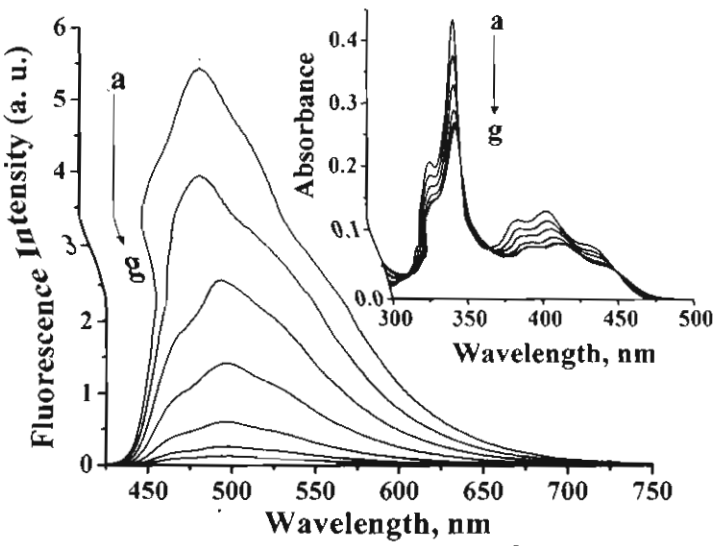

Figure 3.7. Change in fluorescence spectra of bisacridinium derivative **2** (12.8 μM) in 10 mM phosphate buffer containing 2 mM NaCl with increasing concentration of CT DNA. [DNA] (a) 0, (b) 0.024, (c) 0.048, (d) 0.072, (e) 0.096, (f) 0.12 and (g) 0.14 mM. Inset shows the corresponding changes in the absorption spectra. Excitation wavelength, 363 nm.

the absorption and fluorescence emission spectra of the bisacridinium conjugate **2** in the presence of DNA (Figure 3.7) were significantly higher, when compared to the changes observed for the bisacridinium derivative **1**. The bisacridinium derivative **1** with polymethylene spacer n = 5, showed ca. 20% hypochromicity in the absorption spectrum in presence of 0.14 mM DNA. In contrast, the bisacridinium conjugate **2** with polymethylene spacer n = 10, exhibited nearly ca. 41% hypochromicity under similar conditions. Similarly, contrasting effects were observed in the fluorescence properties of **1** and **2** in the presence of DNA. The bisacridinium derivative **2** undergoes efficient fluorescence quenching upon binding with DNA, when compared to the conjugate **1**. At any DNA concentration, the quenching in fluorescence emission observed in the case of the bisacridinium derivative **2** is more than twice than that of **1**, suggesting its greater affinity for DNA. The quenching in fluorescence of the bisacridinium derivatives is attributed to the favorable electron transfer from the DNA bases to the excited state of the acridinium chromophore.[30,37]

The DNA association constants (K_{DNA}) of **1-3** were determined based on the fluorescence titrations and according to the method of McGhee and von Hippel using the data points of the Scatchard plot.[31] The bisacridinium conjugate **1**, exhibited an association constant of $K_{DNA} = 4.3 \times 10^6\ M^{-1}$, which is around 6-fold lower value than that of the bisacridinium derivative **2** ($K_{DNA} = 2.5 \times 10^7\ M^{-1}$). Since these derivatives are cationic in nature, the involvement of the electrostatic

interactions in these derivatives was confirmed by the observation of lesser extent of quenching in fluorescence emission in buffer containing 100 mM NaCl. The binding constant for the bisacridinium derivative **1** ($K_{DNA} = 4 \times 10^5\ M^{-1}$) was found to be one order less in buffer containing 100 mM NaCl, when compared to the value obtained at 2 mM NaCl (Table 1). In the case of the derivative **2**, the binding constant at 100 mM NaCl was found to be two orders of magnitude less than that observed at 2 mM NaCl. Similarly at even higher ionic strengths, for example, at 1 M NaCl the binding constants were found to be in the order of $10^4\ M^{-1}$ for these derivatives. The changes in the fluorescence and absorbance spectra of the bisacridinium derivatives with increasing DNA concentrations at higher ionic strengths shown in Figures 3.8-3.11

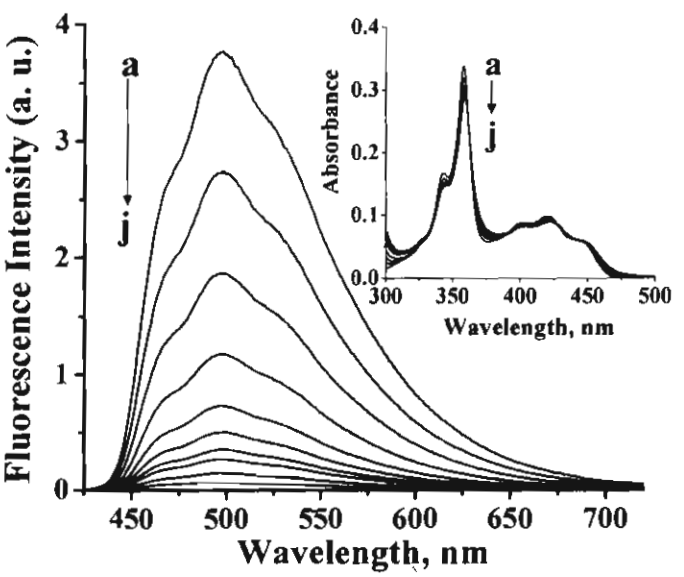

Figure 3.8. Change in fluorescence spectra of **1** (10 μM) in 10 mM phosphate buffer containing 100 mM NaCl with increasing concentration of CT DNA. Inset shows the corresponding changes in the absorption spectra. [DNA] (a) 0, (b) 0.048, (c) 0.096, (d) 0.14, (e) 0.19, (f) 0.24, (g) 0.28, (h) 0.33, (i) 0.47 and (j) 0.9 mM. Excitation wavelength, 363 nm.

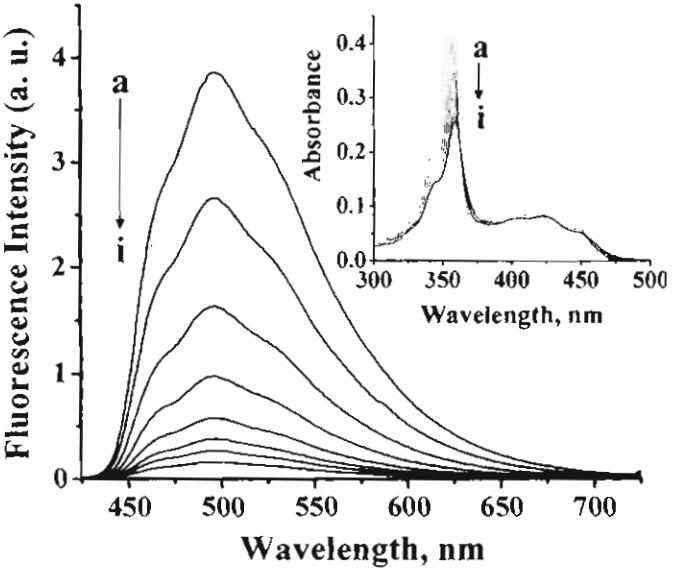

Figure 3.9. Change in fluorescence spectra of **2** (12 μM) in 10 mM phosphate buffer containing 100 mM NaCl with increasing concentration of CT DNA. Inset shows the corresponding changes in the absorption spectra. [DNA] (a) 0, (b) 0.048, (c) 0.096, (d) 0.14, (e) 0.19, (f) 0.24, (g) 0.28, (h) 0.38 and (i) 0.47 mM. Excitation wavelength, 363 nm.

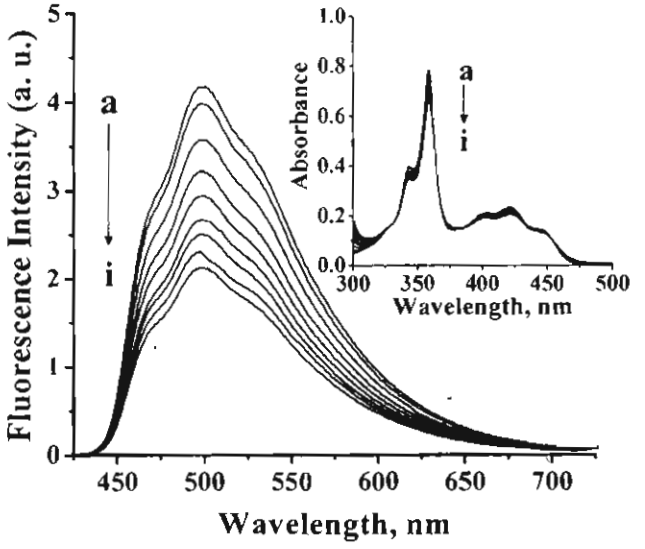

Figure 3.10. Change in flourescence spectra of **1** (12 μM) in 10 mM phosphate buffer containing 1 M NaCl with increasing concentration of CT DNA. Inset shows the corresponding changes in the absorption spectra. [DNA] (a) 0, (b) 0.048, (c) 0.096, (d) 0.14, (e) 0.19, (f) 0.24, (g) 0.28, (h) 0.38 and (i) 0.47 mM. Excitation wavelength, 363 nm.

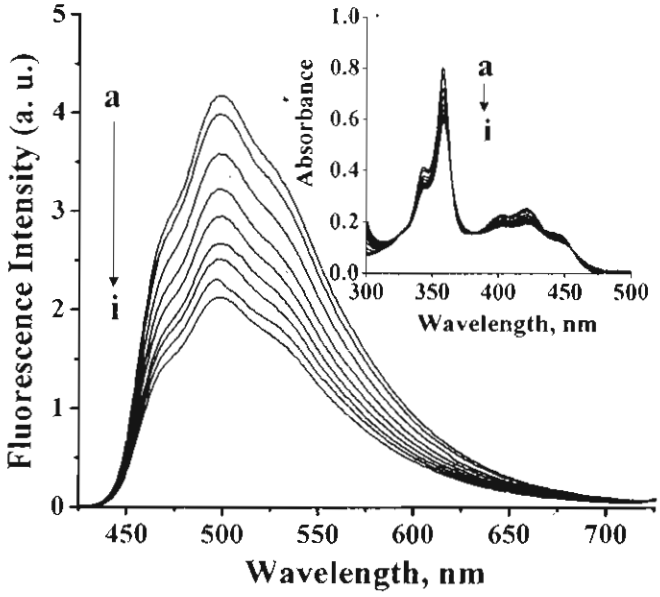

Figure 3.11. Change in fluorescence spectra of **2** (12 μM) in 10 mM phosphate buffer containing 1 M NaCl with increasing concentration of CT DNA. Inset shows the corresponding changes in the absorption spectra. Excitation wavelength, 363 nm. [DNA] (a) 0, (b) 0.048, (c) 0.096, (d) 0.14, (e) 0.19, (f) 0.24, (g) 0.28, (h) 0.38 and (i) 0.47 mM.

indicates that the extent of quenching in fluorescence emission of both the bisacridinium derivatives decreases as the salt concentration increased. Further, we observed significant decrease in fluorescence quenching at or above 1 M NaCl concentration.

3.3.4. Characterization of DNA Binding Interactions

Circular dichroism and viscometry have been used extensively to elucidate the mode of interaction of various DNA binding drugs. The process of intercalation occurs by the unwinding of the double helix to accommodate the ligand that gets stacked between the DNA bases. This process results in

lengthening of the DNA leading to an increased viscosity of DNA.[32] Hence, viscometric studies were carried out to understand the preferred mode of interactions of these derivatives with DNA. *In the* case of the bifunctional derivative **2**, we observed significant change in viscosity of DNA than that observed for the derivative **1** (Figure 3.12). The derivative with longer spacer

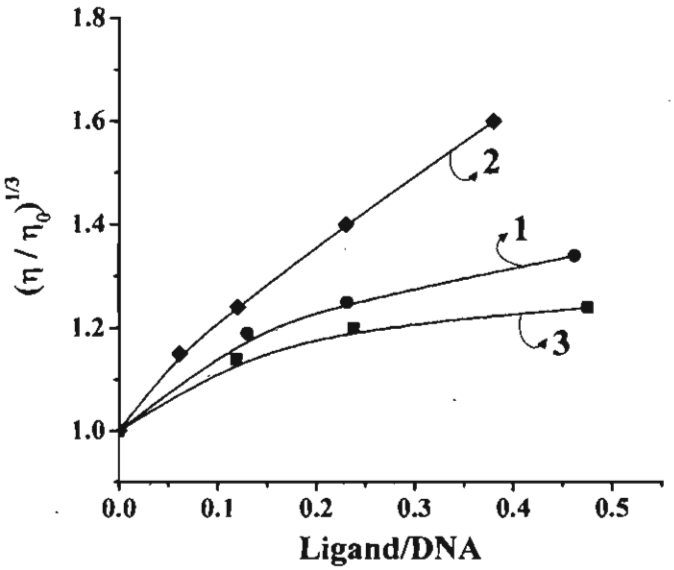

Figure 3.12. Effect of increasing concentrations of the bifunctional derivatives **1**, **2** and **3** on the relative viscosity of CT DNA (0.72 mM) at 26 ± 0.2 ^{0}C in 10 mM phosphate buffer (pH 7.4) containing 2 mM NaCl.

length (n = 10) preferentially undergoes bisintercalation leading to the marked increase in the DNA viscosity when compared to the monointercalating derivatives **1** with shorter spacer length of n = 5 and the model compound **3**.

The complexation of an achiral molecule in a chiral environment can exhibit an induced circular dichroic (ICD) signal in the region of absorption of the achiral ligand.[33] DNA, owing to the presence of asymmetric sugar moieties and helical

structure, exhibits strong CD signal in the wavelength region 180-300 nm. Interaction of ligands with DNA can result in changes in the CD spectrum of the DNA along with the formation of an ICD corresponding to the ligand absorption. Based on the assumption that the interacting molecular systems are at van der Waals distances, ICD can be attributed to the coupling of electrical transition moments of the DNA moiety and the ligand. Hence, knowledge of the magnitude and direction of DNA and ligand transition moments can give significant information regarding the mode of binding.[33] The acridinium derivatives under investigation, being achiral, do not show any CD signal. However, as shown in Figure 3.13, in the presence of DNA, an ICD signal is observed in the chromophore absorption region of the bisacridinium derivatives **1** and **2**, indicating the formation of a strong complex between the derivatives and DNA.

At 3 μM concentration of the derivative **2**, a bisignated CD signal is observed with a positive band and a weak negative band. Under similar conditions, the CD signal observed for **1** has only positive signal, however as shown in the inset of the Figure 3.13, similar bisignated CD signal with comparatively lesser intensity is obtained at higher concentrations of the ligand. This result further supports the observation that the derivative **2** with longer space length (n = 10), forms stronger complex with DNA when compared to the monointercalating derivative **1** with shorter spacer length of n = 5. Increasing the ligand to DNA

ratio increases the intensity of the ICD signal indicating excitonic coupling between the acridinium moieties when bound to DNA.

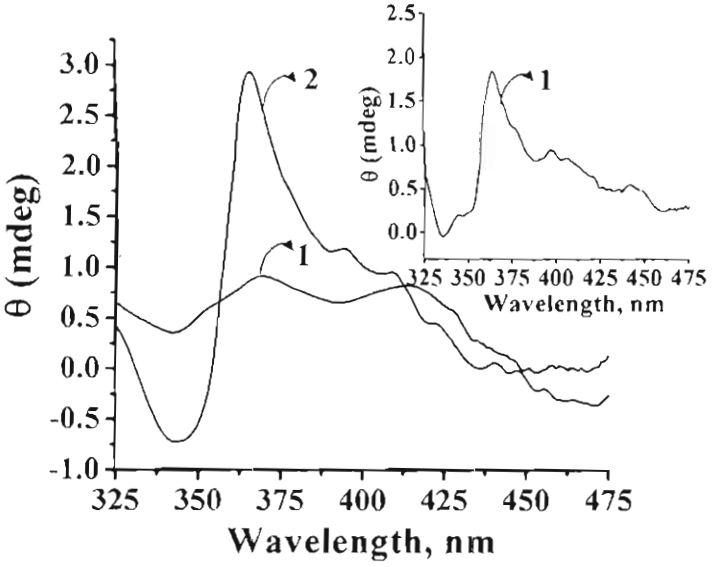

Figure 3.13. Circular dichroism (CD) spectra of **1** (3 μM) and **2** (3 μM) in the presence of dsDNA (0.5 mM) in 10 mM phosphate buffer (pH 7.4) containing 2 mM NaCl. Inset shows the CD spectra of **1** (8.7 μM) under similar conditions.

The dependence of the association constants on the Na^+ ion concentration indicates the role of electrostatic interactions in the binding of these derivatives with DNA. The effect of salt on the binding constant was used to calculate the sodium ion release per bound ligand.[34] The number of released Na^+ ions obtained from the slopes of the plots of $\log K_{assn}$ vs $-\log[Na^+]$ were found to be 1.9, 2.04 and 0.97, respectively for the bisacridinium derivatives **1** and **2** and the model derivative **3** (Figure 3.14). The values obtained correlates well with the number of positive charges on these derivatives. The non-electrostatic contributions to the binding interactions of these derivatives were calculated using equation 3.1,

$$\ln K_{obs} = \ln K_T^0 + Z\xi^{-1} \ln(\gamma_{\pm}\delta) - Z\Psi \ln [Na^+] \quad (3.1)$$

where, K_T^0 is the equilibrium constant that does not include the free energy of ion release. For the B-form of dsDNA, the dimensionless polymer charge density ξ is 4.2. The variable δ is $0.33b$, where b is the average axial charge spacing (1.7 Å) for B-DNA, while $\gamma_{\pm}$ is the mean activity coefficient at a particular salt concentration. Using the NaCl concentration of 100 mM and its mean activity at

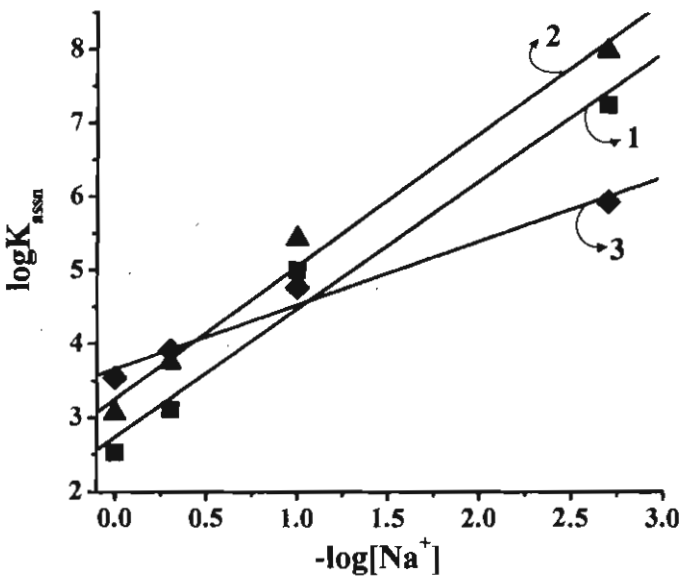

Figure 3.14. Change in the log of association constants of the acridinium derivatives **1-3** with the log of NaCl concentration.

this concentration as 0.78, the non-electrostatic contributions to the free energies of association at 298 K (ΔG_n) were calculated to be -40.6, -41.3 and -31.7 kJ/mol, respectively for the derivatives **1**, **2** and **3**. The ΔG_n values for the bisacridinium derivatives at 100 mM NaCl is less than double the value of the model acridinium derivative, indicating monointercalative interactions of the derivatives at this ionic

strength. The bisacridinium derivatives **1** and **2** have comparable non-electrostatic contributions to the free energy of association at 100 mM NaCl, which is 11 kJ/mol greater than the model acridinium derivative **3**. The similar ΔG_n values for **1** and **2** at 100 mM are consistent with the observation that the bisacridinium derivatives exhibit monointercalation at higher ionic strengths.

The bifunctional derivatives **1** and **2** contain two DNA binding motifs; acridinium chromophores separated by a distance of 7.6 and 12.6 Å, respectively. The observation of higher DNA association constant (ca. 36-fold) for **2**, when compared to the model compound **3**, clearly suggests that both the acridinium moieties present in **2** undergo interactions with DNA through bisintercalation. In contrast, the bifunctional system **1** exhibited only ca. 6-fold higher value of K_{DNA} than that of the model compound **3**, indicating thereby that **1** interacts with DNA through mono-interacalation. The length of the spacer group in this case is not sufficient enough to allow the interaction of both acridinium chromophores through bisintercalation. Furthermore, a comparison of the absorption and fluorescence changes of **1** and **2**, in presence of DNA at different ionic strengths (Figures 3.15-3.16), clearly indicates that these two molecules exhibit different modes of binding interactions with DNA.[40,41] Interestingly, at lower ionic strength (2 mM NaCl), the bisacridinium derivative **1** exhibits relatively small changes in the absorption as well as fluorescence properties with increasing DNA concentration, when compared to that of the derivative **2**. The observed saturation

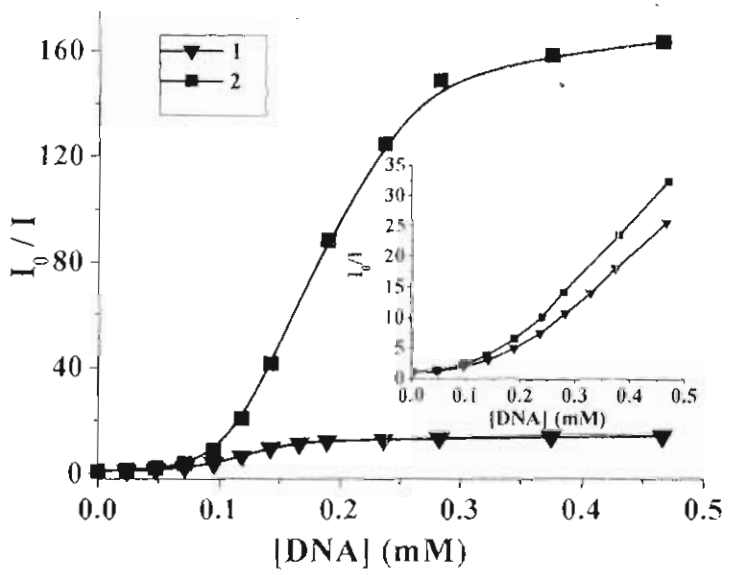

Figure 3.15. Change in fluorescence intensity of the bifunctional derivatives **1** and **2** with increasing concentration of DNA in 10 mM phosphate buffer (pH 7.4) containing 2 mM NaCl. Inset shows the changes in fluorescence intensity of **1** and **2** at higher ionic strength (100 mM NaCl).

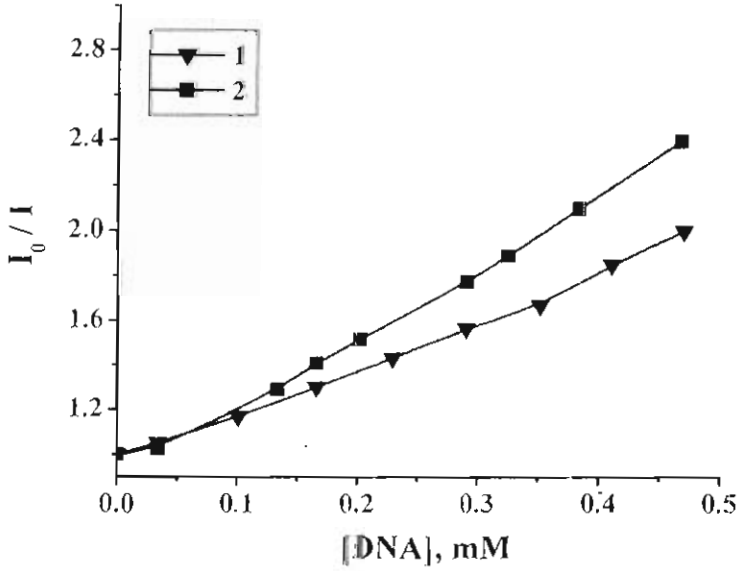

Figure 3.16. Change in fluorescence intensity of the bifunctional derivatives **1** and **2** with increasing concentration of DNA in 10 mM phosphate buffer (pH 7.4) containing 1 M NaCl.

in the fluorescence changes and significant increase in the absorption bands at higher concentrations of DNA, show that at lower ionic strength of the buffer, **1** binds through monointercalation, whereas **2** interacts through bisintercalative interactions. In contrast, at the higher ionic strength of the buffer medium (Inset of Figure 3.15 and Figure 3.16), both these derivatives exhibited identical saturation behavior as well as DNA association constants, confirming thereby that both these systems undergo preferentially monointercalating interactions with DNA under these conditions.

3.3.5. Photosensitized Oxidation of Nucleotides and DNA

Interaction with DNA results in efficient quenching of fluorescence emission of the acridinium derivatives **1**, **2** and the model compound **3**. Based on theoretical calculations this observation could be attributed to the electron transfer from DNA bases to the excited state of acridinium chromophore. Change in free energy values calculated for electron transfer from DNA bases to the singlet excited state of acridinium are ΔG = –0.89, –0.76, –0.58 and –0.48, respectively for guanosine, adenosine, cytidine and thymidine.[35] The reduction potential of acridinium moiety was taken as -0.57 eV *vs* SCE.[36] In order to confirm the electron transfer process, laser flash photolysis studies of the acridinium derivatives were carried out in the presence of DNA and guanosine-5'-monophosphate, which has the lowest oxidation potential among the nucleotides. The electron transfer should in principle lead to the formation of the radical cation

of DNA and the reduced acridine radical. In the case of the bisacridinium derivatives **1** and **2**, the formation of the base radical cation could not be observed clearly, however in the presence of strong electron acceptors such methyl viologen, a transient absorption spectrum with three distinct maxima is observed. Figure 3.17 shows the transient absorption spectrum of the bisacridinium derivative **1** in buffer which could be attributed to the triplet excited state of the acridinium, while Figure 3.18 shows the transient spectrum observed in the presence of DNA and methyl viologen. On the basis of experimental evidence and

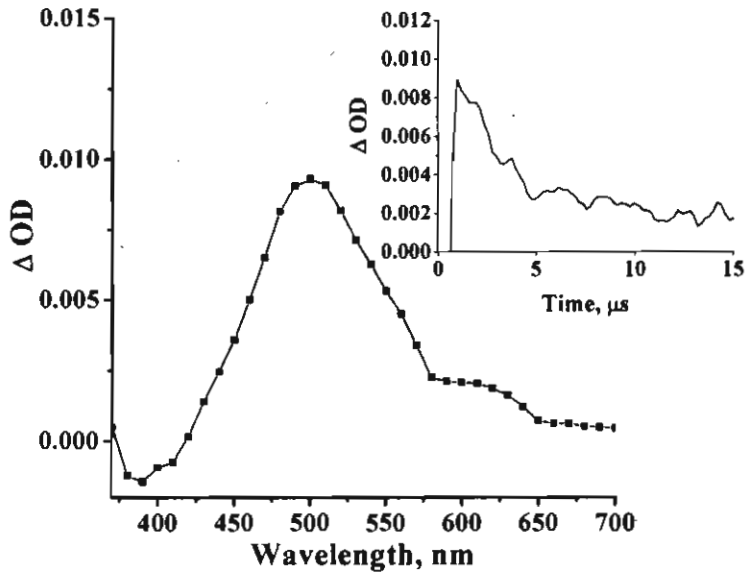

Figure 3.17. Transient absorption spectrum of **1** (40 μM) in argon saturated phosphate buffer (10 mM; pH 7) recorded immediately after 355 nm laser excitation. Inset shows the transient decay at 500 nm.

literature reports,[37,38] the species with a lifetime of 2.2 μs could be attributed to the viologen radical cation and while the transient at 520 nm with a lifetime of 8.10 μs is

attributed to the oxidized DNA base. Similar observations were made in the case of the derivative **2** and the model compound **3**.

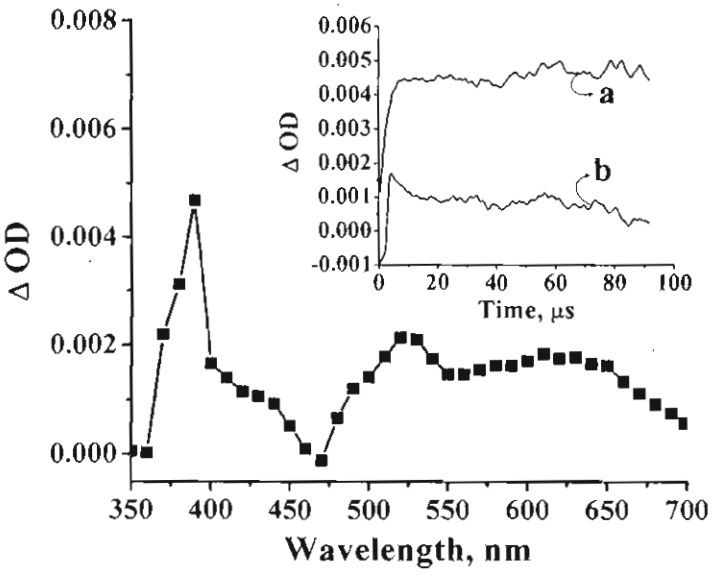

Figure 3.18. Transient absorption spectrum of **1** (40 μM) in the presence of DNA (1 mM) and methyl viologen in argon saturated phosphate buffer (10 mM; pH 7) recorded at 0.8 μs after 355 nm laser excitation. Inset shows the transient decays of (a) viologen radical cation at 390 nm and (b) DNA radical cation at 520 nm.

In order to assess the importance of π-stacking of ligands for efficient electron transfer between the DNA bases and ligands, we had selected the acridinium derivative **4**, which was shown to have no intercalative interactions with the double strand DNA (dsDNA).[30] Figure 3.19 shows the transient absorption spectrum of **4** in buffer. On the basis of quenching experiments with molecular oxygen (Figure 3.20), the transient species with absorption maximum at 500 nm could be assigned to the triplet excited state of **4**. As shown in the inset of Figure 3.19, there was no observation of transient absorption corresponding to the

DNA radical cation on exciting the derivative **4** in the presence of dsDNA. Similar observation was made in the presence of methyl viologen.

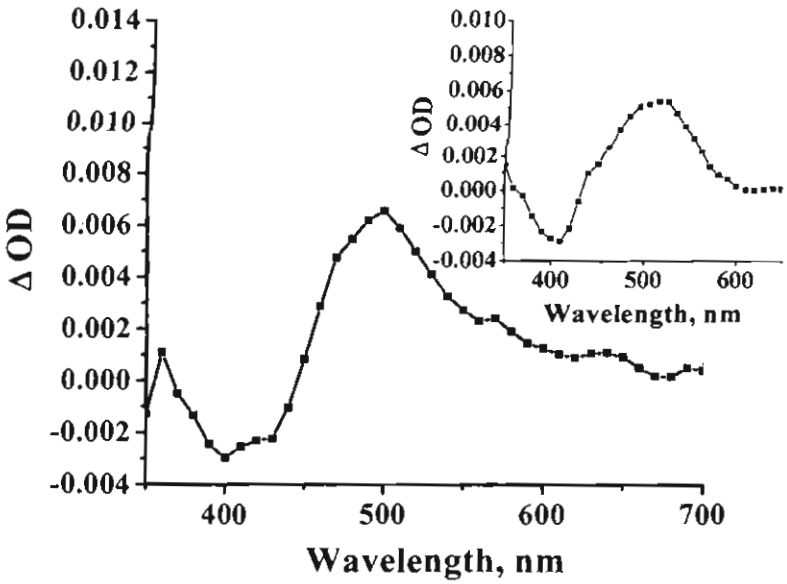

Figure 3.19. Transient absorption spectrum of **4** (40 μM) in the presence of dsDNA (1 mM) in argon saturated phosphate buffer (10 mM, pH 7) recorded at 1.4 μs after 355 nm laser excitation.

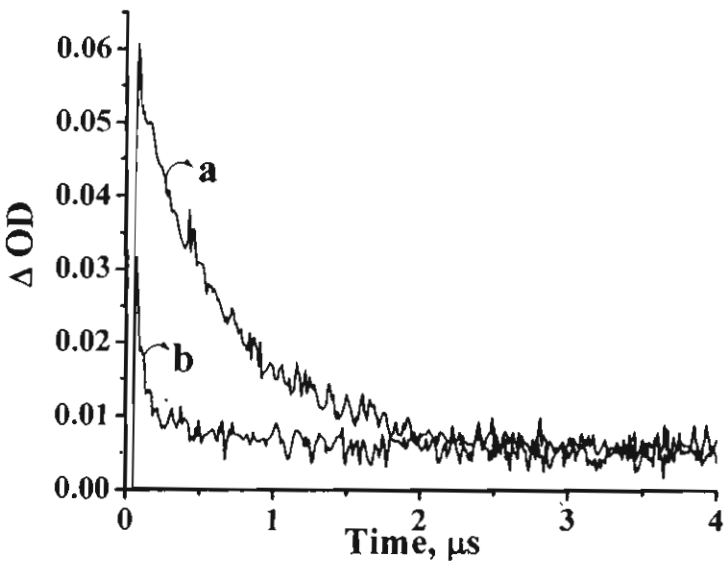

Figure 3.20. Transient decay of **4** (40 μM) in (a) argon saturated phosphate buffer (10 mM, pH 7) and (b) oxygen purged conditions, immediately after 355 nm laser excitation.

However, in the presence of ssDNA where the acridinium derivative **4** was reported to intercalate efficiently, a transient absorption spectrum was obtained with two maxima having distinct lifetimes (Figure 3.21). We observed a blue shift of 10 nm in the absorption maximum to 490 nm and a shoulder appears at 520 nm. The lifetime of the transient with absorption maximum at 490 nm in the presence of ssDNA is found to be 1.6 μs, while 0.85 μs was observed for the species with absorption maximum at 520 nm. These transients at 490 nm and 520 nm can be attributed to the formation of the acridine radical and the radical cation of DNA, respectively as per the experimental evidence and literature reports.[37,38]

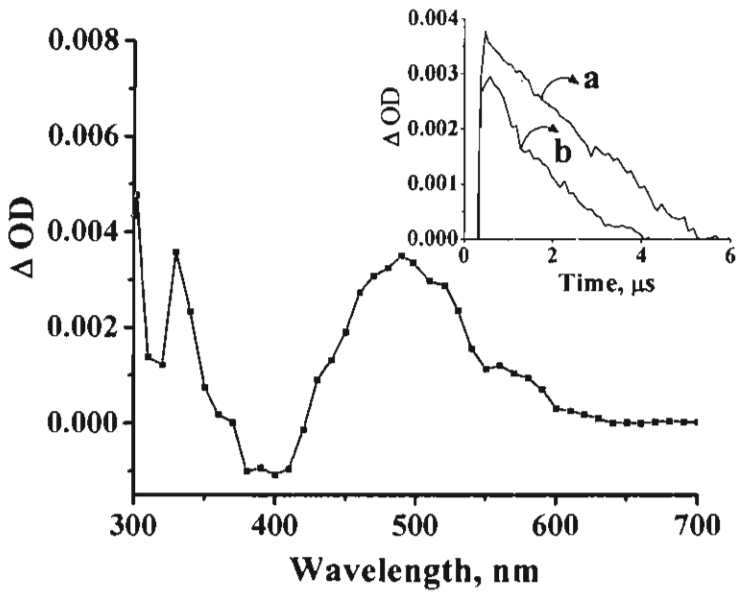

Figure 3.21. Transient absorption spectrum of **4** (40 μM) in the presence of ssDNA (1 mM) in argon saturated phosphate buffer (10 mM, pH 7) recorded at 1 μs after 355 nm laser excitation. Inset shows the transient decays of (a) acridine radical at 490 nm and (b) DNA radical cation at 520 nm.

To further confirm the formation of the DNA radical cation, similar studies have been carried out in the presence of guanosine 5'-monophosphate (GMP), which gives two transient absorption maxima at 500 nm and 520 nm with lifetimes of 4.3 μs and 83 μs. These transients could be assigned to the formation of which could be assigned to the formation of acridine radical and guanosine radical cation, respectively (Figure 3.22). On comparison with results obtained with DNA,

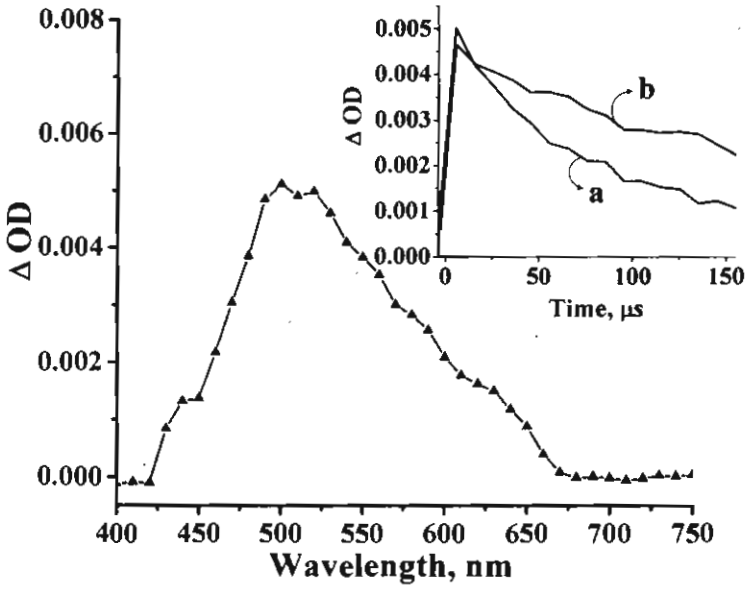

Figure 3.22. Transient absorption spectrum of **4** (40 μM) in the presence of GMP (1 mM) in argon saturated phosphate buffer (10 mM, pH 7) recorded at 1 μs after 355 nm laser excitation. Inset shows the transient decays of (a) acridine radical at 500 nm. (b) GMP radical cation at 520 nm.

the formation of the guanosine radical cation could be seen distinctly in the presence of methyl viologen, as shown in Figure 3.23, which showed three absorption maxima at 395 nm, 520 nm and 610 nm. While the maxima at 395 nm and 610 nm with lifetimes of 2.95 μs, corresponds to the methyl viologen radical

cation, that at 520 nm with a lifetime of 0.43 μs is due to the radical cation of ssDNA. Since no photoproduct formation was observed upon the laser excitation of **4** in the presence of methyl viologen, the observed formation of the viologen radical cation could be due to the efficient electron transfer reaction from the DNA base or GMP to the viologen moiety via the excited state of the acridinium chromophore. This is was supported by free energy calculations which shows that while electron transfer from the nucleobases to the excited state of acridinium is possible, the electron transfer from the acridinium to methyl viologen is not feasible.

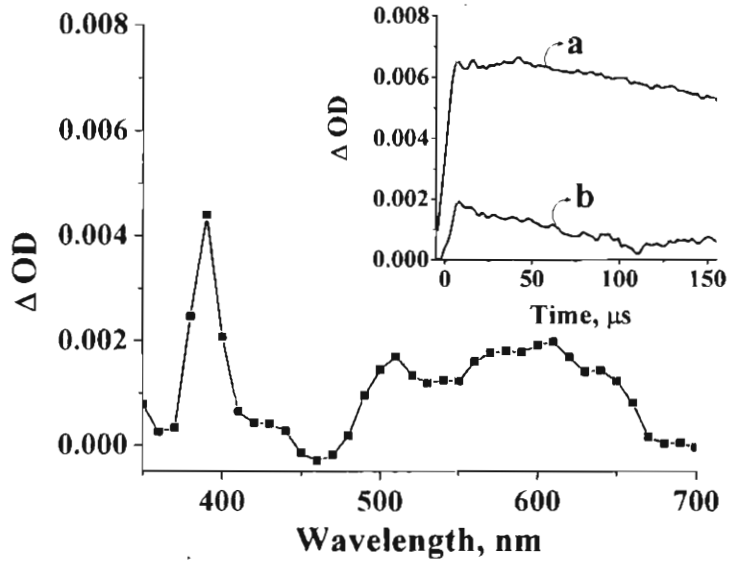

Figure 3.23. Transient absorption spectrum of **4** (40 μM) in the presence of GMP (1 mM) and methyl viologen (1 mM) in argon saturated phosphate buffer (10 mM, pH 7) recorded at 1 μs after 355 nm laser excitation. Inset shows (a) viologen radical cation at 395 nm and (b) GMP radical cation at 520 nm.

3.4. Conclusions

In summary, we have demonstrated the chromophore dependent electron transfer and competitive DNA binding interactions of systems containing two DNA binding motifs. The bifunctional derivatives **1** and **2** at lower ionic strength, exhibit respectively, mono-intercalative and bis-intercalative interactions with DNA, but both undergo only mono-intercalative interactions at the higher ionic strength of the buffer medium. Laser flash photolysis studies of these systems in buffer gave transients, which can be attributed to their triplet exited states based on the quenching studies with molecular oxygen. Excitation of these derivatives in presence of DNA and guanosine-5'-monophosphate (GMP) led to the formation of oxidized species like radical cations of DNA and GMP. The efficiency of oxidation of GMP and DNA by these derivatives was further increased in the presence of an efficient electron acceptor such as methylviologen. These results indicate that ionic strength has a profound influence on the DNA mono- and bisintercalating properties of the novel bisacridinum derivatives and further demonstrate that depending on the spacer and substituents present, these molecules can act as efficient DNA photo-oxidizing agents. These novel bifunctional systems, which are highly soluble in aqueous medium, stable under irradiation conditions and exhibit significant fluorescence quantum yields can have potential applications as fluorescent probes for biological applications.

3.5. Experimental Section

3.5.1. General Techniques

All melting points are uncorrected and were determined on a Mel-Temp II melting point apparatus.[39,40] ^{1}H and ^{13}C NMR spectra were recorded on a Brucker DPX-300 MHz NMR spectrometer using tetramethylsilane as the internal standard. CHN analyses were done using a Perkin-Elmer Series-II 2400 CHN analyzer. The electronic absorption spectra were obtained using a Shimadzu UV-3101PC UV-VIS-NIR scanning spectrophotometer. The fluorescence spectra were recorded on a SPEX-Fluorolog F112X spectrofluorimeter. The fluorescence quantum yields were measured by the relative methods using optically dilute solutions, with 9-aminoacridine in methanol (Φ_f = 0.99) or 10-methylacridinium trifluoromethanesulphonate in water (Φ_f = 1) as the reference.[39a]

The nanosecond fluorescence lifetime studies were carried out using an Edinburgh FL900CD single photon counting system. Fluorescence lifetimes were determined by deconvoluting the instrumental function with a mono- or biexponential decay and minimizing the χ^2 values of the fit to 1 ± 0.1.[39] Laser flash photolysis experiments were carried out in Applied Photophysics model LKS-20 laser kinetic spectrometer using the third harmonic (355 nm) of a Quanta Ray GCR-12 series pulsed Nd:YAG laser. Circular dichroism (CD) spectra were recorded on Jasco Corporation, J-810 spectropolarimeter. The cyclic voltammograms were recorded on a BAS CV-50W Voltammetric Analyser. A

glassy carbon working electrode was used along with platinum auxiliary and Ag/AgCl (3 M NaCl) reference electrodes. The redox potentials obtained were calibrated using ferrocene as an internal standard.[39,40]

DNA binding studies of the acridinium derivatives were carried out in 10 mM phosphate buffer containing either 2 mM or 100 mM NaCl (pH 7). Solution of Calf thymus DNA (Pharmacia Biotech, USA) was sonicated for 1 h and filtered through a 0.45 μM Millipore filter. The concentrations of DNA solutions were determined by using the average value of 6600 M^{-1} cm^{-1} for the extinction coefficient of a single nucleotide at 260 nm.[41] The DNA binding affinities were calculated according to the method of McGhee and von Hippel by using the data points of the Scatchard plot.[31]

3.5.2. Materials

9-Methylacridine, mp 116-117 ^{0}C (lit. mp 115-116 ^{0}C)[25] and 9,10-dimethylacridinium iodide (**3**), mp 248-249 ^{0}C (lit. mp 249-250 ^{0}C)[25] and 2,4-dimethylphenylacridinium iodide mp 242-245 ^{0}C were prepared as per the reported procedures.[25] Commercially available starting materials and solvents were purified and distilled before use. Petroleum ether used was the fraction boiling at 60-80 ^{0}C.

Synthesis of bisacridines.[29] A mixture of diphenylamine (**5**, 2.5 mol), 1,7-heptanedioic acid (1 mol) and anhydrous $ZnCl_2$ (10 mol) was heated at 230 ^{0}C for

40 h. To the reaction mixture was added 20% H_2SO_4 (100 mL) and refluxed for 4 h. It was then cooled and neutralized with 25% ammonia solution and the solid product obtained was chromatographed over silica gel. Elution of the column with a mixture (1:4) of ethyl acetate and petroleum ether gave bisacridine (n = 5) (57%), mp 219-220 ^{0}C, after recrystallization from a mixture (1:9) of petroleum ether and dichloromethane. ^{1}H NMR (300 MHz, $CDCl_3$) δ 1.15-1.95 (6H, m), 3.61 (4H, t, J = 7.5 Hz), 7.53 (4H, t, J = 7.6 Hz), 7.76 (4H, t, J = 7.6 Hz), 8.15-8.30 (8H, m); ^{13}C NMR ($CDCl_3$, 75 MHz) δ 27.44, 30.55, 31.16, 124.19, 124.85, 125.58, 129.71, 130.41, 146.46 and 148.65; MS (FAB) m/z 427.10 (MH^+). Anal. Calcd for $C_{31}H_{26}N_2$: C, 87.29; H, 6.14; N, 6.57. Found: C, 87.12; H, 6.15; N, 6.62.

In a separate experiment, when the reaction of diphenylamine with 1,12-dodecanedioic acid in presence of anhydrous $ZnCl_2$ was carried out as described above, gave 61% of the bisacridine **7** (n = 10) (mp 158-159 ^{0}C), after recrystallization from a mixture (1:9) of petroleum ether and dichloromethane. ^{1}H NMR (300 MHz, $CDCl_3$) δ 1.25-1.95 (16H, m), 3.61 (4H, t, J = 7.9 Hz), 7.54 (4H, t, J = 7.7 Hz), 7.76 (4H, t, J = 7.7 Hz) and 8.21-8.25 (8H, m); ^{13}C NMR ($CDCl_3$, 75 MHz) δ 27.71, 29.49, 29.54, 30.26, 31.42, 124.34, 124.89, 125.47, 129.69, 130.39, 147.16 and 148.69; MS (FAB) m/z 497.10 (MH^+). Anal. Calcd for $C_{36}H_{36}N_2$: C, 87.05; H, 7.31; N, 5.64. Found: C, 87.28; H, 7.36; N, 5.88.

Synthesis of the bisacridinium derivatives 1-2. 1,5-Bis(acridin-9-yl)pentane (1 mmol) was dissolved in dry dichloromethane (20 mL) and methyl

ifluoromethanesulphonate (2 mmol) was added slowly with stirring at room emperature. The reaction mixture was refluxed for 4 h and the residue obtained after recrystallization from a mixture (1:4) of ethyl acetate and acetonitrile gave the bisacridinium derivative **1** in 74% yield, mp 260-261 °C. ^{1}H NMR (DMSO-d_6, 300 MHz) δ 1.82-1.89 (6H, m), 3.97 (4H, t, J = 8.1 Hz), 4.81 (6H, s), 8.0 (4H, t, J = 7.8 Hz), 8.43 (4H, t, J = 8 Hz), 8.77 (4H, d, J = 9.3 Hz), 8.68 (4H, d, J = 8.5 Hz); ^{13}C NMR (DMSO-d_6, 75 MHz) δ 29.30, 30.15, 32.54, 44.91, 124.42, 127.73, 129.86, 130.39, 136.33, 141.64, 158.63. Anal. Calcd for $C_{35}H_{32}F_6N_2O_6S_2$: C, 55.70; H, 4.27; N, 3.71; S, 8.50. Found: C, 55.44; H, 4.03; N, 3.78; S, 8.40.

Similar reaction of 1,10-bis(acridin-9-yl)decane (1 mmol) with methyl trifluoromethanesulphonate (2 mmol) in dry dichloromethane, followed by the recrystallization of the residue obtained, from a mixture (1:4) of ethyl acetate and acetonitrile yielded 76% of bisacridinium derivative **2**, mp. 255-256 ^{0}C. ^{1}H NMR (DMSO-d_6, 300 MHz) δ 1.15-1.78 (16H, m), 3.98 (4H, t, J = 8 Hz), 4.81 (6H, s), 8.02 (4H, t, J = 8.3 Hz), 8.42 (4H, t, J = 8.3 Hz), 8.76 (4H, d, J = 9.2 Hz), 8.88 (4H, d, J = 8.8 Hz); ^{13}C NMR (DMSO-d_6, 75 MHz) δ 29.30, 30.15, 32.54, 44.91, 124.42, 127.73, 129.86, 130.39, 136.33, 141.64, 158.63. Anal. Calcd for $C_{35}H_{32}F_6N_2O_6S_2$: C, 55.70; H, 4.27; N, 3.71; S, 8.50. Found: C, 55.44; H, 4.03; N, 3.78; S, 8.40.

3.6. References

1. Lerman, L.S. *J. Mol. Biol.* **1961**, *3*, 18-30.
2. Le Pecq, J.-B.; Bret, M. L.; Barbet, J.; Roques, B. *Proc. Natl. Acad. USA* **1975**, *72*, 2915-2919.
3. Waring, M. J. *Annu. Rev. Biochem.* **1981**, *50*, 159-192.
4. Denny, W. A.;Wakelin, L. P. G. *Anti-Cancer Drug Des.* **1990**, *5*, 189-200.
5. Wilson, W. D. DNA intercalators. In Kool, E. T (ed.), *DNA and Aspects of Molecular Biology,* of Barton, D., Nakanishi, K. (Eds.), *Comprehensive Natural Products Chemistry*, Pergamon Press, Elsevier, 1999, Vol. 7, Chapter 12.
6. Demeunynck, M., Bailly, C., Wilson, W.D. (Eds.), *Small Molecule DNA and RNA Binders: From Synthesis to Nucleic Acid Complexes*, Wiley-VCH, Weinheim, 2002, Vols. 1 and 2.
7. Armitage, B. *Chem. Rev.* **1998**, *98*, 1171-1200 and references cited therein.
8. Kochevar, I. E.; Dunn, D. A. In Morrison, H. (Ed.), *Bioorganic Photochemistry: Photochemistry and the Nucleic Acids*. John Wiley and Sons, New York, 1990, Vol. 1, pp. 273-315.
9. Joseph, J.; Eldho, N. V.; Ramaiah, D. *J. Phys. Chem. B* **2003**, *107*, 4444-4450.
10. Joseph, J.; Eldho, N. V.; Ramaiah, D. *Chem. Eur. J.* **2003**, *9*, 5926-5935.
11. Akerman, B.; Tuite, E. *Nucleic Acids Res.* **1996**, *24*, 1080-1090.

12. Canellakis, E. S.; Bono, V.; Bellantone, R. A.; Krakow, J. S.; Fico, R. M.; Schulz, R. A. *Biochim. Biophys. Acta,* **1976**, *418*, 300-314.

13. Lown, J. W.; Gunn, B. C.; Chang, R. -Y.; Majumdar, K. C.; Lee, J. S. *Can. J. Biochem,* **1978**, *56*, 1006-1015.

14. Wakelin, L. P. G.; Romanos, M.; Chen, T. K.; Glaubiger, D.; Canellakis, E. S.; Waring, M. J. *Biochemistry* **1978**, *17*, 5057-5063.

15. Zimmerman, S. C.; Lamberson, C. R.; Cory, M.; Fairley, T. A. *J. Am. Chem. Soc.* **1989**, *111*, 6805-6809.

16. Wirth, M.; Buchardt, O.; Koch, T.; Nielsen, P. E.; Norden, B. *J. Am. Chem. Soc.* **1988**, *110*, 932-939.

17. Slam-Schwok, A.; Teulade-Fichou, M. -P.; Vigneron, J. -P.; Taillandier, E.; Lehn, J. -M. *J. Am. Chem. Soc.* **1995**, *117*, 6822-6830.

18. Jourdan, M. ; Garcia, J. ; Lhomme, J. ; Teulade-Fichou, M. P. ; Vigneron, J. P. ; Lehn, J. -M. *Biochemistry* **1999**, *38*, 14205-14213.

19. Slama-Schwok, A.; Peronnet, F.; Hantz-Brachet, E.; Taillandier, E.; Teulade-Fichou, M. P.; Vigneron, J. P.; Best-Belpomme, M.; Lehn, J. -M. *Nucleic Acids Res.* **1997**, *25*, 2574-2581.

20. Takenaka, S.; Shigemoto, N.; Kondo, H. *Supramol. Chem.* **1998**, *9*, 47-56.

21. King, H. D.; Wilson, W. D.; Gabbay, E. J. *Biochemistry* **1982**, *21*, 4982-4989.

22. Atwell, G. J.; Stewart, G. M.; Leupin, W.; Denny, W. A. *J. Am. Chem. Soc.* **1985**, *107*, 4335-4337.

23. Blackburn, G. M.; Gait, M. J. (Eds.), *Nucleic Acids in Chemistry and Biology*. Oxford University Press, Oxford, 1996, pp. 329-374 and references cited therein.

24. Denny, W. A.; Baguley, B. C.; Cain, B. F.; Waring, M. J. In Neidle, S., Waring, M. J. (Eds.), *Molecular Aspects of Anticancer Drug Action.* Macmillan, London, 1984, pp. 1-34.

25. Albert, A. *The Acridines.* Edward Arnold Publishers Ltd., London, 2nd Edition. 1966.

26. Kohn, K. W. *Cancer Res.* **1996**, *56,* 5533-5546.

27. Harris, C. C. *J. Natl. Can. Inst.* **1996**, *88,* 1442-1455.

28. Ramaiah, D.; Koch, T.; Orum, H.; Schuster, G. B. *Nucleic Acids Res.* **1998**, *26*, 3940-3943.

29. Eldho, N. V.; Saminathan, M.; Ramaiah, D. *Synth. Commun.* **1999**, *29*, 4007-4014.

30. Joseph, J.; Kuruvilla, E.; Achuthan, T. A.; Ramaiah, D.; Schuster, G. B. *Bioconjugate Chem.* **2004**, *15*, 1230-1235.

31. (a) McGhee, J. D.; von Hippel, P. H. *J. Mol. Biol.* **1974**, *86*, 469-489. (b) Adam, W.; Cadet, J.; Dall'Acqua, F.; Epe, B.; Ramaiah, D.; Saha-Moeller, C. R. *Angew. Chem., Int. Ed. Engl.* **1995**, *34*, 107-110.

32. (a) Reinert, K. E. *Nucleic Acids. Res.* **1983**, *11*, 3411-3430. (b) Breslin, D. T.; Coury, J. E.; Anderson, J. R.; McFail-Isom, L.; Kan, Y.; Williams, L. D.; Bottomley, L. A.; Schuster, G. B. *J. Am. Chem. Soc.* **1997**, *119*, 5043-5044.

33. (a) Ardhammar, M.; Kurucsev, T.; Nordén, B. (2000) *Circular Dichroism: Principles and Application* (Berova, N.; Nakanishi, K., Woody, R. W., Eds.); Chapter 26, Wiley-VCH. (b) Becker, H.; Nordén, B. *J. Am. Chem. Soc.* **1997**, *119*, 5798-5803.

34. Petty, J. T.; Bordelon, J. A.; Robertson, M. E. *J. Phys. Chem. B* **2000**, *104*, 7221-7227.

35. Steenken, S.; Jovanovich, S. V. *J. Am. Chem. Soc.* **1997**, *119*, 617-618.

36. Mann, C. K.; Barnes, K. K. In *Electrochemical Reactions in Non-aqueous Systems*, Marcel Dekker, Inc., New York, 1970.

37. Ohkubo, K.; Yukimoto, K.; Fukuzumi, S. *Chem. Comm.* **2006**, *23*, 2504-2506.

38. Hariharan, M.; Joseph, J.; Ramaiah, D. *J. Phys. Chem. B* **2006**, *110*, 24678-24686.

39. (a) Kuruvilla, E.; Joseph, J.; Ramaiah; D. *J. Phys. Chem. B* **2005**, *109*, 21997-22002. (b) Avirah, R. R.; Jyothish, K.; Ramaiah, D. *Org. Lett.* **2007**, *9*, 121-124. (c) Jyothish, K.; Avirah, R. R.; Ramaiah, D. *Org. Lett.* **2006**, *8*,

111-114. (d) Jyothish, K.; Arun, K. T.; Ramaiah, D. *Org. Lett.* **2004**, *6*, 3965-3968.

40. (a) Neelakandan, P. P.; Hariharan, M.; Ramaiah, D. *J. Am. Chem. Soc.* **2006**, *128*, 11334-11335. (b) Jisha, V. S.; Arun, K. T.; Hariharan, M.; Ramaiah, D. *J. Am. Chem. Soc.* **2006**, *128*, 6024-6025. (c) Neelakandan, P. P.; Hariharan, M.; Ramaiah, D. *Org. Lett.* **2005**, *7*, 5765-5768.

41. Baguley, B. C.; Falkenhang, E. –M. *Nucleic Acid Res.* **1978**, *5*, 161-171.

Chapter 4

DEVELOPMENT OF A FLUORIMETRIC ASSAY FOR QUANTIFICATION OF SINGLE STRAND DNA AND RATIO OF SINGLE STRAND TO DOUBLE STRAND DNA

4.1. Abstract

DNA binding properties of the acridinium based simple fluorescent probes **1** and **2** were studied and the remarkable selectivity exhibited by these derivatives for single strand DNA (ssDNA) over double strand DNA (dsDNA) has been employed to develop a fluorimetric assay for the quantification of ssDNA. The acridinium derivatives **1** and **2** with sterically hindered aryl group on the acridinium moiety undergoes selective binding with ssDNA involving both electrostatic and intercalative interactions as analyzed through photophysical, biophysical and microscopic techniques. Studies with different oligonucleotides indicate that these derivatives show greater affinity for guanosine rich sequences $(dG)_{19}$, whereas least affinity (ca. 3-fold) was observed for the cytosine rich sequences $(dC)_{19}$. The significant fluorescence changes observed with these derivatives led to the development of a sensitive method for the quantification of ssDNA and the ratio of ssDNA to dsDNA. This method showed linearity over a wide range of ssDNA concentrations with high correlation coefficients and slope

values. Only marginal error was observed even in the presence of additives like RNA, free nucleotides, proteins, surfactants and in biological fluid. Our results demonstrate that the acridinium derivatives **1** and **2**, exhibit high solubility and stability in buffer media and quantitative fluorescence yields and hence can be used as a sensitive fluorescent probes for the quantification of ssDNA (20-1000 μM) and the ratio of ssDNA to dsDNA in buffer and biofluids.

4.2. Introduction

Study of interactions of small molecules with nucleic acids is important from the view point of developing new probes for quantification of nucleic acids, in establishing carcinogenic potential of a chemical and in developing drugs targeted to DNA.[1-3] Quantification of nucleic acids is an essential step in most of the molecular biological applications, in clinical diagnostics and in the detection of DNA damage.[4,5] Significant advances have been made over the years in the detection techniques of DNA damage. However, most of these techniques are either labor intensive or based on the detection of DNA cleavage products, which are rapidly repaired in cells.[6,7] Hence, there is a growing interest in recent years in the development of new and simpler methods for the detection and quantification of DNA damage.

Some of the general strategies employed to quantify DNA damage caused by ionizing radiation or chemical modification include gel electrophoresis, capillary electrophoresis, optical and electrochemical methods.[8-11] DNA damage

include base alterations, DNA-protein cross links and both single strand and double strand breaks.[12] Ethidium bromide binding assay, comet assay, alkaline unwinding and elution assays are some of the methods reported for the detection of single strand breaks.[7,13-15] These methods use alkaline conditions to denature or unwind damaged DNA. Under controlled conditions, the degree of denaturation is dependent on the number of single strand breaks, which can be quantified by measuring the ratio of single strand DNA (ssDNA) to double strand DNA (dsDNA) and thereby the extent of DNA damage. However, most of these methods are tedious and time consuming. In this context, the direct measurement of DNA damage through optical methods offers several advantages. Of the optical methods used for the quantification of nucleic acids, the fluorescence based methods have attracted much attention primarily because of the high sensitivity and rapidity of the technique.[16]

The fluorescence based methods generally rely on measuring either enhancement or quenching in fluorescence intensity and lifetimes of the probe when bound to DNA.[17] However, most of the available nucleic acid probes cannot efficiently differentiate between dsDNA and ssDNA. As a result, the development of fluorescent probes as well as methods to distinguish between various forms of DNA, and particularly ssDNA and dsDNA is gaining importance.[18,19] Dyes which detect only the ssDNA are important not only for the determination of extent of DNA damage but also for the detection and quantification of synthetic

oligonucleotides that are used in a number of different molecular biological techniques.[20] Furthermore, ssDNA is believed to play a major role in various biological functions.[21,22] For example, ssDNA is an important intermediate in the processes of DNA replication, recombination and repair. It is also an important mediator of DNA damage-dependent cell cycle arrest in a range of organisms. In *Escherichia coli*, double strand breaks (DSBs) must be proceeded by the RecBC helicase/exonuclease and pyrimidine dimers must be replicated to generate ssDNA, to activate RecA and induce the SOS response and cell cycle arrest.[23] In budding yeast, meiotic cell DSBs needs to be processed to ssDNA inorder to signal arrest.[24,25] In mammalian cells, a p53-dependent DNA damage sensor also responds to ssDNA, but not to the nicked or covalently closed circular DNA.[26] ssDNA has also been associated with DNA replication[27], transcription[28], *trans*-lesion synthesis[29], apoptosis[30], DNA repair[31], mitotic and meiotic recombination[32,33] and telomeres.[34] Hence, ssDNA selective probes will be highly useful in understanding the role of ssDNA in cells.

Oligreen, a product by the Molecular Probes is an example of ssDNA quantitation reagent. However this dye shows fluorescence enhancement in the presence of dsDNA, albeit to a lesser extent when compared to the ssDNA.[16] Another example of a dye, which has been used to quantify ssDNA in the presence of dsDNA is the PicoGreen. PicoGreen is a widely used dsDNA quantitation reagent[16] and in combination with ethidium bromide, it was reported to be efficien

in determining the ssDNA to dsDNA ratio.[18] However, a drawback of the system was the variation in the linearity of the calibration curve with the concentration of the dye, owing to aggregation of the dye. In this context, our objective has been to develop sensitive fluorescent probes for the detection and quantification of ssDNA and the ratio of ssDNA to dsDNA. With this objective we had selected two acridinium based probes **1** and **2** (Chart 4.1) and studied their interactions with ssDNA, dsDNA and a few synthetic oligonucleotides in the presence and absence of additives such as RNA, proteins and surfactants. Our results demonstrate that the derivatives exhibit quantitative fluorescence yields and high selectivity toward ssDNA and hence can be successfully used as a fluorescent probe for the detection and quantification of ssDNA and the ratio of ssDNA to dsDNA.

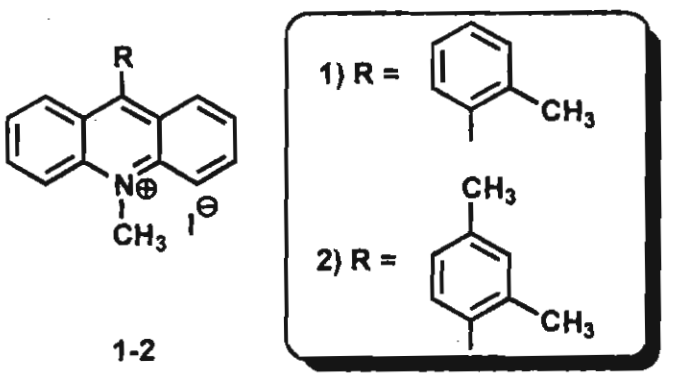

Chart 4.1

4.3. Results and Discussion

4.3.1 Synthesis and DNA Binding Properties

Reaction of 9-(2-methylphenyl)-acridine and 9-(2,4-dimethylphenyl)-acridine with methyl iodide gave the derivatives **1** and **2** in good yields (60-

65%).[35] These derivatives exhibited high solubility in aqueous medium and buffer and obeyed Beer's law under the experimental conditions. They showed characteristic absorption of the acridinium chromophore in the range 300–475 nm with molar extinction coefficient of 1.9×10^4 $M^{-1}cm^{-1}$ at the absorption maximum (361 nm). In buffer media, they exhibited quantitative fluorescence quantum yields ($\Phi_f = 1$) with an emission maximum around 500 nm.

To evaluate the potential of these derivatives as fluorescent probes, we monitored their absorption and fluorescence changes in presence and absence of both single strand DNA (ssDNA) and double strand (dsDNA) in phosphate buffer at pH 7.4 under identical conditions. As shown in Figure 4.1, the fluorescence

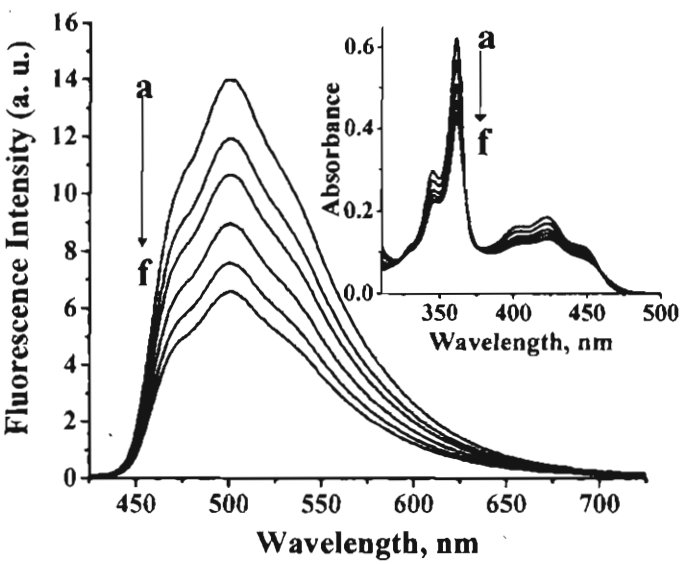

Figure 4.1. Change in fluorescence spectra of **1** (30 μM) with increasing concentration of ssDNA. [ssDNA] (a) 0, (b) 0.20, (c) 0.43, (d) 0.63, (e) 0.82 and (f) 1 mM. Inset shows the corresponding changes in the absorption spectra of **1** with the gradual addition of ssDNA. Excitation wavelength, 366 nm.

emission spectrum of **1** is efficiently quenched (60%) with increasing concentrations of calf thymus ssDNA. The increase in addition of ssDNA resulted in significant hypochromicity (17%) at 361 nm, corresponding to the absorption of the acridinium chromophore of **1** (Inset of Figure 4.1). Similar results were observed in the case of the derivative **2**. In contrast, we observed negligible changes in the absorption and fluorescence emission properties of **1** with increasing in addition of dsDNA. Figure 4.2 shows the extent of fluorescence changes obtained in the presence of ssDNA and dsDNA. Inset of Figure 4.2 shows the visual observation of the change in fluorescence intensity of **1** (40 μM) in the

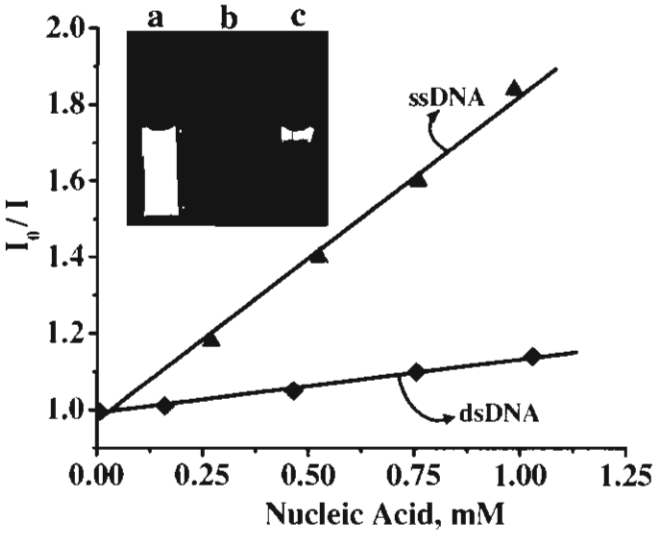

Figure 4.2. Change in fluorescence intensity of **1** (40 μM; monitored at 501 nm) with increasing concentrations of ssDNA and dsDNA. Inset shows the visual observation of change in fluorescence intensity of (a) **1** alone (40 μM) (b) **1** in the presence of ssDNA (1 mM) and (c) **1** in the presence of dsDNA (1 mM). Excitation wavelength, 365 nm.

presence and absence of equimolar concentrations (1 mM) of dsDNA and ssDNA. While the fluorescence intensity of **1** is retained in the presence of dsDNA, it gets completely quenched when ssDNA is added, leading to the visual and selective detection of ssDNA in the solution by the acridinium derivative **1**.

To assess the sequence specificity of the probe **1**, we investigated its interactions with different single strand homooligomers under identical conditions. We chose oligonucleotides consisting of 19 nucleotides such as $(dA)_{19}$, $(dC)_{19}$, $(dT)_{19}$ and $(dG)_{19}$ and a random sequence of $(dN)_{19}$. Figures 4.3-4.7 shows the fluorescence changes of probe **1** with increase in concentration of the oligonucleotides $(dA)_{19}$, $(dC)_{19}$, $(dT)_{19}$, $(dG)_{19}$ and random sequence $(dN)_{19}$, respectively. Figure 4.8 shows a comparison of the fluorescence intensity changes

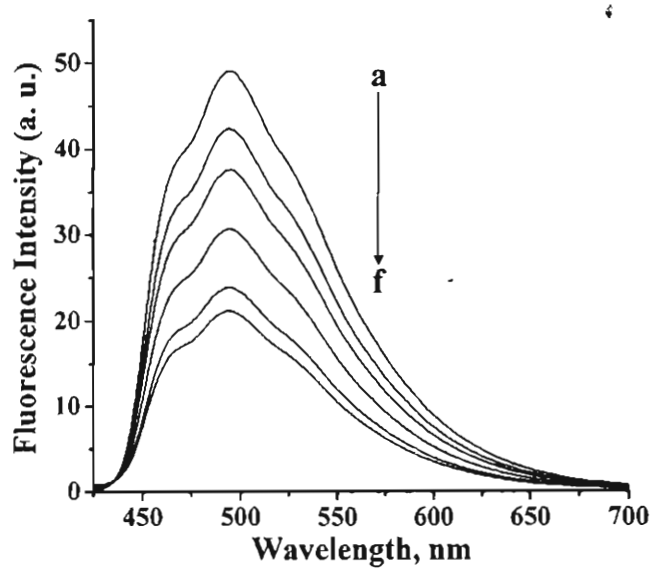

Figure 4.3. Change in fluorescence spectra of probe **1** (30 μM) with increasing concentration of $(dA)_{19}$. [$(dA)_{19}$] (a) 0, (b) 0.03, (c) 0.08, (d) 0.13, (e) 0.20 and (f) 0.34 mM. Excitation wavelength, 366 nm.

of probe **1** at 501 nm, with different concentrations of various homooligomers. The derivative **1** showed a significant quenching (77%) in fluorescence intensity when titrated with $(dG)_{19}$ followed by $(dA)_{19}$ (55%) and $(dT)_{19}$ (53%) whereas very low quenching of 30% was observed with $(dC)_{19}$. In contrast, the random sequence oligomer $(dN)_{19}$ led to 70% quenching in the fluorescence intensity of probe **1**. The data indicates that **1** exhibits greater affinity for guanosine rich sites

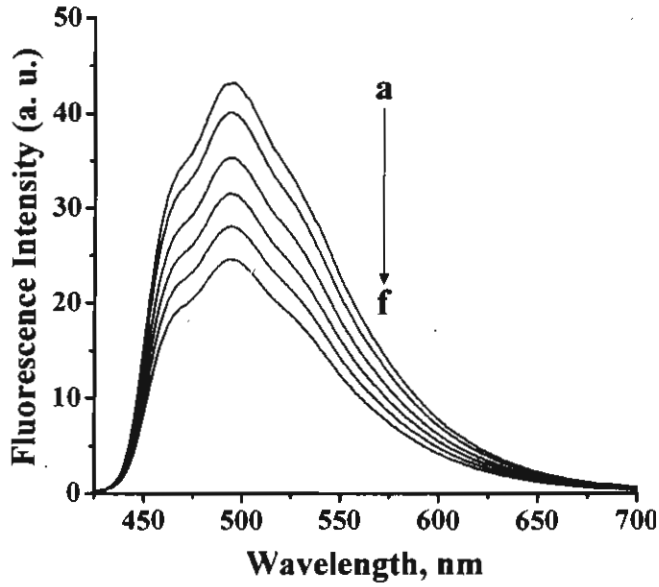

Figure 4.4. Change in fluorescence spectra of probe **1** (30 μM) with increasing concentration of $(dC)_{19}$. $[(dC)_{19}]$ (a) 0, (b) 0.02, (c) 0.10, (d) 0.19, (e) 0.27 and (f) 0.34 mM. Excitation wavelength, 366 nm.

as compared to the cytidine homooligomer. Time resolved fluorescence changes of the probe **1** in the presence of calf thymus ssDNA and oligonucleotides with 19 bases were studied and the changes in the decay profile of probe **1** with the mixed

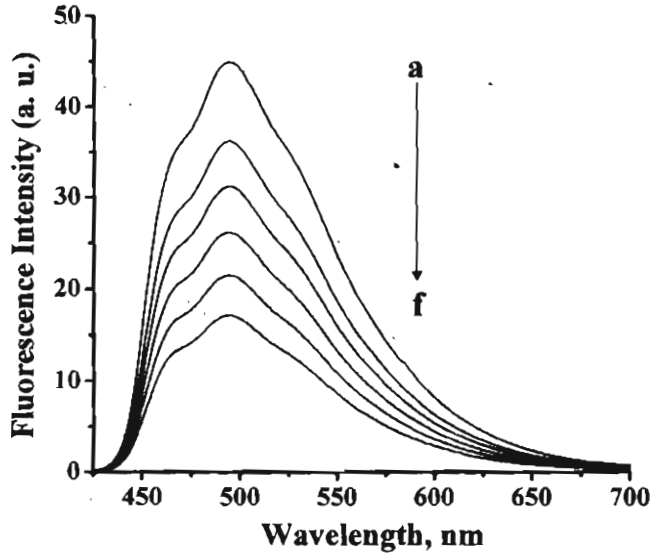

Figure 4.5. Change in fluorescence spectra of probe **1** (30 μM) with increasing concentration of $(dT)_{19}$. $[(dT)_{19}]$ (a) 0, (b) 0.05, (c) 0.09, (d) 0.15, (e) 0.23 and (f) 0.33. Excitation wavelength, 366 nm.

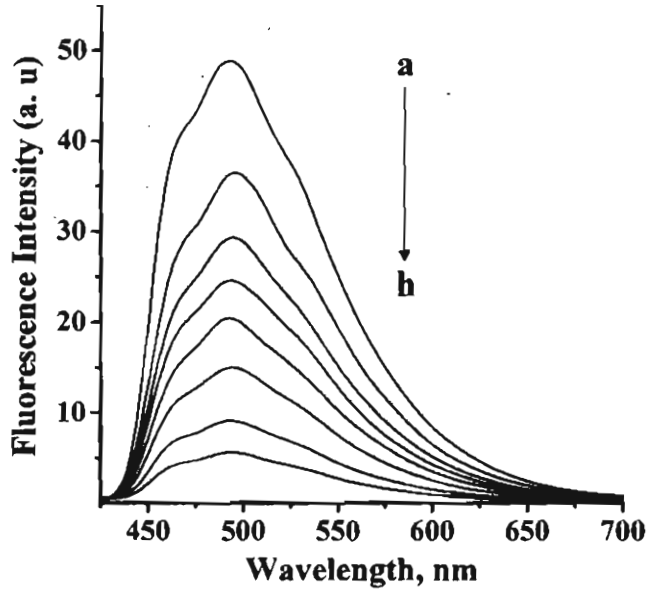

Figure 4.6. Change in fluorescence spectra of probe **1** (30 μM) with increasing concentration of $(dG)_{19}$. $[(dG)_{19}]$ (a) 0, (b) 0.03, (c) 0.07, (d) 0.11, (e) 0.14, (f) 0.2, (g) 0.3 and (h) 0.35 mM. Excitation wavelength, 366 nm.

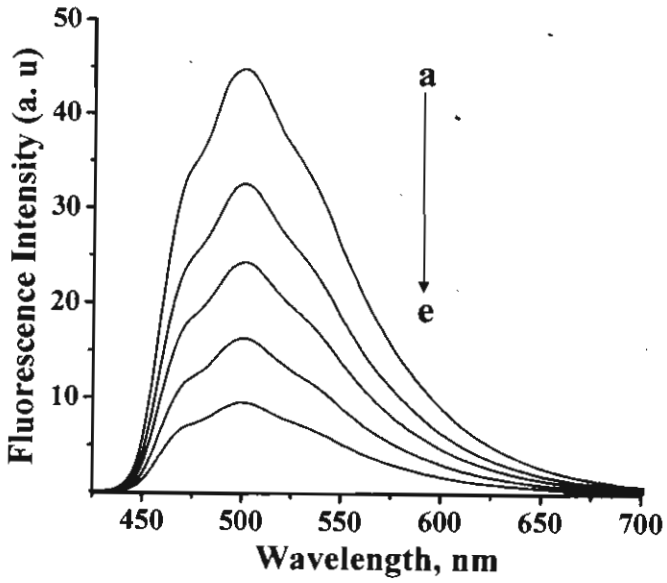

Figure 4.7. Change in fluorescence spectra of probe **1** (30 μM) with increasing concentration of $(dN)_{19}$. [$(dN)_{19}$] (a) 0, (b) 0.05, (c) 0.09, (d) 0.19, and (e) 0.35mM. Excitation wavelength, 366 nm.

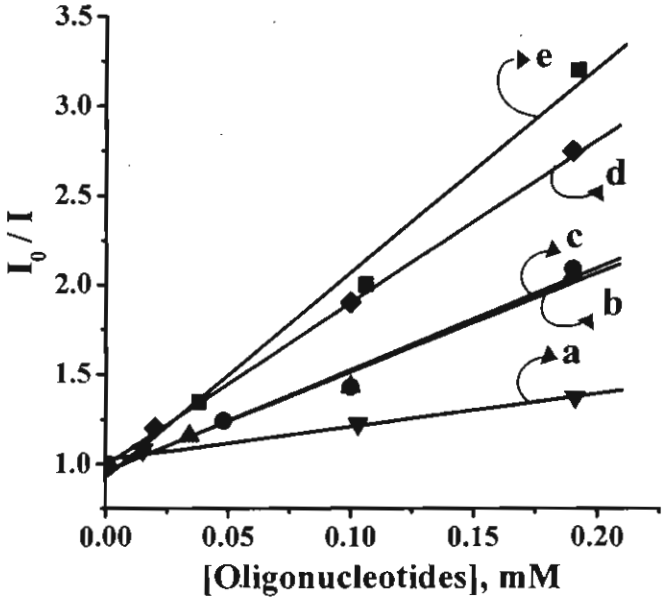

Figure 4.8. Change in fluorescence intensity of probe **1** with increase in addition of various oligonucleotide sequences (a) $(dC)_{19}$, (b) $(dT)_{19}$, (c) $(dA)_{19}$, (d) $(dN)_{19}$ and (e) $(dG)_{19}$. Excitation wavelength, 366 nm.

base sequence oligonucleotide, $(dN)_{19}$ is shown in Figure 4.9. While only negligible changes were observed in the presence of long chain CT ssDNA, biexponential decay with lifetimes 42 ps and 20 ns were observed in the presence of $(dN)_{19}$.

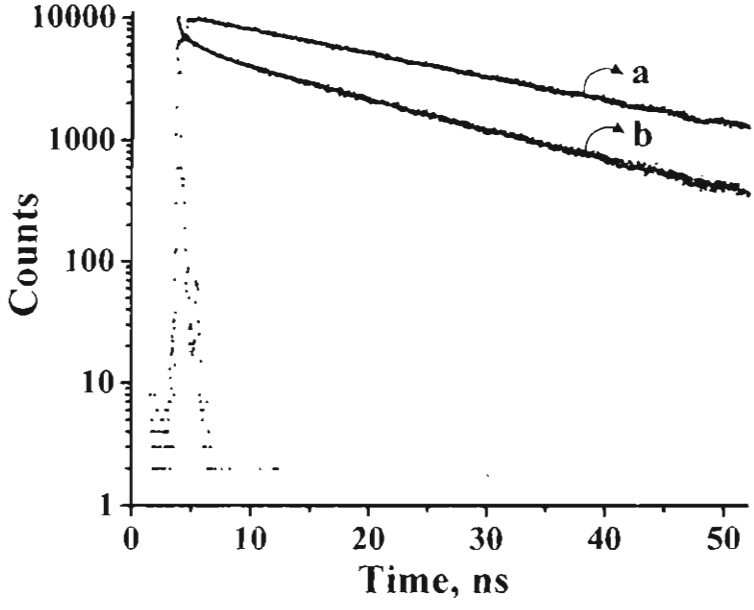

Figure 4.9. Fluorescence decay profiles of **1** (32 μM) in the presence and absence of $(dN)_{19}$ in phosphate buffer (10 mM; pH 7.4). [DNA] (a) 0 and (b) 0.45 mM.

The association constants of the complexes formed between the probe **1** and the oligonucleotide were determined by fluorescence titration experiments, according to the method of McGhee and von Hippel using the data points of the Scatchard plot.[36] These results are summarized in Table 4.1. Significant association constant of $K_{DNA} = 8.5 \times 10^4\ M^{-1}$ was observed for the guanosine homooligomer $(dG)_{19}$, while nearly ca. 3-fold less value of $K_{DNA} = 3 \times 10^4\ M^{-1}$ was obtained for $(dC)_{19}$. Fluorescence emission of **1** is efficiently quenched by ssDNAs of different

Table 4.1. Association constants of the probe **1** with different DNA structures in phosphate buffer (10 mM, pH 7.4).[a]

DNA Code	DNA Sequence	K_{DNA} (M^{-1})[b]	k (s^{-1})[c] × 10^8
$(dA)_{19}$	5'-AAA AAA AAA AAA AAA AAA A-3'	7×10^4	0.9
$(dT)_{19}$	5'-TTT TTT TTT TTT TTT TTT T-3'	3.3×10^4	0.6
$(dC)_{19}$	5'-CCC CCC CCC CCC CCC CCC C-3'	3×10^4	0.32
$(dG)_{19}$	5'-GGG GGG GGG GGG GGG GGG G-3'	8.5×10^4	3.1
$(dN)_{19}$	5'-CGT GGA CAT TGC ACG GTA C-3'	7.5×10^4	1.4

[a] Average of more than two experiments. [b]DNA association constants were determined by the Scatchard analysis of the fluorescence titration data. [c]Rate of static quenching by DNA calculated as reported earlier.[37]

sequences and the mechanism of quenching is attributed to the electron transfer from DNA bases to the singlet excited state of the acridinium chromophore. This assignment is based on the redox species characterized through laser flash studies[35] and theoretically calculated favorable change in free energy values (ΔG = -0.89, -0.76, -0.58 and -0.48 for guanosine, adenosine, cytosine and thymidine, respectively). Among the nucleobases, the electron transfer from the guanosine to the excited state of the acridinium chromophore is expected to be more facile

theoretically and hence we observed an efficient fluorescence quenching with $(dG)_{19}$ sequence as compared to $(dC)_{19}$. As shown in Table 4.1, the probe **1** showed selectivity for all the ssDNA sequences but with binding affinity in the order $(dG)_{19} > (dN)_{19} > (dA)_{19} > (dT)_{19} > (dC)_{19}$.

4.3.2 Quantification of Single Strand DNA in Buffer

A solution of probe **1** (30 μM) in 10 mM phosphate buffer at pH 7.4 was treated with aliquots of single strand DNA (ssDNA) obtained by boiling CT DNA in water bath for 30 min, followed by sudden quenching on ice and repeating the process for minimum of three times. The compound-DNA solutions were incubated at room temperature (20 ^{0}C) for 1 min. The solutions were excited at 366 nm, which is the isosbestic point observed in the absorption spectrum and the emission intensity was monitored at 501 nm, which is the emission maximum of of the probe **1**. The fluorescence intensity ratio at 501 nm in the presence and absence of ssDNA was plotted against increasing concentrations (20 – 1000 μM) of ssDNA. As shown in Figure 4.10, the data points give a linear fit with high correlation coefficient of 0.99 and a slope value of 1.07. Similar changes in the fluorescence emission intensity were observed in the case of the probe **2** where a linear fit was obtained for the plot of the fluorescence intensity ratios at 505 nm (emission maximum) against the ssDNA concentrations (Figure 4.11).

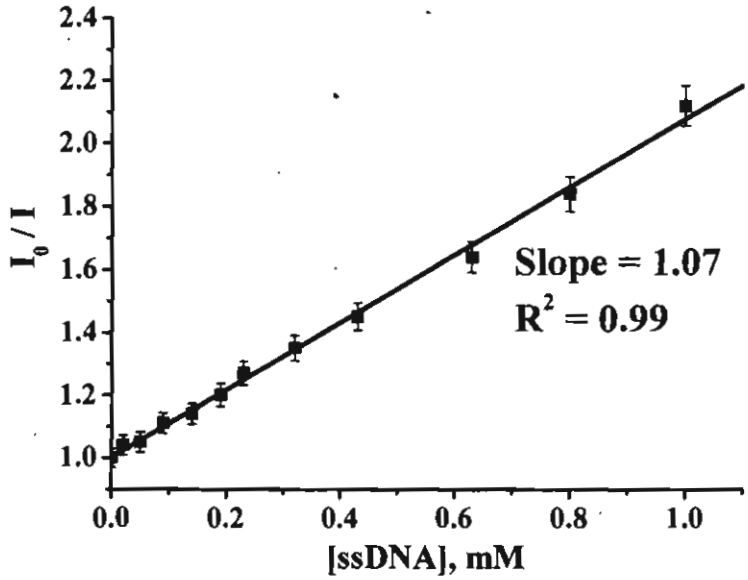

Figure 4.10. Demonstration of the linearity of the fluorescence assay using the probe **1** for the quantitation of ssDNA (20-1000 μM) in phosphate buffer (10 mM; pH 7.4).

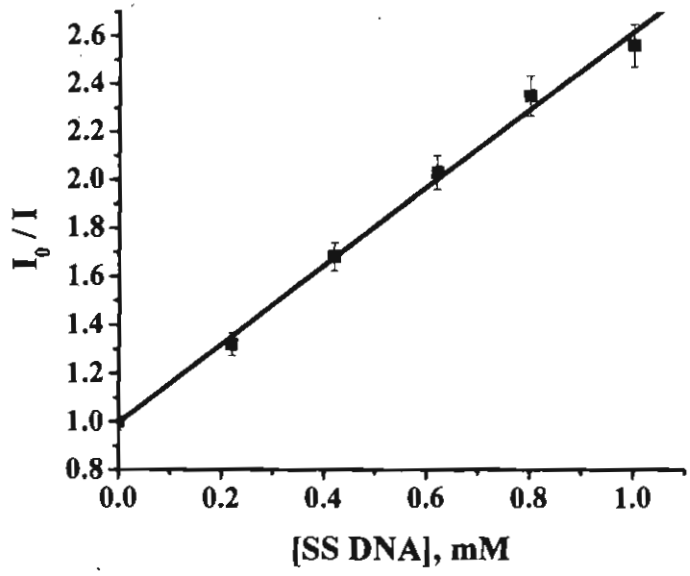

Figure 4.11. Demonstration of the linearity of the fluorescence assay using the probe **2** for the quantitation of ssDNA (20-1000 μM) in phosphate buffer (10 mM; pH 7.4).

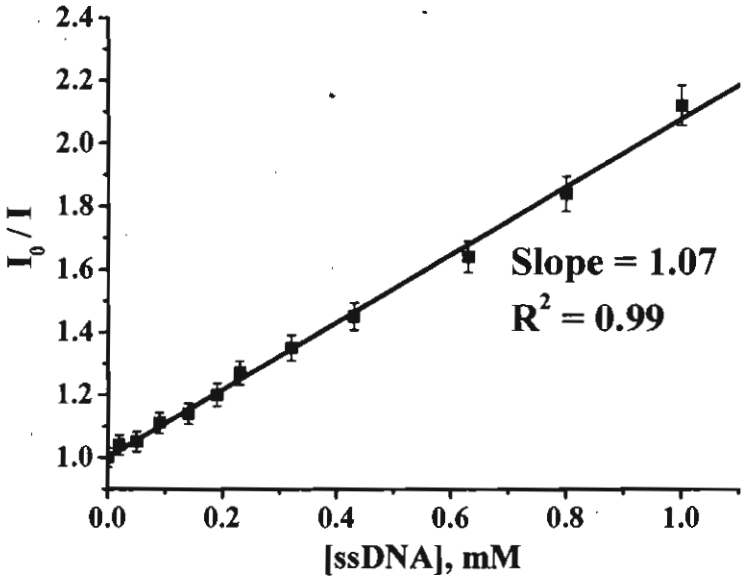

Figure 4.10. Demonstration of the linearity of the fluorescence assay using the probe **1** for the quantitation of ssDNA (20-1000 μM) in phosphate buffer (10 mM; pH 7.4).

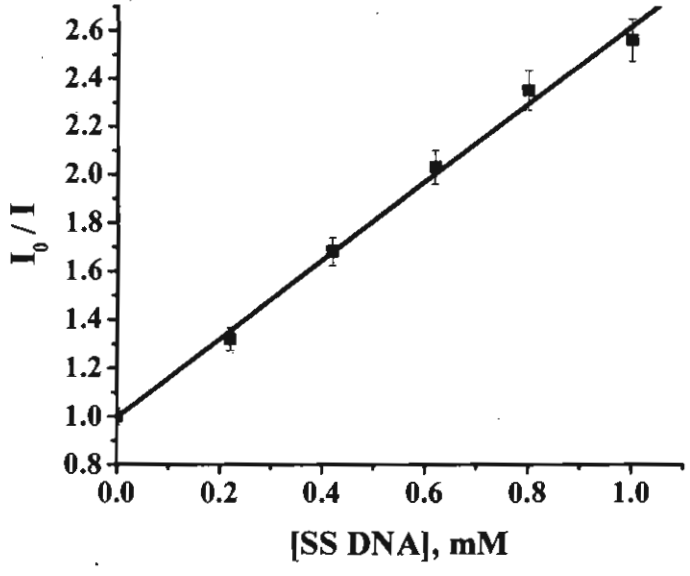

Figure 4.11. Demonstration of the linearity of the fluorescence assay using the probe **2** for the quantitation of ssDNA (20-1000 μM) in phosphate buffer (10 mM; pH 7.4).

In order to ascertain whether these derivatives showed any interaction with RNA and proteins, we had monitored the fluorescence intensity changes of these derivatives with increasing concentrations of RNA and bovine serum albumin. As shown in Figures 4.12 and 4.13, only marginal quenching was observed in the fluorescence emission of the acridinium derivatives. These results indicate the selectivity of the derivatives for the ssDNA. Proteins, detergents, inorganic salts

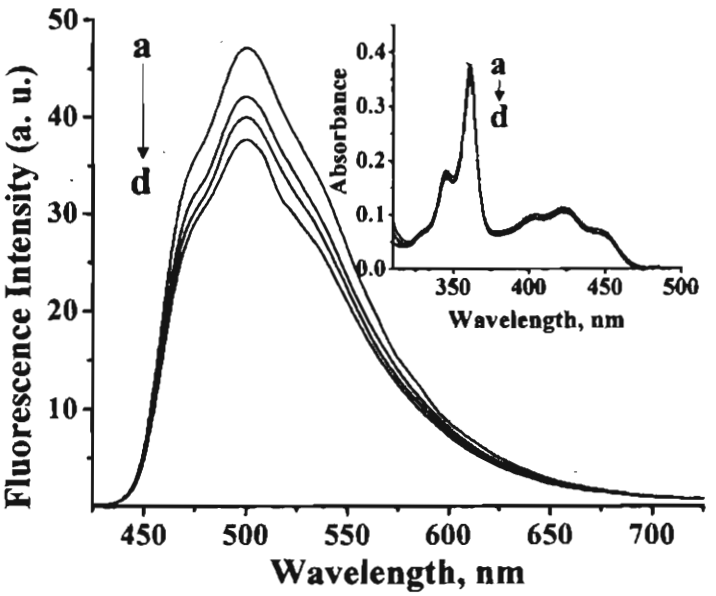

Figure 4.12. Change in fluorescence spectra of the probe **1** (30 μM) with increasing concentration of RNA. [RNA] (a) 0, (b) 0.20, (c) 0.43 and (d) 1mM. Excitation wavelength, 366 nm.

and agarose are some of the contaminants, which usually skew the nucleic acid assays.[38] The DNA which is extracted from the cells can contain small amounts of proteins, enzymes and RNA, which brings about error in the nucleic acid quantification. Besides these, the separation process involves the treatment of

the nucleic acid samples with detergents such as sodium dodecylsulphate (SDS), buffers containing various inorganic salts and organic solvents.

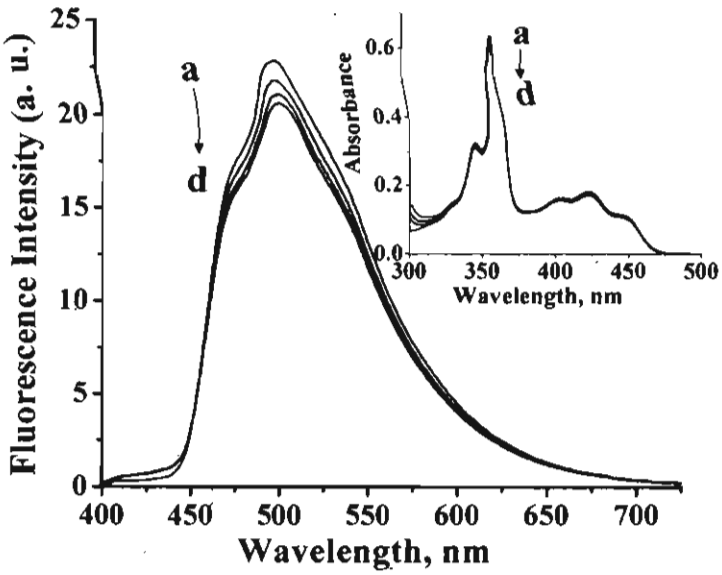

Figure 4.13. Change in fluorescence spectra of the probe **1** (30 μM) with increasing concentration of BSA. [BSA] (a) 0 and (d) 10 μg/mL. Excitation wavelength, 366 nm.

To understand the extent to which these contaminants can affect the ssDNA quantification assay, we have investigated the fluorescence changes of the probe **1** with ssDNA in the presence of RNA, bovine serum albumin, salts and detergents like SDS and Triton X-100. Since the extraction and separation of the nucleic acids from the biological extracts involves time consuming protocols, experiments were carried out to assess whether the fluorescence assay was affected by the presence of biological fluids. Linearity of the assay in biological fluids was assessed by conducting the assay in blood serum. Figure 4.14 shows the change in fluorescence of the probe **1** with increasing concentration of ssDNA in the presence

of bovine serum albumin as additive, while the inset shows the fluorescence changes in the presence of RNA as additive. In both cases only negligible effect of the additives were observed in the fluorescence changes.

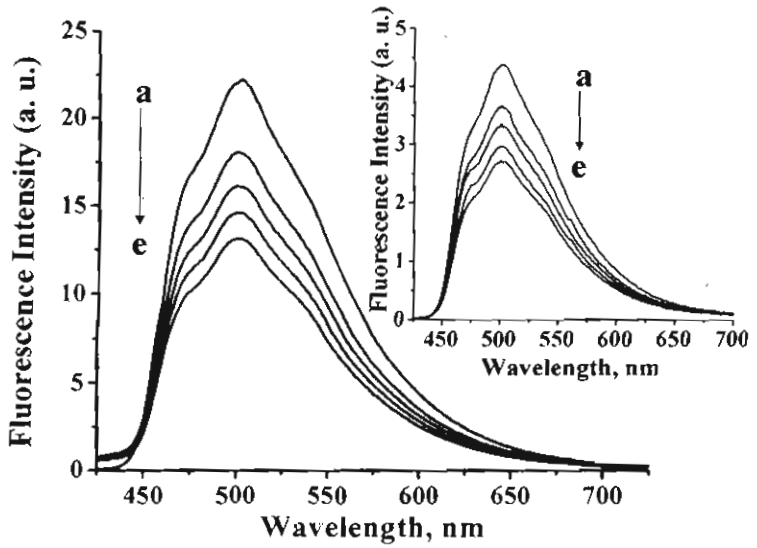

Figure 4.14. Change in fluorescence spectra of probe **1** (30 μM) with increase in addition of ssDNA in 10 mM phosphate buffer (pH 7.4) containing 1% BSA. [ssDNA] (a) 0, (b) 0.20, (c) 0.43, (d) 0.63 and (e) 0.8 mM. Inset shows the change in fluorescence of probe **1** in the presence of 0.25 mM RNA under similar conditions. Excitation wavelength, 366 nm.

Similarly, Figure 4.15 shows the change in fluorescence of the probe **1** with ssDNA in blood serum and in the presence of 0.1% triton (inset), while Figure 4.16 shows the fluorescence changes with increasing concentrations of ssDNA in the presence of SDS and 100 mM NaCl (inset). While SDS shows only negligible effects, the extent of quenching in the fluorescence emission of probe **1** with ssDNA is decreased in the presence of 100 mM NaCl. The relative effects of all these additives on the ssDNA detection by the probe **1** are shown in Figures 4.17-

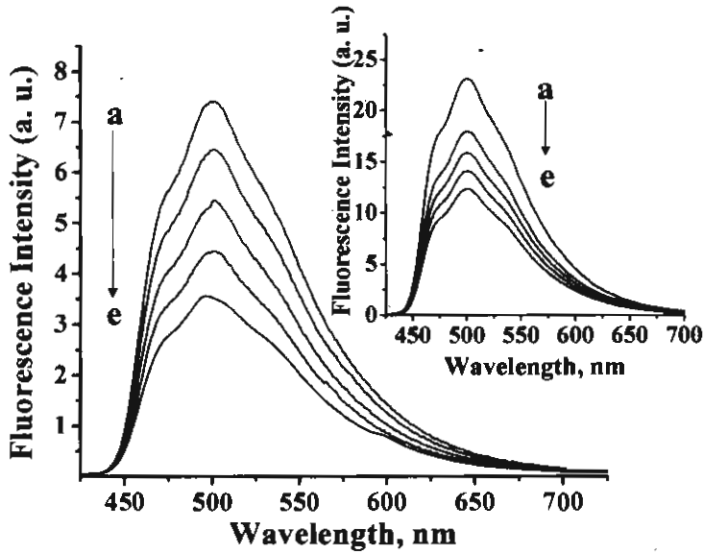

Figure 4.15. Change in fluorescence spectra of probe **1** (30 μM) with increase in addition of ssDNA in 10 mM phosphate buffer (pH 7.4) containing 0.8% blood serum. [ssDNA] (a) 0, (b) 0.20, (c) 0.43, (d) 0.63 and (e) 0.8 mM. Inset shows the change in fluorescence of probe **1** in the presence of 0.1% Triton X-100 under similar conditions. Excitation wavelength, 366 nm.

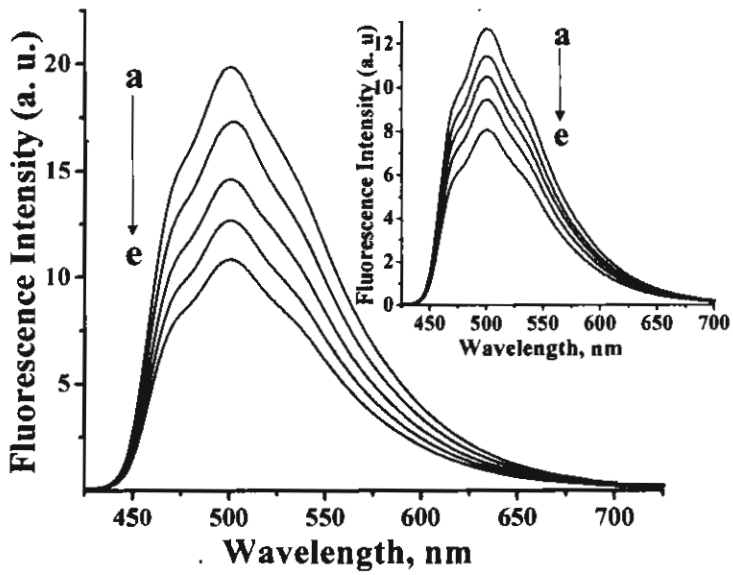

Figure 4.16. Change in fluorescence spectra of probe **1** (30 μM) with increase in addition of ssDNA in 10 mM phosphate buffer (pH 7.4) containing 0.01% SDS. [ssDNA] (a) 0, (b) 0.20, (c) 0.43, (d) 0.63 and (e) 0.8 mM. Inset shows the change in fluorescence of probe **1** in the presence of 100 mM NaCl under similar conditions. Excitation wavelength, 366 nm.

4.18. It was observed that the additives caused only slight or negligible changes in the fluorescence emission characteristics of the probes **1** and **2**. Interestingly, in all cases, the linearity of the assay is maintained. While the slope of the linear fit obtained in the presence of ssDNA is 1.04, those obtained in the presence of BSA (1%), SDS (0.01%) and RNA (100 μg/mL) are 0.85, 1.33 and 0.75, respectively. The slope of the assay in blood serum was found to be 1.04, while a slope value of 1.22 was observed in the presence of 500 μM dsDNA. These observations confirm that the commonly found contaminants have negligible influence on the slope value of the fluorimetric quantification of ssDNA by probe **1**.

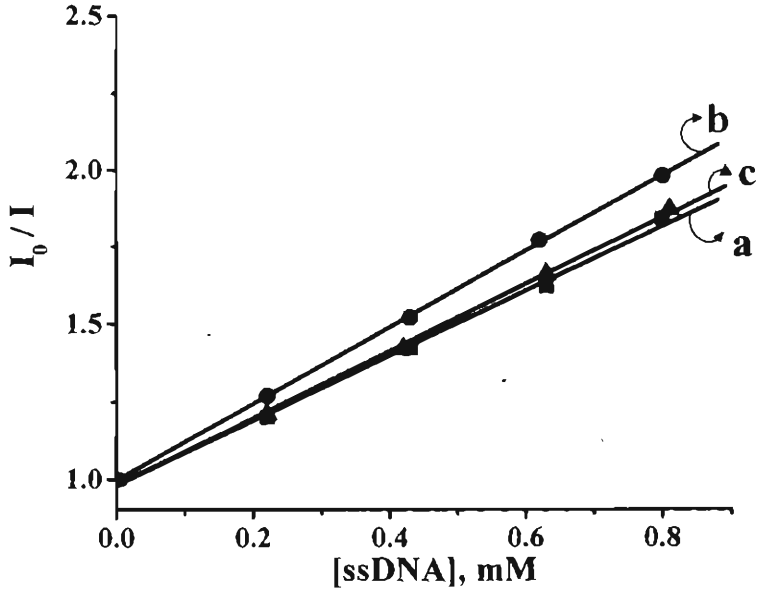

Figure 4.17. Effect of various additives on the linearity of the assay based on the probe **1** for the quantitation of ssDNA. (a) ssDNA alone, and in the presence of (b) dsDNA (0.5 mM), and (c) blood serum.

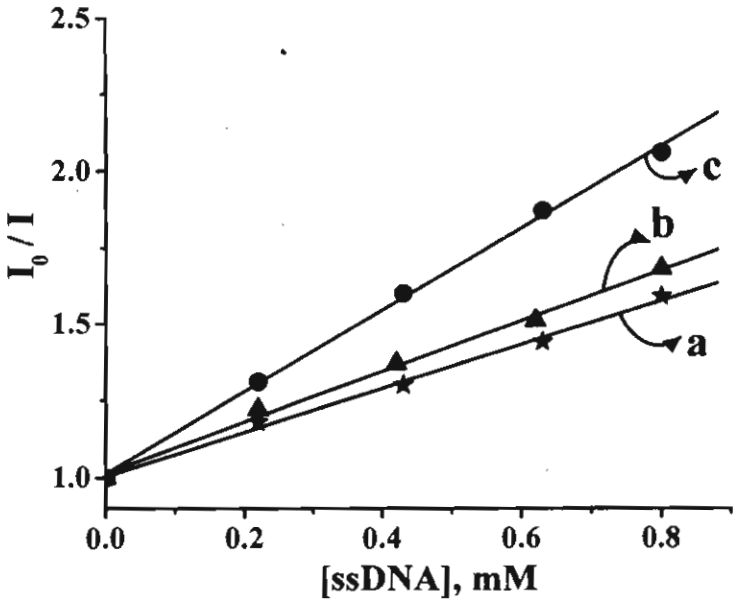

Figure 4.18. Effect of various additives on the linearity of the assay based on the probe **1** for the quantitation of ssDNA. (a) *E.Coli* RNA (100 μg/mL), (b) BSA (1%) and (c) SDS (0.01%).

Thus, the concentration of ssDNA in an unknown sample can be estimated from equation 4.1,

$$\text{ssDNA} = \frac{(I / I_0) - 1}{M} \qquad (4.1)$$

where, I_0 is the fluorescence intensity of the probe in the absence of ssDNA and I is the fluorescence intensity of the probe in the presence of ssDNA. M is the slope of the linear fit obtained from the plot of I_0/I vs the concentration of ssDNA and was found to be 1.0 ± 0.2 under the experimental conditions described.

4.3.3 Quantification of Ratio of Single Strand DNA to Double Strand DNA

The fluorimetric method based on the probe **1** showed high selectivity for ssDNA and also in the presence of various additives including the duplex DNA (dsDNA). Figure 4.19 shows the changes in fluorescence emission of the probe **1** with increasing concentrations of ssDNA in the presence of 0.25 mM dsDNA. In this context, it was of our interest to evaluate the potential use of the probe **1** for quantification of the ratio of ssDNA to dsDNA, since such a ratio is directly proportional to the extent of the DNA damage.[9] To test this view, the DNA samples

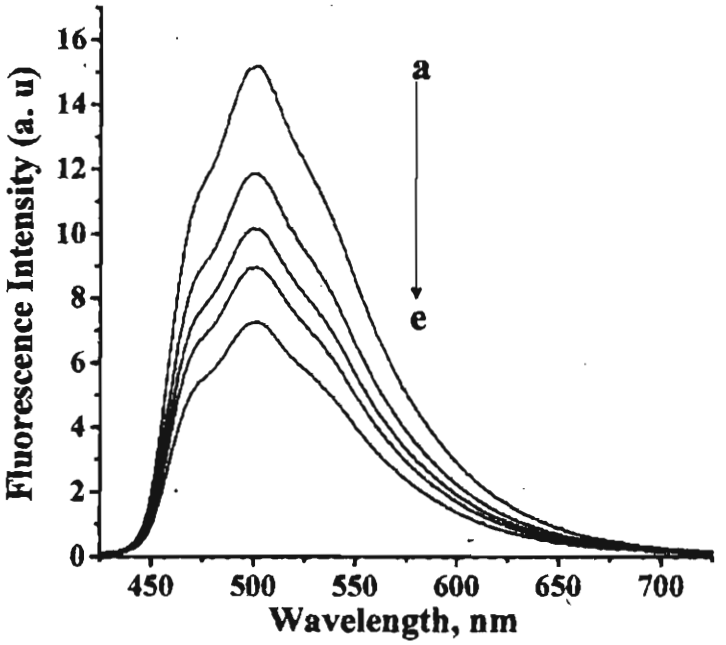

Figure 4.19. Change in fluorescence spectra of probe **1** (30 μM) with increase in addition of single stranded (ssDNA) in 10 mM phosphate buffer (pH 7.4) containing 0.25 mM dsDNA. [ssDNA] (a) 0, (b) 0.20, (c) 0.43, (d) 0.63 and (e) 0.8 mM. Excitation wavelength, 366 nm.

samples containing both ssDNA and dsDNA in different ratios of 0, 1, 2.1, 3.2 and 4.4 were prepared and titrated with 30 μM of the probe **1**. These samples were excited at 366 nm and the emission intensity was monitored at 501 nm, corresponding to the maximum of the acridinium chromophore. The ratio of fluorescence intensity (I_0/I) in the absence and presence of DNA was then plotted against the ratios of ssDNA to dsDNA. A linear regression was obtained with a correlation coefficient of 0.99 and the slope value of 0.26 (Figure 4.20) under the physiological pH conditions.

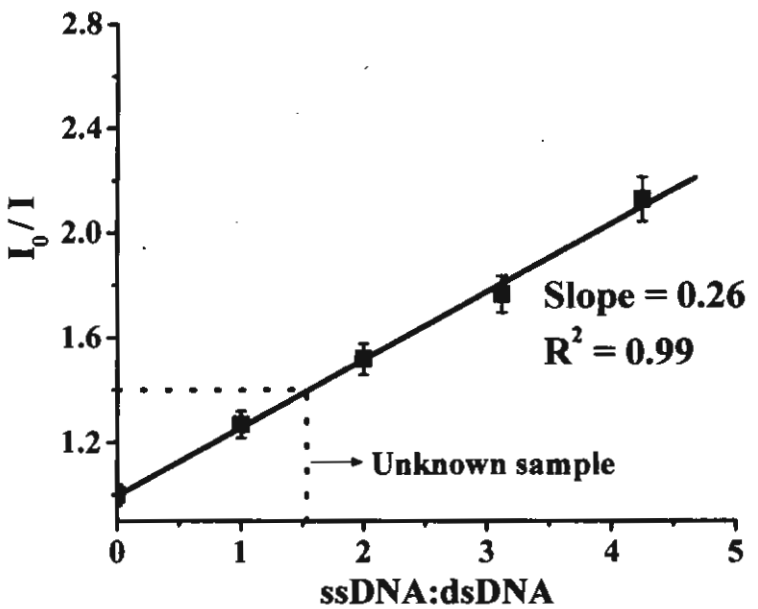

Figure 4.20. Variation in the fluorescence intensity of the probe **1** (30 μM) with the addition of samples containing different ratios of ssDNA to dsDNA.

To assess the ability of this assay to measure the ratio of ssDNA to dsDNA, a sample containing ssDNA and dsDNA in the ratio of 2:1 was prepared and classified as unknown. The fluorescence intensity at 501 nm was measured in the

absence and presence of the unknown concentration of DNA. The fluorescence intensity ratio (I_0/I) value measured is found to be very close to the predicted valuefor the corresponding ratio of ssDNA to dsDNA in the standard curve as shown by the dotted lines in Figure 4.20. On the other hand, the ratio of ssDNA to dsDNA and the percentage of ssDNA in a sample containing ssDNA and dsDNA can be accurately determined in an unknown sample from equations 4.2 and 4.3,

$$\text{ssDNA} = \frac{(I / I_0) - 1}{0.26} \qquad (4.2)$$

$$\% \text{ ssDNA} = \left(\frac{(I / I_0) - 1}{0.26} \right) \times 100 \qquad (4.3)$$

where, I_0 is the fluorescence intensity of the probe in the absence of DNA and I is the fluorescence intensity of the probe in the presence of DNA and 0.26 is a constant slope value obtained from the graph. To determine the sensitivity and robustness of the method for quantification of ssDNA, we have evaluated the effect of concentration of the probe **1** on the fluorimetric detection of ssDNA and ratio of ssDNA to dsDNA. The plot of (I_0/I) vs the ratio of ssDNA to dsDNA, gave a slope value of 0.23 ± 0.04 at all concentrations of the (5 - 40 μM) tested (Figure 4.21). These results demonstrate that the probe concentration has negligible effect on the fluorimetric quantification method for ssDNA as well as the ratio of ssDNA to dsDNA.

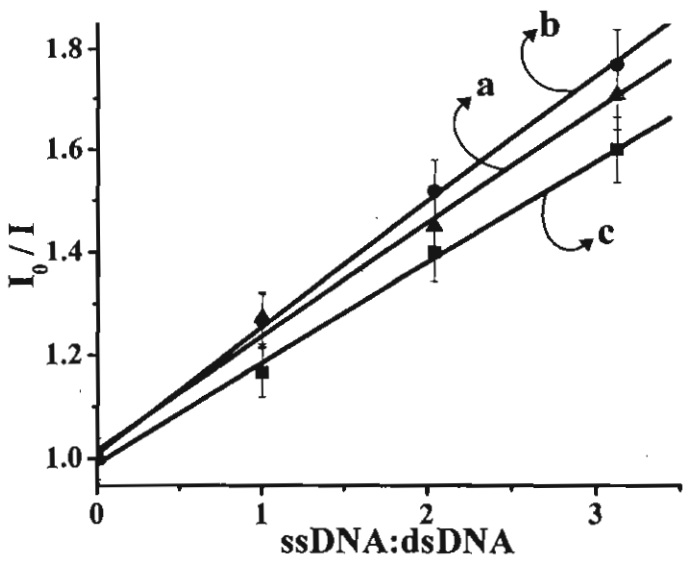

Figure 4.21. Effect of the probe concentration on the linearity of assay by following the change in fluorescence intensity with DNA samples containing different ratios of ssDNA to dsDNA. [**1**] (a) 20, (b) 30 and (c) 40 μM.

4.4. Conclusions

In conclusion, of the two probes investigated, we observed that the probe **1** with quantitative fluorescence quantum yield (Φ_f = 1) exhibited unusually high selectivity for ssDNA as compared to dsDNA due to the inherent steric factors (Figure 4.22). It showed significantly high binding affinity for various single strand DNA sequences in the range K_{DNA} = 3-8.5 x 10^4 M^{-1} and the mode of binding involves both intercalative and electrostatic interactions. The unusual selectivity of the probe **1** was effectively employed to develop and demonstrate a sensitive fluorimetric method for the quantification of ssDNA and also the ratio of ssDNA to dsDNA. This assay showed linearity over a wide range of ssDNA concentrations (20–1000 μM), the probe concentrations (10-50 μM) and have

negligible error even in the presence of dsDNA, RNA, proteins and surfactants. These results clearly demonstrate the use of the probe **1** as an efficient and sensitive fluorescent probe for the quantification of ssDNA under the physiological pH conditions and also in biological fluids.

Figure 4.22. Visual detection of ssDNA by the probe **1**. Excitation Wavelength, 365 nm.

4.5. Experimental Section

4.5.1. General Aspects

The equipment and procedure for spectral recordings are described elsewhere.[35,39,40] The fluorescence spectra were recorded on a SPEX-Fluorolog F112X spectrofluorimeter. The fluorescence quantum yields were measured by the relative methods using optically dilute solutions, with 10-methylacridinium-trifluoromethane sulfonate in water (Φ_f = 1) as the standard.[40] Circular dichroism (CD) spectra were recorded on Jasco Corporation, J-810 spectropolarimeter. The fluorescence lifetimes were measured on an IBH picosecond single photon counting system using a 401 nm IBH NanoLED source and a Hamamatsu C4878-

02 MCP detector. The fluorescence decay profiles were deconvoluted using IBH Data Station software V2.1, fitted with a mono-, bi- or tri-exponential decay and minimizing the χ^2 values of the fit to 1 ± 0.1.

4.5.2. Chemicals

Calf thymus DNA (from Sigma Aldrich, India) was used without further purification. The RNA (Sigma Aldrich) used was RNA-Core Type from Baker's Yeast and RNA Transfer Type from *E. Coli*. The oligonucleotide sequences 5'-AAA AAA AAA AAA AAA AAA A-3', $(dA)_{19}$; 5'-TTT TTT TTT TTT TTT TTT T-3', $(dT)_{19}$; 5'-CCC CCC CCC CCC CCC CCC C-3', $(dC)_{19}$; 5'-GGG GGG GGG GGG GGG GGG G-3' $(dG)_{19}$; and 5'-CGT GGA CAT TGC ACG GTA C-3' $(dN)_{19}$; were purchased from Sigma Genosys (India). All solvents used were distilled and purified before use. The synthesis of the compounds **1** and **2** were carried out by first synthesizing the corresponding acridines in 50-60% yields by a modified Bernthsen procedure as described in chapter 2. The quarternization of these acridine derivatives with methyl iodide gave the corresponding acridinium derivatives **1** (60 %), mp 224-225 °C and **2** (65 %), mp 242-2453 °C.

4.5.3. DNA Binding Studies

All binding studies were carried out in 10 mM phosphate buffer (pH 7.4) containing either 2 mM or 100 mM NaCl. Solution of calf thymus DNA (CT DNA) was filtered through a 0.45 μM Millipore filter. The concentrations of CT

DNA solutions were determined by using the average extinction coefficient value of 6600 M^{-1} cm^{-1} for a single nucleotide at 260 nm.[41] The absorption and fluorescence titrations with DNA were carried out by adding small aliquots of DNA solution containing the same concentration of the probe as that in the test solution. For ssDNA, all conditions were the same except that the CT DNA solution was heated in a boiling water bath for 30 min in order to denature the DNA. Complete denaturation was confirmed by comparing the absorption ratio at 260 nm for the heated (ssDNA) and non-heated (dsDNA) samples. A value of 1.32 was obtained in good agreement with the literature value.[42]

DNA association constants were calculated using fluorescence quantum yields, and according to the method of McGhee and von Hippel by using the data points of the Scatchard plot.[36] By using the fluorescence data, the concentration of the free probe was determined from equation 4.4,

$$C_F = C_T \left(\frac{I}{I_0} - p \right) \Big/ (1 - p) \qquad (4.4)$$

where, C_T is the total concentration of the added probe, C_F is the concentration of the free ligand, I and I_0 are the fluorescence intensities in the presence and absence of DNA and p is the ratio of the observed fluorescence quantum yield of the probe in bound form to that of free form. The value of p was obtained from a plot of I/I_0 vs 1/[DNA] such that the limiting fluorescence yield is given by the Y-intercept.

The amount of bound probe (C_B) at any concentration is given by the equation 4.5,

$$C_B = C_T - C_F \qquad (4.5)$$

Scatchard analysis was done according to the McGhee and von Hippel equation 3,

$$\frac{r}{C_F} = K_{ass}(1 - nr)\left(\frac{1 - nr}{1 - (n - 1)r}\right)^{n-1} \qquad (4.6)$$

where, r is the extent of ligand molecules bound per unit amount of macromolecule at a free ligand concentration of C (M), K_{ass} is the intrinsic binding constant to an isolated site, n is the number of nucleotides occluded by the compounds. The analysis was done using the plot of r / C_F vs r, where r is equal to C_B / [DNA].

4.5.4. Processing of Blood Samples

Fresh blood samples were immediately treated with EDTA and centrifuged at 3000 rpm for 5 min and the supernatant was collected. This supernatant was divided into two portions. One of the portions was subjected to deproteinization by stirring with 20% trichloroacetic acid followed by centrifugation at 3000 rpm for 5 min as described in the literature,[43] and used for further studies after diluting with water (100-fold). The other portion was used as such after dilution with water. The pH of all blood samples is maintained at 7.4.

4.6. References

1. (a) Blackburn, G. M., Gait, M. J., Eds. *Nucleic Acids in Chemistry and Biology*; Oxford University Press: Oxford, 1996, and references cited therein. (b) Glazer, A. N.; Rye, H. S. *Nature* **1992**, *359*, 859-861.

2. (a) Armitage, B. A. *Chem. Rev.* **1998**, *98*, 1171-1200. (b) Marin, V. L.; Armitage, B. A. *J. Am. Chem. Soc.* **2005**, *127*, 8032-8033. (c) Mugesh, G.; du Mont, W.; Sies, H. *Chem. Rev.* **2001**, *101*, 2125-2179.

3. (a) Wilson, W. D. DNA Intercalators. DNA and Aspects of Molecular Biology; Kool, E., Ed. In *Comprehensive Natural Products Chemistry*; Barton, D., Nakanishi, K., Eds.; Pergamon Press: Elsevier, 1999; Vol. 7, Chapter 12. (b) Goodwin, K. D.; Lewis, M. A.; Tanious, F. A.; Tidwell, R. R.; Wilson, W. D.; Georgiadis, M. M.; Long, E. C. *J. Am. Chem. Soc.* **2006**, *128*, 7846-7854. (c) Cutler, R. G.; Rodriguez, H., Eds. *Critical Reviews of Oxidative Stress and Aging*; World Scientific Publishing Co.: New York, 2003; Vol 2.

4. (a) Levy, M. S.; Lotfian, P.; O'Kennedy, R.; Lo-Yim, M. Y.; Shamlou, P. A.; *Nucleic Acids Res.* **2000**, *28*, e57. (b) Gaylord, B. S.; Heeger, A. J.; Bazan, G. C. *J. Am. Chem. Soc.* **2003**, *125*, 896-900. (c) Rogers, K. R.; Apostol, A.; Madsen, S. J.; Spencer, C. W. *Anal. Chem.* **1999**, *71*, 4423-4426.

5. Ramaiah, D.; Koch, T.; Orum, H.; Schuster, G. B. *Nucleic Acids Res.* **1998**, *26*, 3940-3943.

6. (a) Pfeifer, G. P., Ed. *Technologies for Detection of DNA Damage and Mutations*; Plenum Press: New York, 1996. (b) Siede, W., Kow, Y. W., Doetsch, P. W., Eds. *DNA Damage Recognition*; Taylor and Francis: New York, 2006. (c) Ostling, O.; Johanson, K. J. *Biochem. Biophys. Res. Commun.* **1984**, *123*, 291-298.

7. (a) Epe, B. *Biol. Chem.* **2002**, *383*, 467-475. (b) Olive, P. L. *Int. J. Radiat. Biol.* **1999**, *75*, 395-405. (c) Zhang, Y. J.; Geacintov, N. E.; Santella, R. M. *Chem. Res. Toxicol.* **1997**, *10*, 948-952.

8. (a) Kohn, K. W. *Pharmacol. Ther.* **1991**, *49*, 55-77. (b) Hitchelson, K. R.; Cheng, J. Eds. *Capillary Electrophoresis of Nucleic Acids*; Humana Press: Totowa, New Jersey, 2001; Volume 1.

9. Potter, J. A.; Gollahon, K. A.; Palanca, B. J. A.; Harbert, M. J.; Choi, Y. M.; Moskovitz, A. H.; Potter, J. D.; Rabinovitch, P. S. *Carcinogenesis* **2002**, *23*, 389-401.

10. Epe, B.; Pflaum, M.; Häring, M.; Hegler, J.; Rüdiger, H. *Toxicology Letters* **1993**, *67*, 57-72. (c) Möller, M.; Stopper, H.; Häring, M.; Schleger, Y.; Epe, B.; Adam, W.; Saha-Möller, C. A. *Biochem. Biophys. Res. Commun.* **1995**, *216*, 693-701.

11. (a) Zhou, L.; Rusling, J. F. *Anal. Chem.* **2001**, *73*, 4780-4786. (b) Zhou, L.; Yang, J.; Estavillo, C.; Stuart, J. D.; Schenkman, J. B.; Rusling, J. F. *J. Am. Chem. Soc.* **2003**, *125*, 1431-1436. (c) Hou, C. J.; Milovic, N.; Godin, M.;

Russo. P. R.; Chakrabarti, R.; Manalis, S. R. *Anal. Chem.* **2006**, *78*, 2526-2531.

12. (a) von Sonntag, C. *Chemical Basis of Radiation Biology*; Taylor and Francis: Philladelphia, 1989. (b) Melvin, M. S.; Tomlinson, J. T.; Saluta, G. R.; Kucera, G. L.; Lindquist, N.; Manderville, R. A. *J. Am. Chem. Soc.* **2000**, *122*, 6333-6334. (c) Noll, D. M.; Mason, T. M.; Miller, P. S. *Chem. Rev.* **2006**, *106*, 277-301.

13. (a) Angelov, D.; Spassky, A.; Berger, M.; Cadet, J. *J. Am. Chem. Soc.* **1997**, *119*, 11373-11380. (b) Wagner, J. R.; Decarroz, C.; Berger, M.; Cadet, J. *J. Am. Chem. Soc.* **1999**, *121*, 4101-4110. (c) Douki, T.; Angelov, D.; Cadet, J. *J. Am. Chem. Soc.* **2001**, *123*, 11360-11366. (d) Frelon, C. G.; Douki, T.; Ravanat, J. L.; Pouget, J. P.; Tornabene, C.; Cadet, J.; *Chem. Res. Toxicol.* **2000**, *25*, 1002-1010.

14. (a) Ramaiah, D.; Eckert, I.; Arun, K. T.; Weidenfeller, L.; Epe, B. *Photochem. Photobiol.* **2004**, *79*, 99-104. (b) Ramaiah, D.; Eckert, I.; Arun, K. T.; Weidenfeller, L.; Epe, B. *Photochem. Photobiol.* **2002**, *76*, 672-677.

15. Collins, A. R.; Dobson, V. L.; Dŭsinská, M.; Kennedy, G.; Štětina, R. *Mutat. Res.* **1997**, *466*, 63-69.

16. Haugland, R. P., Ed. *Handbook of Fluorescent Probes and Research Products*; Molecular Probes Inc, 2002.

17. (a) Cosa, G.; Focsaneanu, K. -S.; McLean, J. R. N.; McNamee, J. P.; Scaiano, J. C. *Photochem. Photobiol.* **2001**, *73*, 585-599. (b) Cosa, G.; Vinette, A. L.; McLean, J. R. N.; Scaiano, J. C. *Anal. Chem.* **2002**, *74*, 6163-6169. (c) Chen, Q.; Li, D.; Zhao, Y.; Yang, H.; Zhu, Q.; Xu, J. *Analyst* **1999**, *124*, 901-906.

18. (a) Cosa, G.; Focsaneanu, K. -S.; McLean, J. R. N.; Scaiano, J. C. *Chem. Commun.* **2000**, 689-690. (b) Beach, L.; Schweitzer, C.; Scaiano, J. C. *Org. Biomol. Chem.* **2003**, *1*, 450-451.

19. (a) Liu, B.; Bazan, G. C. *J. Am. Chem. Soc.* **2006**, *128*, 1188-1196. (b) Pang, D.; Abruña, H. D. *Anal. Chem.* **2000**, *72*, 4700-4706. (c) Singhal, P.; Kuhr, W. G. *Anal. Chem.* **1997**, *69*, 4828-4832.

20. Hames, B. D., Higgins, S. J., Eds. *Gene Probes 1*; IRL Press: New York, 1995.

21. (a) Booth, C.; Griffith, E.; Brady, G.; Lydall, D. *Nucleic Acids Res.* **2001**, *29*, 4414-4422. (b) Rye, H. S.; Glazer, A. N. *Nucleic Acids Res.* **1995**, *23*, 1215-1222.

22. (a) Wang, X.; Nau, W. M. *J. Am. Chem. Soc.* **2004**, *126*, 808-813. (b) Kawai, K.; Yoshida, H.; Sugimoto, A.; Fujitsuka, M.; Majima, T. *J. Am. Chem. Soc.* **2005**, *127*, 13232-13237.

23. Sassanfar, M.; Roberts, J. W. *Nucleic Acids Res.* **1990**, *212*, 79-96.

24. Bishop, D. K.; Park, D.; Xu, L.; Kleckner, N. *Cell* **2001**, *69*, 439-456.

25. Lydall, D.; Nikolsky, Y.; Bishop, D. K.; Weinert, T. *Nature,* **1996**, *383*, 840-843.

26. Huang, L. C.; Clarkin, K. C.; Wahl, G. M. *Proc. Natl. Acad. Sci. USA,* **1996**, *93*, 4827-4832.

27. (a) Okazaki, R.; Okazaki, T.; Sakabe, K.; Sugimoto, K.; Sugino, A. *Proc. Natl. Acad. Sci. USA* **1968**, *59*, 598-605. (b) Henson, P. *J. Mol. Biol.,* **1978**, *1198*, 487-506. (c) Wanka, F.; Brouns, R. M.; Aelen, J. M.; Eygensteyn, A.; Eygensteyn, J. *Nucleic Acids Res.* **1977**, *4*, 2083-2097.

28. Tapiero, H.; Leibowitch, S. A.; Shaool, D.; Monier, M. N.; Harel, J. *Nucleic Acids Res.* **1976**, *3*, 953-963.

29. Cordeiro-Stone, M.; Makhov, A. M.; Zaritskaya, L. S.; Griffith, J. D. *J. Mol. Biol.* **1999**, *289*, 1207-1218.

30. (a) Watanabe, I.; Toyoda, M.; Okuda, J.; Tenjo, T.; Tanaka, K.; Yamamoto, T.; Kawasaki, H.; Sugiyama, T.; Kawarada, Y.; Tanigawa, N. *Jpn J. Cancer Res.* **1999**, *90*, 188-193. (b) Frankfurt, O. S.; Robb, J. A.; Sugarbaker, E. V.; Villa, L. *Exp. Cell Res.* **1996**, *226*, 387-397.

31. Raderschall, E. Golub, E. I.; Haaf, T. *Proc. Natl. Acad. Sci. USA* **1999**, *96*, 1921-1926.

32. Sugawara, N.; Haber, J. E. *Mol. Cell. Biol.* **1992**, *12*, 563-575.

33. Sun, H.; Treco, D.; Szostak, J. W. *Cell* **1991**, *64*, 1155-1161.

34. (a) Dionne, I.; Wellinger, R. J. *Proc. Natl. Acad. Sci. USA* **1996**, *93*, 13902-13907. (b) Makarov, V. L.; Hirose, Y.; Langmore, J. P. *Cell* **1997**, *88*, 657-

666. (c) Garvik, B.; Carson, M.; Hartwell, L. *Mol. Cell. Biol.* **1995**, *15*, 6128-6138.

35. (a) Joseph, J.; Eldho, N. V.; Ramaiah, D. *Chem. Eur. J.* **2003**, *9*, 5926-5935. (b) Joseph, J.; Eldho, N. V.; Ramaiah, D. *J. Phys. Chem. B* **2003**, *107*, 4444-4450. (c) Kuruvilla, E.; Joseph, J.; Ramaiah, D. *J. Phys. Chem. B* **2005**, *109*, 21997-22002.

36. (a) McGhee, J. D.; Von Hippel, P. H. *J. Mol. Biol.* **1974**, *86*, 469-489. (b) Adam, W.; Cadet, J.; Dall'Acqua, F.; Epe, B.; Ramaiah, D.; Saha-Möller, C. R. *Angew. Chem. Int. Ed. Engl.*, **1995**, *34*, 107-110. (c) Kumar, C. V.; Asuncion, E. H *J. Am. Chem. Soc.* **1993**, *115*, 8547-8553.

37. Rogers, J. E.; Le, T. P.; Kelly, L. A. *Photochem. Photobiol.* **2001**, *73*, 223-229.

38. Ahn, S. J.; Costa, J.; Emanuel, J. R. *Nucleic Acids Res.* **1996**, *24*, 2623-2625.

39. (a) Jisha, V. S.; Arun, K. T.; Hariharan, M.; Ramaiah, D. *J. Am. Chem. Soc.* **2006**, *128*, 6024-6025. (b) Avirah, R. R.; Jyothish, K.; Ramaiah, D. *Org. Lett.* **2007**, *9*, 121-124. (d) Hariharan, M.; Karunakaran, S. C.; Ramaiah, D. *Org. Lett.* **2007**, *9*, 417-420. (c) Arun, K. T.; Ramaiah, D. *J. Phys. Chem. A* **2005**, *109*, 5571-5578.

40. (a) Joseph, J.; Kuruvilla, E.; Achuthan, A. T.; Ramaiah, D.; Schuster, G. B. *Bioconjugate Chem.* **2004**, *15*, 1230-1235. (b) Ramaiah, D.; Kuruvilla, E. Fluorescent marker for the detection and quantitation of single strand DNA

under physiological pH conditions, Patent application No. 0603DEL2006, March 3, 2006.

41. Baguley, B. C.; Falkenhaug, E. M. *Nucleic Acids Res.* **1978**, *5*, 161-171.

42. Ausubel, F. M.; Brent, R.; Kingston, R. E.; Moore, D. D.; Seidman, J. G.; Smith, J. A.; Struhl, K. Eds. *Current Protocols in Molecular Biology*; Wiley Interscience: New York, 1994.

43. Koshiishi, I.; Imanari, T. *Anal. Chem.* **1997**, *69*, 216.

List of Publications

1. Selective interactions of a few acridinium derivatives with single strand DNA: Study of photophysical and DNA binding interactions,
Kuruvilla, E.; Ramaiah, D. *J. Phys. Chem. B* **2007**, *111*, 000 (In Press).

2. Fluorescent marker for the detection and quantitation of single strand DNA under physiological pH conditions,
Ramaiah, D.; **Kuruvilla, E.** Patent Application Number 0603Del2006 dated March 8, **2006**.

3. Novel bifunctional acridine-acridinium conjugates: Synthesis and study of their chromophore selective electron transfer and DNA binding properties,
Kuruvilla, E.; Joseph, J.; Ramaiah, D. *J. Phys. Chem. B* **2005**, *109*, 21997-22002.

4. Tuning of intercalation and electron transfer processes between DNA and acridinium derivatives through steric effects,
Joseph, J.; **Kuruvilla, E.**; Achuthan, A. T.; Ramaiah, D.; Schuster, G. B. *Bioconjugate Chem.* **2004**, *15*, 1230-1235.

5. Direct evidence on the external stimuli induced dissembly of DNA through microscopic techniques,
Hariharan, M.; **Kuruvilla, E.**; Ramaiah, D. *J. Am. Chem. Soc.* (Communicated).

Papers Presented at Conferences

6. Bifunctional acridine-acridinium conjugates: Synthesis and study of their chromophore selective electron-transfer and DNA binding properties,
Kuruvilla, E.; Joseph, J.; Ramaiah, D. Poster presented at the *International Conference on Frontiers of Radiation and Photochemistry*, M. G. University, Kottayam, **2007**, February 8-12.

7. Bisacridinium derivatives: Synthesis and study of photophysical and DNA binding properties,
Kuruvilla, E.; Joseph, J.; Ramaiah, D. Poster presented at the *7th Chemical Research Society of India Symposium*, IACS, Kolkatta, **2005**, February 4-6.

8. DNA interactions of 9-substituted acridinium derivatives: Steric and conformational effects,
Joseph, J.; **Kuruvilla, E.**; Achuthan, A. T. ; Ramaiah, D. Poster presented at the *6th Chemical Research Society of India Symposium*, IIT, Kanpur, **2004**, February 6-8.

9. Photophysical and DNA binding properties of bisacridinium derivatives,
Kuruvilla, E.; Joseph, J.; Ramaiah, D. Poster presented at the *3rd Trivandrum International Symposium on Recent Trends in Photochemical Sciences,* Regional Research Laboratory, Trivandrum, **2004**, January 5-7.